IITRI

IITRI Project G-6003
Summary Report

METAL CARBIDE-GRAPHITE COMPOSITES

Contract No. NASr-65(09)

Prepared for

Office of Research Grants and Contracts
Code BG
National Aeronautics & Space Administration
Washington 25, D. C.

IIT Research Institute

IITRI Project G-6003
Summary Report

METAL CARBIDE-GRAPHITE COMPOSITES

Contract No. NASr-65(09)

Prepared for

Office of Research Grants and Contracts
Code BG
National Aeronautics & Space Administration
Washington 25, D. C.

IIT RESEARCH INSTITUTE

IIT RESEARCH INSTITUTE
10 West 35th Street
Chicago, Illinois 60616

IITRI Project G-6003
Summary Report

For the Period
August 1, 1966 through July 31, 1967

METAL CARBIDE-GRAPHITE COMPOSITES
Contract No. NASr-65(09)

Prepared for

Office of Research Grants and Contracts
Code BG
National Aeronautics & Space Administration
Washington 25, D. C.

September 29, 1967

IIT RESEARCH INSTITUTE

IIT RESEARCH INSTITUTE
10 West 35th Street
Chicago, Illinois 60616

IITRI Project G-6003
Summary Report

For the Period
August 1, 1966 through July 31, 1967

METAL CARBIDE-GRAPHITE COMPOSITES
Contract No. NASr-65(09)

Prepared for

Office of Research Grants and Contracts
Code BG
National Aeronautics & Space Administration
Washington 25, D. C.

September 29, 1967

IIT RESEARCH INSTITUTE

METAL CARBIDE-GRAPHITE COMPOSITES

ABSTRACT

Niobium carbide-graphite and tantalum carbide-graphite composites have been fabricated by hot pressing at 3000° to 3250°C. The effect of carbide content upon physical and mechanical properties has been evaluated, both at room temperature and up to 2800°C. The properties which have been determined include flexural strength and modulus, tensile strength, compressive strength, thermal expansion, thermal conductivity, high temperature plastic deformation, and electrical conductivity.

Room temperature studies show that with increasing carbide content in either the NbC-C or TaC-C system, the various strength properties and electrical conductivity increase, and anisotropy in properties decrease. Tests at 2000°C reveal the following trends with temperature for any particular composite: increase in flexural strength, decrease in flexural modulus, little change in tensile strength, and a decrease in compressive strength. These changes indicate that the material should have an improved thermal shock resistance when rapidly cycled between ambient and 2000°C. Resistance to high temperature deformation does not follow any trend as a function of carbide content. However, the TaC-C system exhibits superior structural integrity at the high temperatures compared to the NbC-C system.

Measurement of thermal expansion and conductivity shows a trend toward isotropic behavior with increasing carbide content. At 80 vol% carbide, the with-grain (W/G) and across-grain (A/G) values for thermal expansion are virtually the same.

Other studies have considered strength-electrical properties relationships and the effect of heat treatment. A linear increase in flexural strength with increasing electrical conductivity in the W/G direction has been observed. The relationship in the A/G direction is nonlinear. Heat treatment of composites at 2500°C subsequent to hot pressing results in dimensional changes which are quite significant for low carbide content materials. These changes diminish with increasing carbide content.

CONTENTS

CONTENTS (Cont'd)

IIT RESEARCH INSTITUTE

ILLUSTRATIONS

IIT RESEARCH INSTITUTE

ILLUSTRATIONS (Cont'd)

IIT RESEARCH INSTITUTE

ILLUSTRATIONS (Cont'd)

IIT RESEARCH INSTITUTE

ILLUSTRATIONS (Cont'd)

TABLES

METAL CARBIDE-GRAPHITE COMPOSITES

I.   INTRODUCTION AND SUMMARY

Metal carbides are the most refractory of all known materials and also exhibit high strength. Their use for high temperature applications has been limited by their susceptibility to thermal shock and also by difficulties in the machining of desired configurations. However, the incorporation of graphite to form a series of metal carbide-graphite composites has yielded materials which minimize the undesirable properties of pure carbides while exploiting their high strength. Our earlier work has dealt with the fabrication and characterization of a wide variety of metal carbide (TiC, ZrC, HfC, VC, NbC, TaC, $MoC_{(1-x)}$, or WC) - graphite composites. The materials were hot pressed at temperatures of 2600° to 3250°C using no binder. Solid and/or liquid state sintering under pressure at these high temperatures is the mechanism by which the raw powder mixture is consolidated into a dense two-phase body.

The investigation for this year has been concerned with characterization of properties in the NbC-C and TaC-C systems. These are the most refractory of the metal carbide-carbon systems and exhibit the best resistance to creep at high temperature. Both room and high temperature behavior in flexure, tension, and compression have been evaluated. Other measurements which have been made include electrical resistivity at room temperature, and thermal expansion and conductivity. High temperature studies have also considered effects of heat treatment on physical and mechanical properties.

Similar trends in properties as a function of carbide content have been observed in both the NbC-C and TaC-C systems. At room temperature the relationships with increasing carbide content from 15 to 85 vol% carbide are the following:

1. Flexural strength - linear increase in the W/G direction from 7000 to 25,000 psi and exponential increase in the A/G direction from 2500 to 18,000 psi.

2. Flexural modulus - exponential increase in both grain directions (W/G: 4.0 to 30 x 10^6 psi, and A/G: 1.0 to 17 x 10^6 psi).

3. Tensile strength - exponential increase in W/G direction from 2000 to 20,000 psi.

4. Compressive strength - exponential increase in both grain directions from 10,000 psi to 100,000-180,000 psi.

5. Electrical conductivity - linear increase in the W/G direction and exponential increase in the A/G direction. For the NbC-C system, 0.7 x 10^4 to 2.6 x 10^4 mho-cm (W/G) and 0.2 x 10^4 to 2.5 x 10^4 mho-cm (A/G). For the TaC-C system, 0.5 x 10^4 to 4.2 x 10^4 mho-cm (W/G) and 0.2 x 10^4 to 3.2 x 10^4 mho-cm (A/G).

At elevated temperatures the following relationships have been observed:

1. Flexural strength - a 10 to 20% increase with temperature showing a peak at 2000°C. Strengths at 2500°C are about the same as that at room temperature.

2. Flexural modulus - a 10 to 50% decrease at 2000°C.

3. Tensile strength - slight loss with temperature, ranging from about 5 to 30% at 2000°C.

4. Compressive strength - slight increase at 2000°C for composites containing about 25 vol% carbide. Materials incorporating 50 vol% carbide or greater exhibited plastic deformation at stresses above 18,000 psi at 2000°C.

5. Thermal expansion - trend toward isotropy with increasing carbide content. At about a 20 vol% carbide level, the W/G and A/G CTE values (x 10^{-6} in./in./°C) are respectively 4.8 and 14.2 for the NbC-C system and 3.3 and 12.2 for the TaC-C

system. Essentially isotropic behavior is shown at about 80 vol% NbC or TaC, the values being about 7.5 and 7.2 x 10^{-6} in./in./°C, respectively.

6. Thermal conductivity - with increasing carbide content, decrease in W/G direction and increase in A/G direction. At about 750°C, thermal conductivity for a 27 vol% NbC-C are .277 (W/G) and .070 (A/G) cal/sec cm °C, and for a 73 vol% NbC-C composite, the values are .167 (W/G) and .126 (A/G) cal/sec cm °C. Decreasing trend with temperature for both grain directions.

7. Compressive deformation - under the conditions 2700°C/ 2000 psi/30 min, no trend observed as a function of carbide content. Maximum deformation for any well-bonded composite would be less than 2% in either the NbC-C or TaC-C system.

Studies conducted to relate flexural strength with electrical conductivity have shown the following trends: a linear increase in flexural strength with increasing electrical conductivity in the W/G direction. In the A/G direction, this relationship is exponential.

The effects of heat treatment of composites subsequent to fabrication has been established. The following changes have been observed after annealing at 2500°C for 1 hr: expansion in the A/G direction (up to 2%) and contraction in the W/G direction (up to 1%). These dimensional changes are most pronounced in graphite matrix composites and decrease with increasing carbide content. At carbide levels of about 80 vol%, no dimensional changes are observed.

Attempts have been made to characterize the behavior of composites by using mixing laws. In considering the relationship between experimental data and predicted mechanical behavior, a better understanding can be obtained as to whether the full potential of these systems is being realized.

In addition to good structural integrity at high temperatures, there is an interest in carbide-graphite composite materials possessing good resistance to thermal shock. Included in this report as Appendix A is an analysis of the effects of microstructure on mechanical and physical properties with respect to thermal shock resistance.

II. EXPERIMENTAL PROCEDURE

A. Preparation and Fabrication

The metal carbide-graphite composites were fabricated by hot pressing of blended powders at temperatures of 2600° to 3250°C. As detailed below, the processing procedures were based on methods suggested by earlier work.[1,2]

1. Raw Materials

The metal source used for composite fabrication was either the metal or metal carbide obtained as -325 mesh (less than 44µ) powder. Tantalum and niobium metal powders were supplied by the Fansteel Metallurgical Corporation and their carbides were furnished by the Wah Chang Corporation. The carbon source was Continental No. 90 coke flour (Union Carbide), a calcined petroleum coke with needle-like particles. This material was screened to -325 mesh.

The average particle size has been determined for representative powder samples by the Fisher subsieve technique. They are: Nb - 9.8µ, NbC - 3.6µ, and calcined petroleum coke - 3.1µ. Metallographic examination of Nb and NbC are shown in Fig. 1. The metal powder is relatively coarse and angular in shape whereas the carbide is finer without the sharp corners observed in the metal particles. These differences are due to the different production techniques used for these materials. The metal powder is crushed to obtain the finer particle size whereas the -325 mesh carbide powder is merely screened from

50μ
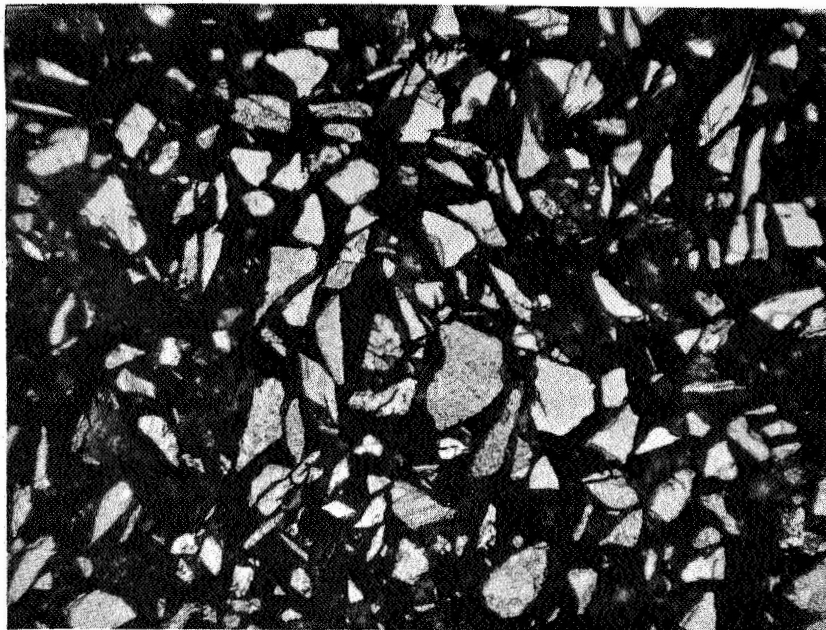
(a) Nb Powder (Fansteel)
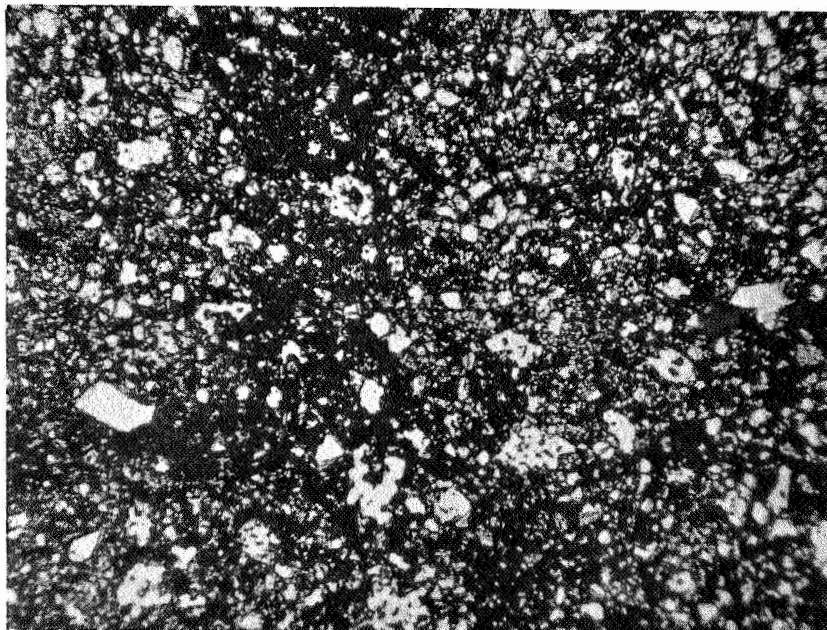
(b) NbC Powder (Wah Chang)

FIG. 1 - PARTICLE SIZE AND SHAPE
OF AS-RECEIVED Nb AND
NbC POWDERS (250x)

powder obtained by chemical reaction. The same relationship in size and shape exists for Ta and TaC.

The effect of contaminants in NbC on composite properties has been studied by Davidson et al.[3] They have observed that high-temperature compressive creep increases with increasing iron content. The deleterious effect becomes particularly pronounced at Fe levels of >500 ppm. Analysis of NbC powders used in our laboratories has revealed iron impurity contents from 80 to 500 ppm. The iron content in Nb metal used in the IITRI experiments have been less than 100 ppm. No correlation has been shown between iron content and deformation for our composites; this may be due to the relatively small amounts of iron present in our materials.

Other investigators have shown that the use of NbC particles which were porous has sometimes resulted in NbC-C composites of poor high-temperature properties.[4] These same investigators have eliminated the porosity by presintering of the NbC powder. Similar porosity has also been observed in our raw material. However, the porosity is no longer evident in hot pressed composites as observed in microstructural examination. This may be due to the longer times used in our processing (as discussed in the next section) which permits some hot working of the billet.

2. Processing Procedure

Compositions were dry blended by tumbling of the powders with rubber stoppers for 16 hr. The mixture was then loaded into the graphite mold and cold-pressed at 1000 psi. The initial pressure (500 psi) applied in hot pressing was maintained until a temperature of 2000°C was attained, at which time it was increased to 3000 psi for the remainder of the heating cycle. The pressure was released on the cooling cycle at about 2500°C.

The temperature of the pressing (2600° to 3250°C) was attained in approximately 1 to 1½ hr from room temperature; at this point temperature was maintained for periods from 5 min to 1 hr depending on the particular experiment. Comparison of our processing cycle with that of Davidson et al[5] appears in Fig. 2.

In general, higher processing temperatures have been shown to be desirable. This is probably due to the increased diffusion occurring at higher temperatures which produces better bonding between the carbide and carbon, and also to the higher degree of graphite orientation.

NbC-C composites were processed at 3100° to 3200°C, or slightly under the eutectic temperature of 3220°C. Composites in the TaC-C system have been hot-pressed at temperatures of 3200° to 3250°C. A closer approach to the eutectic temperature of 3450°C is restricted by practical limitations such as the low creep resistance of the graphite molds. This is reflected in changes in plunger lengths ranging from 10 to 20% depending on the pressing temperature.

3. Temperature Measurement

Temperature measurement during hot pressing is conducted both directly and indirectly. The direct method consists of optical monitoring with a Leeds and Northrup brightness pyrometer by sighting into the mold wall through an argon purged sight tube. Previous studies[2] have been made in which the temperature within the mold, i.e., where the sample would actually be located, was monitored concurrently with the standard mold wall measurement. It was determined that the two temperatures were virtually the same above 2800°C although a lag of about 50°C was observed at lower temperatures.

Temperature is also determined indirectly using time-temperature plots based on experimental data. The latter method
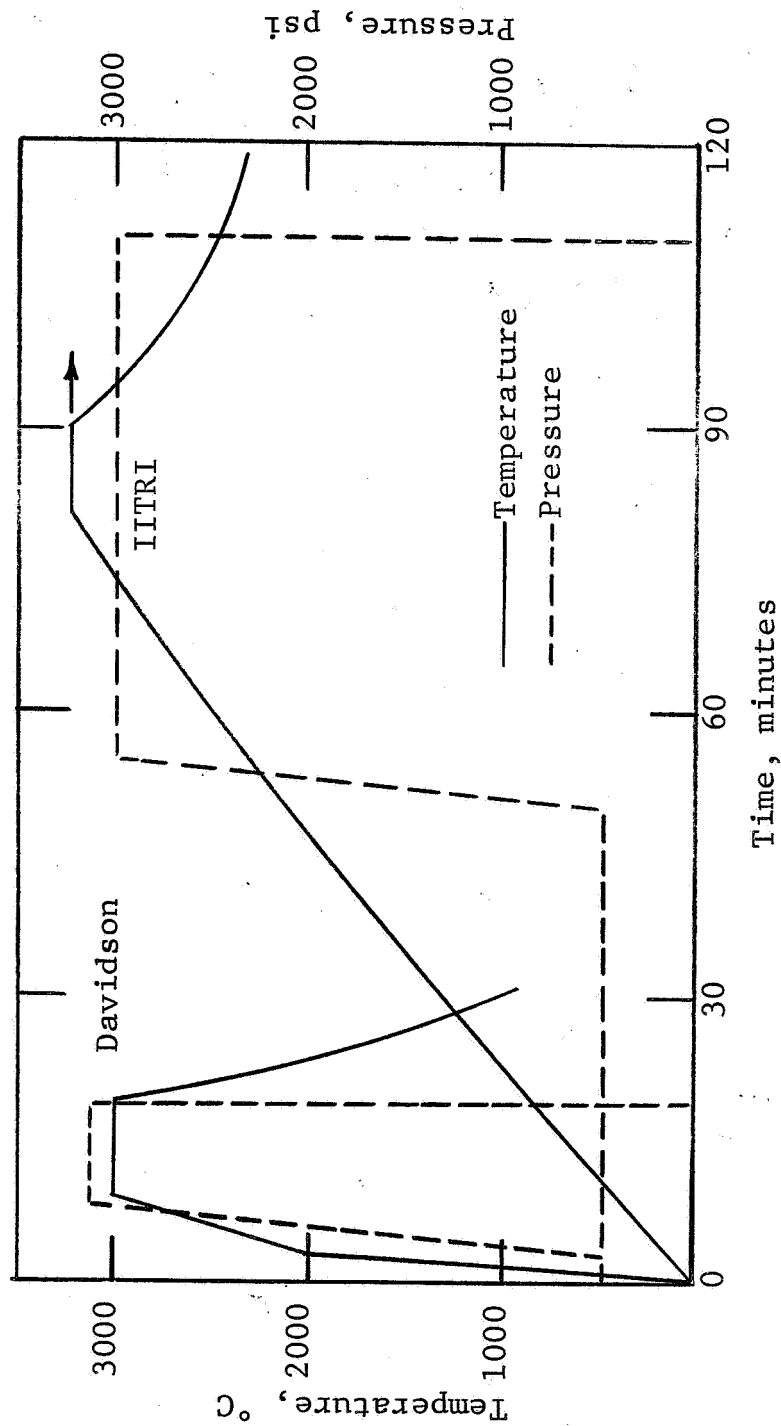
FIG. 2 - COMPARISON OF HOT PRESSING SCHEDULES BETWEEN DAVIDSON (REF. 5) AND IITRI

becomes especially important at the higher temperatures where volatiles occasionally attenuate the transmittance of emitted radiation.

B.   Evaluation of Composites

Evaluation of finished composites included microstructural examination and determination of physical, mechanical, thermal and electrical properties. Samples for metallographic study were prepared using standard techniques of vacuum mounting in plastic, followed by grinding and polishing with silicon carbide and then with 9μ diamond abrasive. Final polishing was accomplished on a silk cloth using a slurry of $\sim 0.05\mu$ alumina (Linde "B") in a 30% hydrogen peroxide solution. The H_2O_2 acted as a chemical polish-etch which minimized smearing and pullouts, and also brightened the sample surface.

Samples of both orientations for physical testing were sectioned and machined from halves of the finished billet which had a diameter of $2\frac{1}{2}$ in. or greater and a height of approximately 2 in. (Fig. 3). Machining of samples containing less than 60 vol% metal carbide could be performed using standard tooling. For composites containing greater amounts of carbide, diamond tooling became necessary. With diamond tooling, however, specimen preparation was relatively simple and a tolerance of $\pm .005$ in. could easily be maintained. Edges were well defined and chipping did not occur.

1.   Designation of Grain Orientation

The composites prepared by hot pressing take on a definite grain orientation. As shown in Fig. 4, the grain direction which would be the ab-axis of the graphite lattice lies perpendicular to the pressing direction and the c-axis would be parallel to the pressing direction. In the literature, several terms have

Pressing direction

(W/G)

With-grain
Samples

(A/G)

Across-grain
Samples
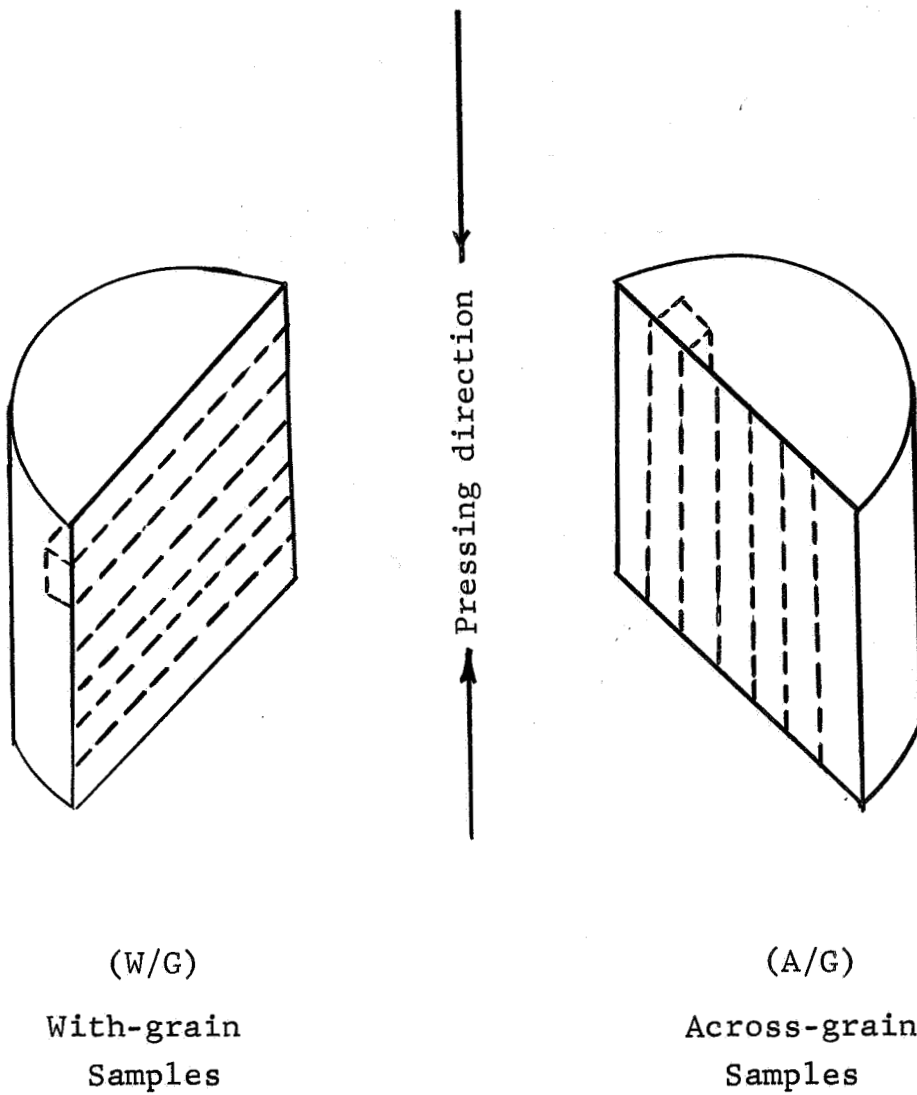
FIG. 3 - SECTIONING OF BILLETS FOR
PROPERTY EVALUATIONS

Pressing Direction

Grain Direction

Microstructure:

W/G

A/G

Flexure :

Tension :

Compression:

Electrical Conductivity,
Thermal Conductivity,
Thermal Expansion:
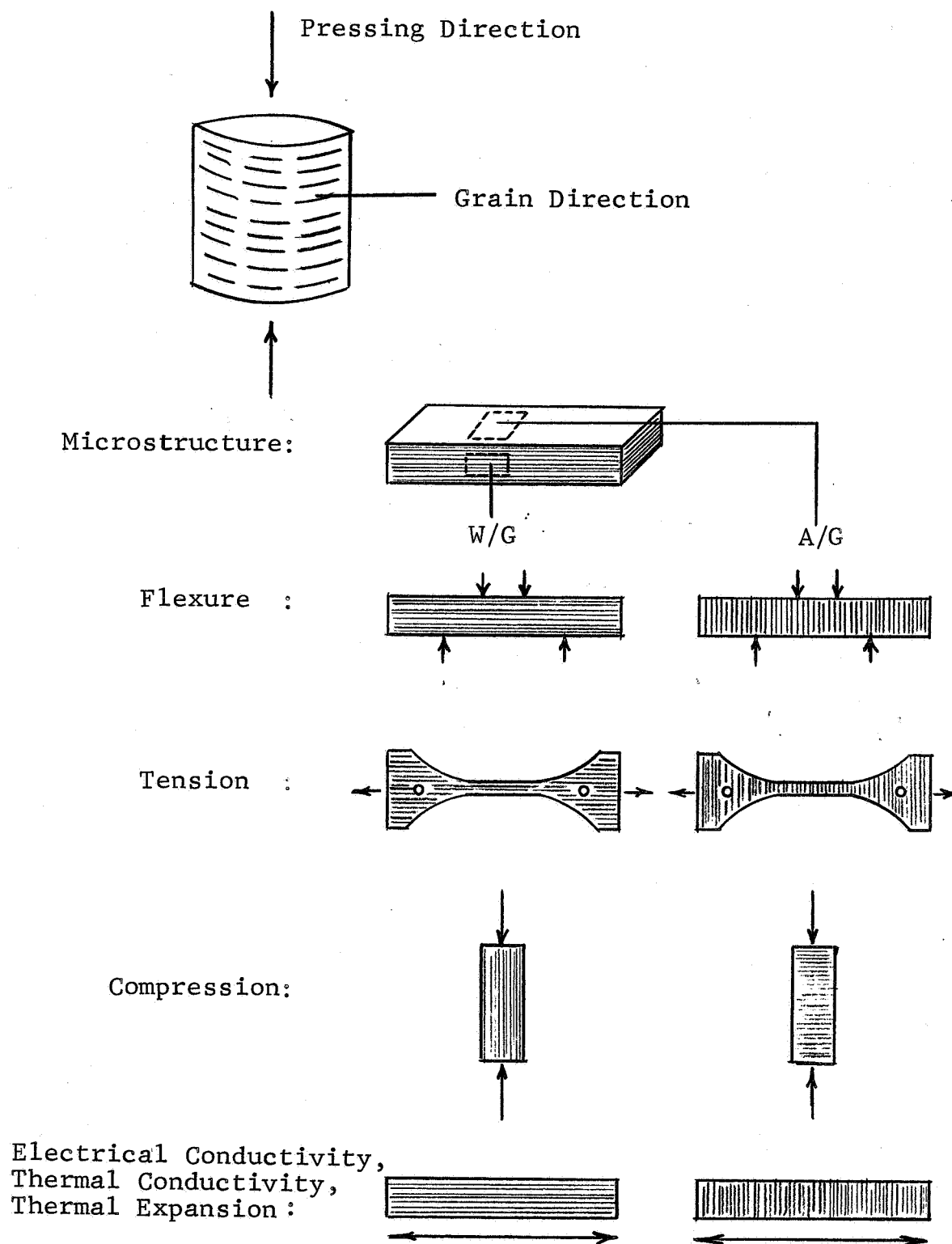
FIG. 4 - GRAIN ORIENTATION DESIGNATION
IN DESCRIPTION OF PROPERTIES

been used to specify grain orientation when discussing graphite properties. Among these are: with-grain (W/G) and across-grain (A/G); transverse and axial; and parallel and perpendicular.

Description of different properties becomes somewhat confusing in using any of these pairs. In order to maintain standard designations, the terms which will be used in this report will be with-grain (W/G) and across-grain (A/G). The drawings in Fig. 4 illustrate the grain orientation under this designation for the various properties which are discussed.

2. Physical Properties

Initial evaluation of samples included determination of bulk density and metal content analysis, as well as microstructural examination. Bulk density values were determined from precise measurements of dimensions and weight and/or by water immersion techniques. The extent of densification was evaluated by comparison of these values to theoretical densities which was calculated simply as: weight of metal carbide plus weight of graphite, all divided by volume of metal carbide plus volume of graphite. The calculations were made based on the x-ray densities of the particular carbide and a value of 2.26 g/cc for the graphite phase.

The need for accurate metal analysis was apparent in that for several of the pressings, significant loss of metal carbide had occurred due to reaction with the mold and extrusion around the plungers. Thus, the actual metal content in the finished billet could vary as much as 80% from that in the as-mixed state. The procedure for determining metal content consisted of oxidizing the metal carbide-graphite under a stream of oxygen at 900°C to obtain the metal oxide while volatilizing the carbon component as the monoxide and/or dioxide. Gravimetric analysis revealed the actual amounts of metal in the samples.

Compositional designations have been reported by various investigators as wt% metal, wt% metal carbide and/or metal carbide vol%. In order to simplify comparison of data, plots of wt% metal carbide vs vol% metal carbide for both NbC and TaC appear in Figs 5 and 6. Also presented in these graphs are curves for theoretical densities as a function of carbide content.

3.   Mechanical Properties

Flexural strengths were determined using four-point loading, the load points being at the 1/3 points of $1\frac{1}{2}$ in. span. Sample dimensions were approximately $\frac{1}{4}$ x $\frac{1}{4}$ x 1 3/4 in. to 2 3/4 in. long. Room temperature measurements were conducted in an Instron testing machine (Fig. 7). An extensometer was employed to record deflection of the sample; flexural modulus was determined from the x-y plot of stress vs strain. The elevated temperature evaluations were made in an argon atmosphere, using a graphite resistor tube furnace. Samples were heated to the respective test temperature in about 5 min and soaked for an additional 10 min prior to testing. Load was monitored with a calibrated deflection ring. To measure sample deflection in high temperature tests, an optical method was used in which sample movements at the supporting pins as well as in the center were monitored visually using Gaertner optical micrometers.

Room temperature compressive and tensile tests were also conducted in the Instron. The compressive cylinders measured $\frac{1}{4}$ in. in diameter x 3/4 in. long. In Fig. 8, the pin-gripped tension specimen used in our evaluations is depicted along with graphite grips used in high-temperature tests. The gage section measured $\frac{1}{2}$ in. long and the cross-section was 1/8 x 3/32 in. The dimensions evolved from modifications which were necessary to obviate failures at the pins in early designs. Composites incorporating more than 70 vol% carbide were machined by EDM;
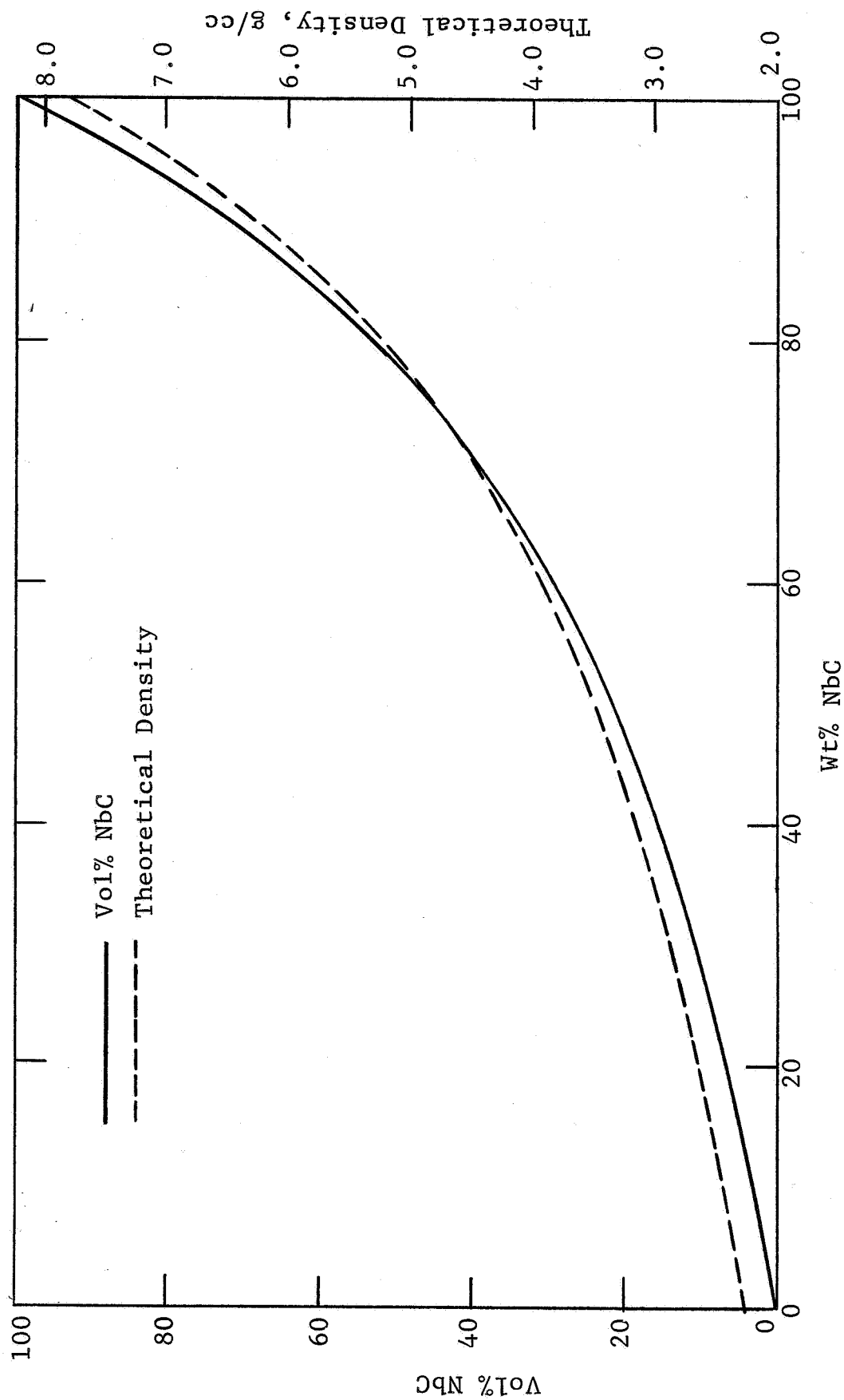
FIG. 5 – VOL% NbC AND THEORETICAL DENSITY AS A FUNCTION
OF WT% NbC FOR NbC-C COMPOSITES
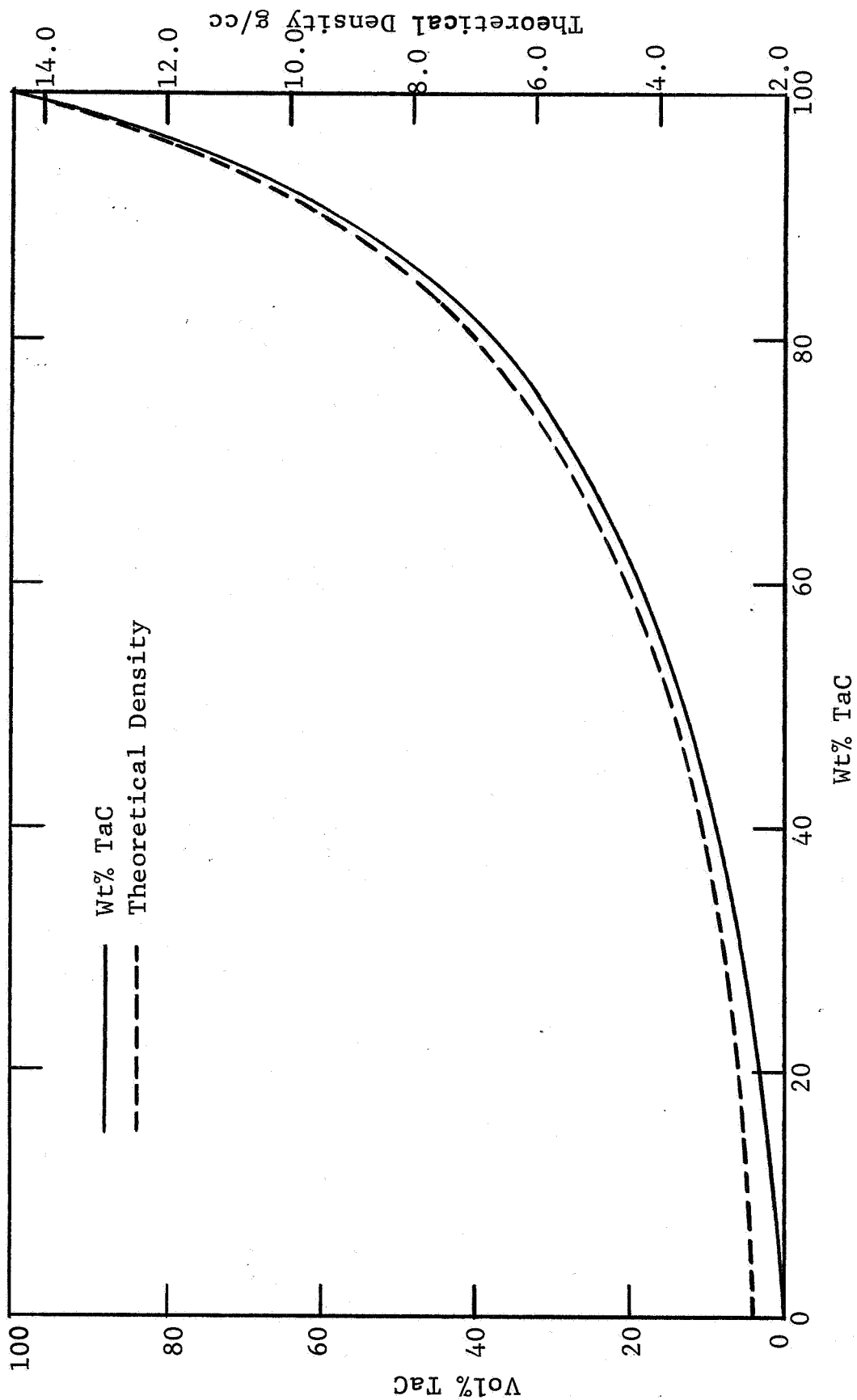
FIG. 6 - VOL%TaC AND THEORETICAL DENSITY AS A FUNCTION OF
WT% TaC FOR TaC-C COMPOSITES
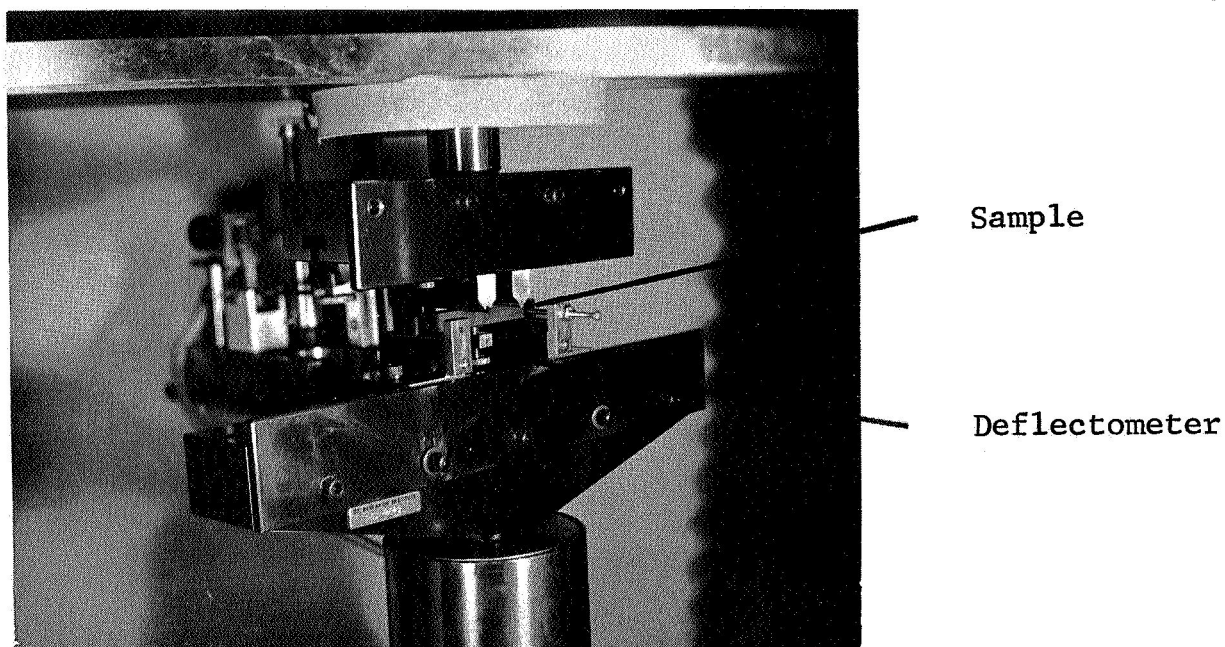
FIG. 7 - FLEXURAL STRENGTH TEST ATTACHMENT
FOR INSTRON TEST MACHINE

PIN-TYPE TENSILE
SPECIMEN
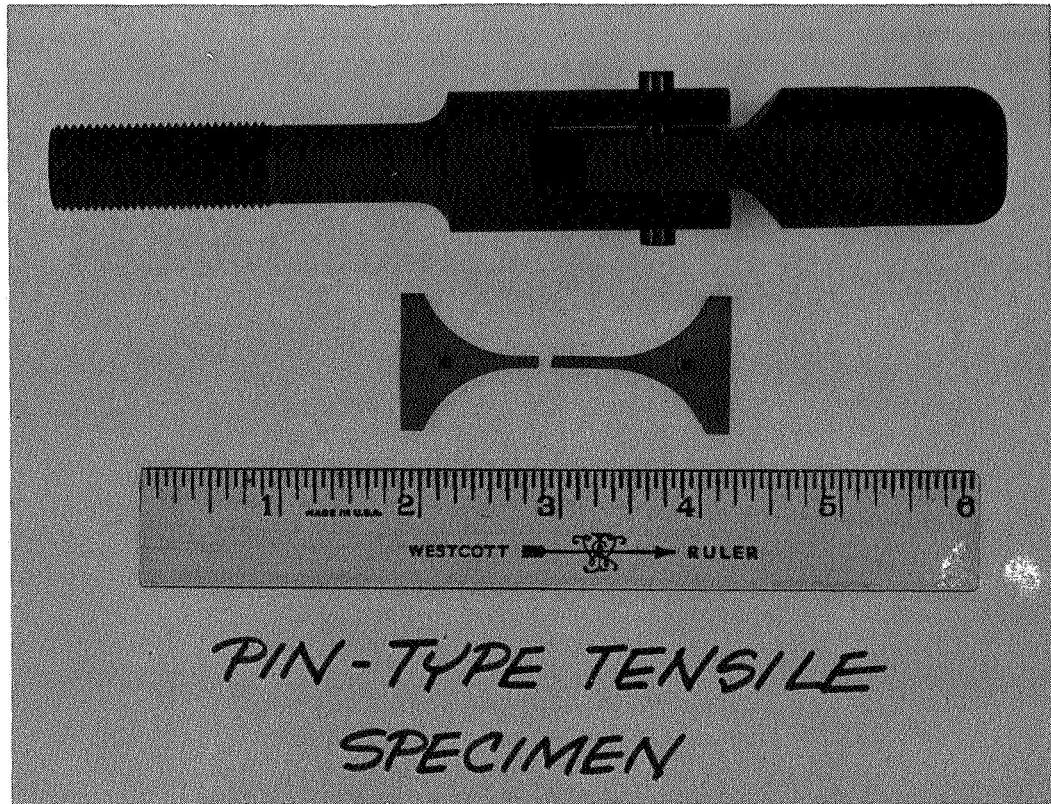
FIG. 8 - SPECIMEN CONFIGURATION
        FOR TENSILE TESTING

those of lower carbide content were machined by standard techniques. Testing of samples at high temperatures was conducted in a Brew 1064 testing furnace.

Each value in the mechanical property data represents an average of three or more determinations.

4. Electrical Properties

Electrical resistivity measurements were made on various samples to determine if any relationship existed between bonding and electrical properties. It was felt that the extent of diffusion of the more conductive carbide or eutectic would lower the electrical resistivity of the composite, and hence, improved bonding would be detected by these experiments. A four-terminal method was used to measure the resistivity. An apparatus constructed for this purpose is shown in Fig. 9. A constant current of 2 amps (CK18-2M Kepco power supply) was passed through the sample clamped between copper electrodes. The potential drop could be measured over a range of distances and positions on the sample by means of 9 tungsten probes positioned over the length of the sample. A Hewlett-Packard 425A-type microvoltmeter was employed for measuring voltage drops.

5. Thermal Expansion and Compressive Creep

Measurements were made of thermal expansion, thermal conductivity, and creep at elevated temperature. The cathetometric method of measuring sample expansion optically was used to determine thermal expansion behavior. Samples were heated in a graphite tube furnace under argon and taken through two cycles of room temperature to 2300°C.

Compressive creep behavior was evaluated in the graphite tube furnace. Sample deformation was monitored visually with a cathetometer. In most of these experiments, the changes were too small to be detected optically since the sensitivity limits
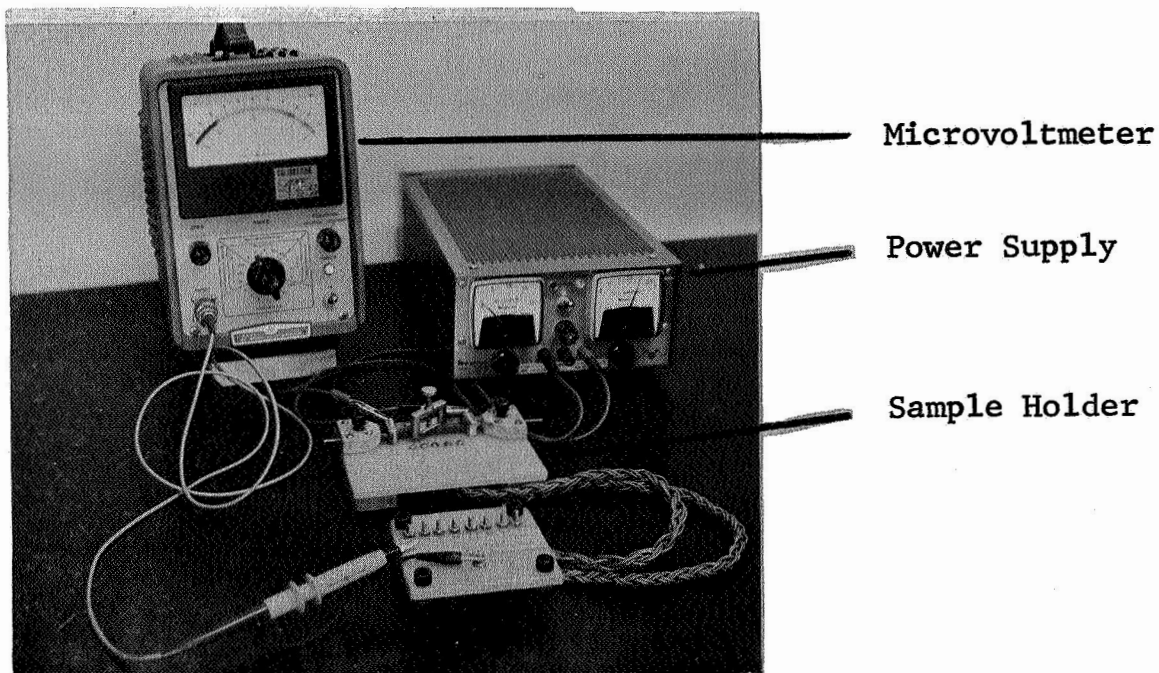
(a) Electrical Resistivity Apparatus
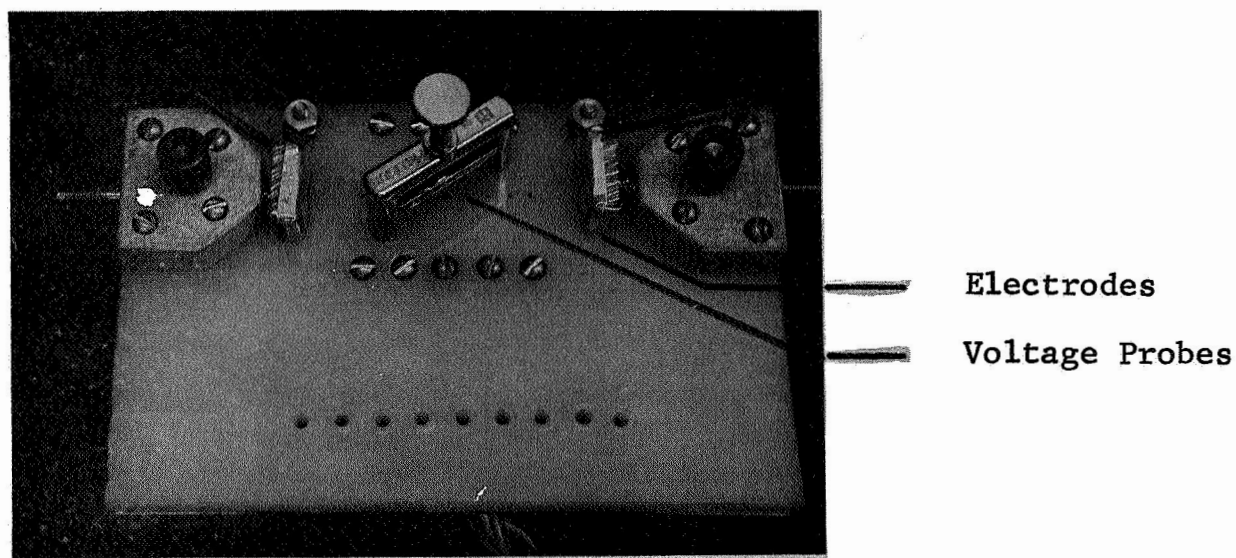
(b) Sample Holder

FIG. 9 - APPARATUS FOR MEASURING ELECTRICAL RESISTIVITY
OF METAL CARBIDE-GRAPHITE COMPOSITES

of the cathetometer was for a Δ of 0.5 to 0.8%. Samples were measured before and after each run.

6. Thermal Conductivity

Thermal conductivity was determined from approximately 100° to 750°C by the split block method and from 750° to approximately 2200°C by determining the thermal inertia and then calculating thermal conductivity from the measured values of thermal inertia, specific heat, and density.

The split block technique has the advantage of requiring a small quantity of test sample material; namely, a solid cylinder 1 in. in diameter by 1¼ in. long, which can also be used in the thermal inertia determinations. In this comparative method, the temperature drop through a material, having a well-known thermal conductivity, is compared to that through the unknown material. A vertical stack of three cylinders, two of which are Armco iron and the other, the test sample, are used (Fig. 10). Heat flows axially through the cylinders from the top of the stack to the bottom. The temperature gradient in both Armco iron standards and the test specimen are measured by thermocouples located in holes along the length of the stack. The stack of cylinders was placed inside an electrically heated furnace in which a helium atmosphere was maintained. Heaters located at the top and bottom of the cylinders are used to adjust the axial flow along the length of the assembly. A guard heater surrounds the cylinder to prevent radial heat losses.

The specimens were machined to the following dimensions; 1 in. in diameter by 1¼ in. long with both faces of the cylinder ground flat and parallel to reduce contact resistance to a minimum. Two 0.065 in. holes were drilled in the specimen; chromel-alumel thermocouple wires in alumina insulators were inserted in each hole. Three thermocouples were similarly installed in each of the Armco iron standards.

$X_A = 0.75$ in.

$X_B = 0.75$ in.

$X_A = 0.75$ in.

2 1/4

1 1/4

2 1/4

1 1/4 Dia.

Argon Outlet →

Bubbled Alumina Insulation

Molybdenum Heater Winding

Armco Iron Standard

Test Sample

Armco Iron Standard

Thermocouples

Water Cooled Furnace Shell

Argon Inlet
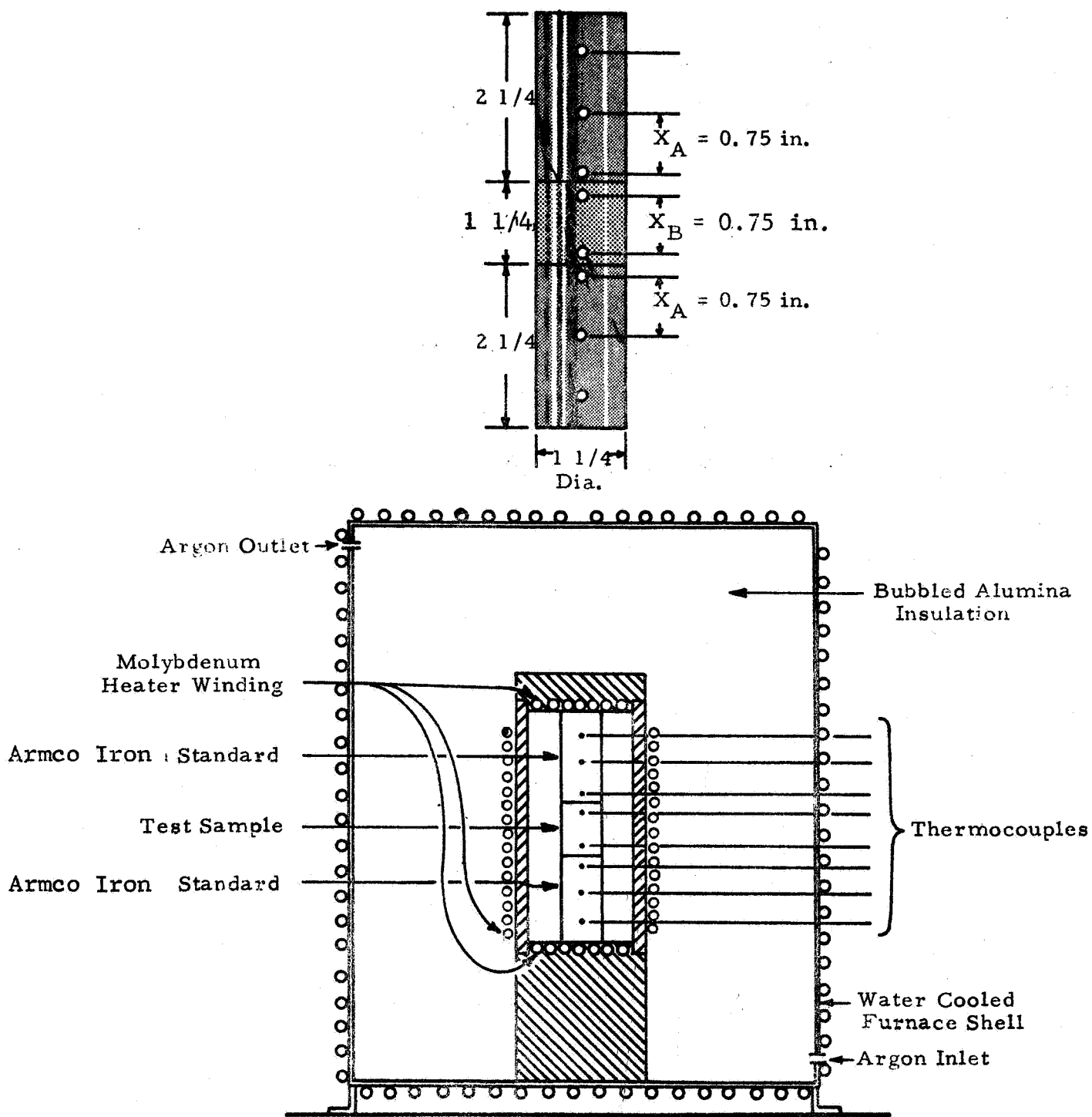
FIG. 10 - APPARATUS FOR MEASURING THERMAL CONDUCTIVITY

After steady-state conditions were reached at each desired temperature level, the thermocouple readings were recorded and the thermal conductivity was calculated as follows:

$$q = \frac{k \, A \, \Delta t}{\Delta x} \tag{1}$$

where q = heat flow, cal/sec

A = cross-sectional area, cm^2

Δt = temperature drop along the cylinder length, °C

k = thermal conductivity, cal/sec cm °C

Δx = distance between thermocouples, cm

By proper guarding, the heat flow through the Armco iron standards and sample are equal. Therefore, we can write:

$$q = \frac{k_a \, A_a \, \Delta t_a}{\Delta x_a} = \frac{k_b \, A_b \, \Delta t_b}{\Delta x_b} \tag{2}$$

where the subscripts a and b refer to the standards and test sample, respectively.

Solving for the thermal conductivity of the test sample, we have:

$$k_b = k_a \cdot \frac{A_a}{A_b} \cdot \frac{\Delta x_b}{\Delta x_a} \cdot \frac{\Delta t_a}{\Delta t_b} \tag{3}$$

Determinations of thermal conductivity of materials by the split block method and by the Powell stacked-disc method (an absolute method) compare very well. Errors in measurement may result from improper guarding which allows heat loss from the periphery of the cylinders or poor contact between cylinder faces which distorts the heat flow pattern. The accuracy of the experimental results obtained with this apparatus is within ±5%.

III. RESULTS AND DISCUSSION

The effect of metal carbide content upon physical, mechanical, thermal and electrical properties have been measured and the observed trends are presented. The results of a study

applying mixing law relationships for composite systems to metal carbide-graphite bodies are discussed.

Some work was conducted to determine the effect of variations in processing parameters on composite properties. Studies have also been conducted on the effect of heat treatment of samples subsequent to hot pressing.
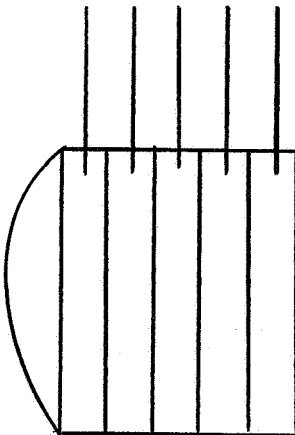
A.   Physical Properties

1.   Density

Initial evaluation of all composites has routinely included determination of density. These measurements reveal not only the extent of densification but also uniformity throughout the particular billet. In general, any variations in density among samples from any one billet have been due to differing carbide contents rather than to different degrees of densification. Such nonuniformity can occur when melting of the sample during hot pressing results in heterogeneous loss of carbide. A diagram of this type of body appears as Fig. 11.

Density, however, is not necessarily a true indication of bonding. It has been shown that composites which have similar metal carbide contents and have shown the same degree of densification can differ significantly in flexural strength. Stronger bonding results at higher processing temperatures due to enhanced diffusion and sintering. Some examples of materials which have shown this relationship appear in Table I.

The degree of densification varies as a function of carbide content for NbC-C composites. Shown in Fig. 12 is a plot of % theoretical density vs composition. Included in this graph are two calculated curves based on assumptions of 2.10 g/cc (92.9%) or 2.00 g/cc (88.5%) for the graphite phase and a 100% dense NbC phase. Obviously, these calculated points will approach theoretical density with increasing carbide content.

Bulk Density, g/cc	Metal Content, Wt% NbC	Theoretical Density, g/cc	% Theoretical Density
2.88	32.7	3.06	94.1
3.01	41.3	3.20	94.2
3.18	45.8	3.35	95.0
3.42	52.4	3.60	95.0
3.62	56.8	3.79	95.6

Sample: C-50Nb

FIG. 11 - NbC-C COMPOSITE SHOWING HETEROGENEITY IN METAL CONTENT AND BULK DENSITY BUT UNIFORMITY IN DEGREE OF DENSIFICATION

Table I

COMPARISON BETWEEN COMPOSITES WHICH EXHIBIT
SIMILARITY IN DEGREE OF DENSIFICATION BUT DIFFERENCE IN STRENGTH

Compositional Designation	Metal Carbide Content		Processing Temp., °C	%Theoretical Density	Flexural Strength psi (W/G)
	Wt%	Vol%			
50Nb	56.9	27.5	3000	92.6	6,100
50Nb-31	54.4	25.6	3100	92.7	14,530
65Ta-B	70.0	26.6	3200	96.6	7,090
65Ta-A	69.0	25.8	3300	97.0	19,160
C3-80Nb	90.0	72.5	2900	97.6	6,660
80Nb-C	90.3	74.4	3050	97.2	16,960
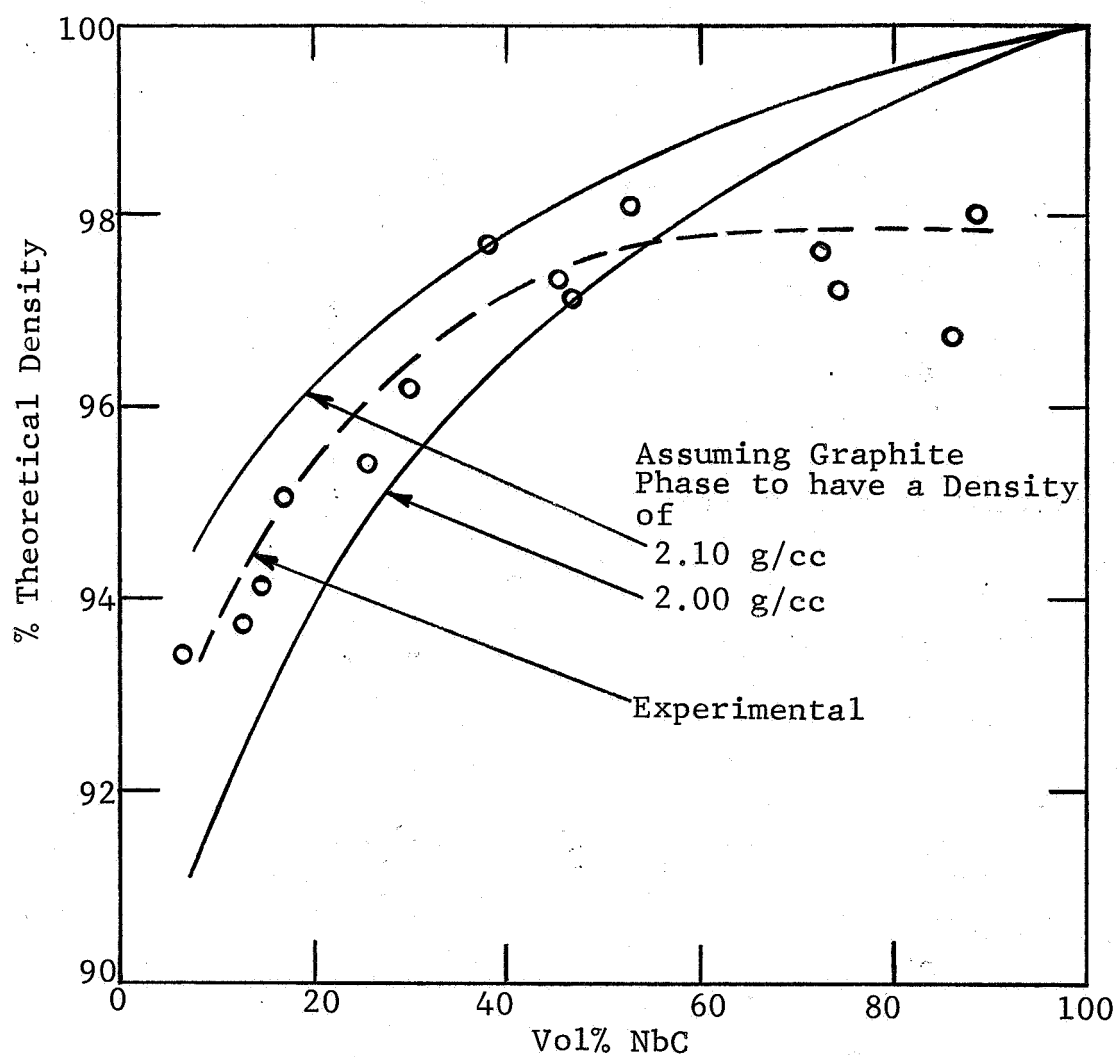
FIG. 12 - DEGREE OF DENSIFICATION AS
A FUNCTION OF CARBIDE CONTENT
FOR NbC-C COMPOSITES

The experimental points in the graphite-rich portion of the diagram suggests a graphite density of about 2.05 g/cc. This curve parallels the calculated curves up to about 50 vol% NbC. At this point a leveling off of the curve occurs and a plateau appears to exist for the carbide matrix composites. This indicates that at these higher carbide levels the graphite phase has a density lower than 2.0 g/cc and/or that the NbC particles are somewhat porous. The former situation may occur in carbide matrix composites in that the carbide may restrict plastic deformation and graphitization of the graphite. The presence of pores in carbide grains has been observed to a very limited extent in metallographic studies of higher carbide content composites.

It would thus appear that a potential exists for producing denser and stronger composites with greater than 50 vol% NbC. This may be accomplished through the use of slightly higher processing temperatures or hot working of bodies. This process may be complicated somewhat by the practical limitations of loss of material through melting. A similar type of % theoretical density vs carbide content curve appears to exist for the TaC-C system.

2. Microstructure

Metallographic examination has been established as a standard procedure in the evaluation of composites. This analysis was used to determine the shape, size and dispersion of particles. Grain directionality and porosity can also be established. Typical microstructures of NbC-C composites with varying carbide contents are shown in Figs. 13 and 14.

In the various bodies, directionality in carbide and graphite phases can be seen in the W/G direction. In the two metallographic photos taken in the A/G direction (Figs. 13d and 14d), such grain oreintation is not seen. These two photographs

50μ
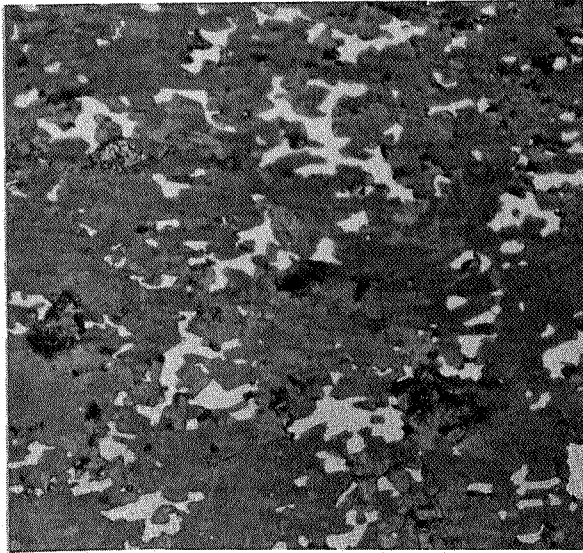
(a) "50Nb-S" (W/G)
    15 vol% NbC
    Added as Metal
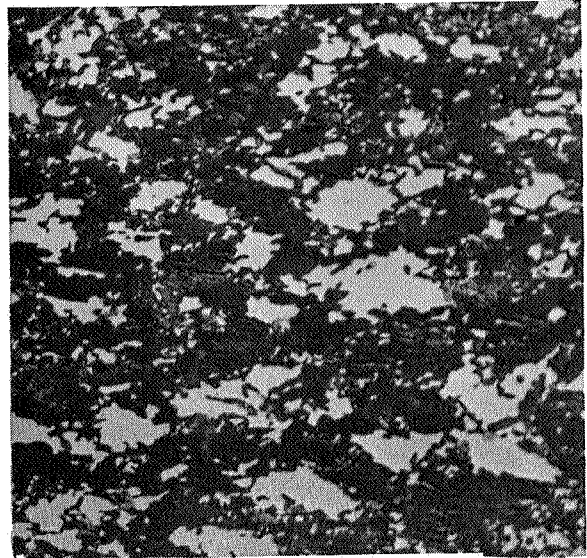
(b) "50Nb-31" (W/G)
    27 vol% NbC
    Added as Metal
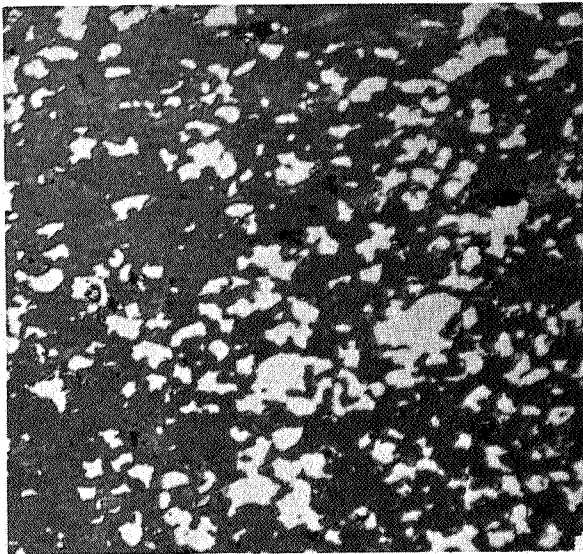
(c) "C-50Nb" (W/G)
    27 vol% NbC
    Added as Carbide
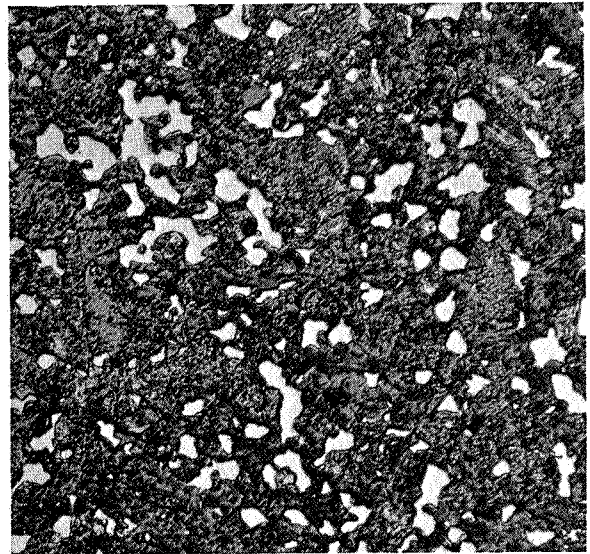
(d) "C-50Nb" (A/G)
    27 vol% NbC
    Added as Carbide

FIG. 13 - TYPICAL MICROSTRUCTURES OF NbC-C COMPOSITES
         CONTAINING LESS THAN 50 VOL% NbC (320x)

$\vdash$ ─── $\dashv$ 50μ
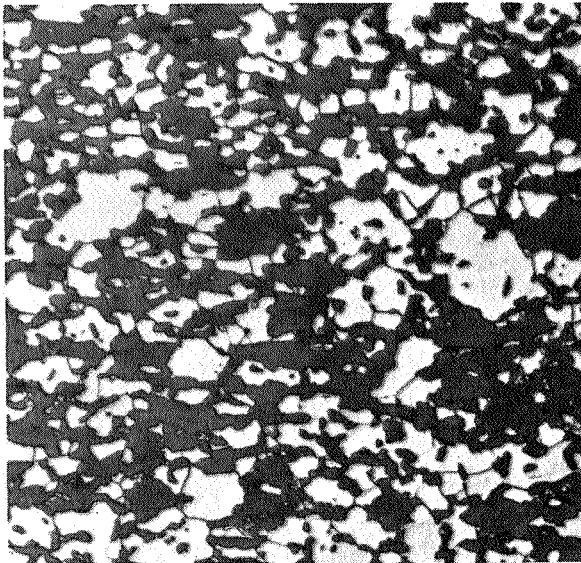
(a) "C2-70Nb" (W/G)
    52 vol% NbC
    Added as Carbide
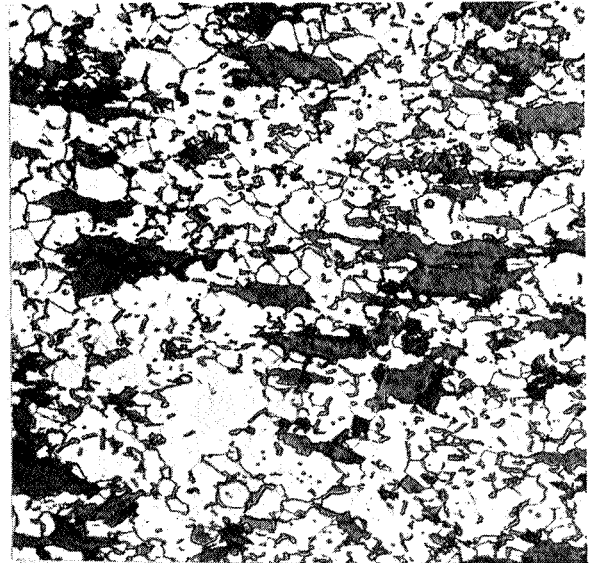
(b) "C3-80Nb" (W/G)
    73 vol% NbC
    Added as Carbide
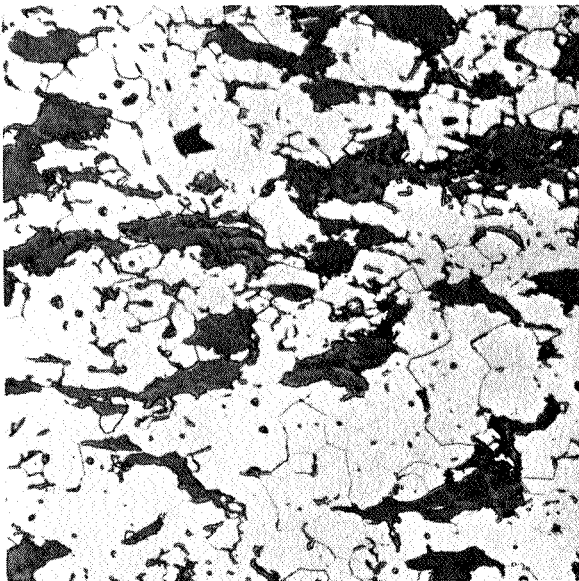
(c) "80Nb-C" (W/G)
    73 vol% NbC
    Added as Metal
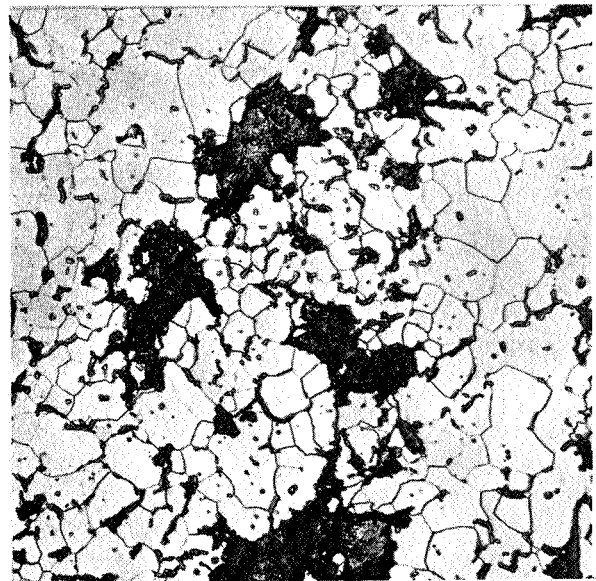
(d) "80Nb-C" (A/G)
    73 vol% NbC
    Added as Metal

FIG. 14 – TYPICAL MICROSTRUCTURES OF NbC-C COMPOSITES
CONTAINING GREATER THAN 50 VOL% NbC (320x)

also show that the graphite is much more susceptible to lamellar pullouts when polished in the A/G direction.

A comparison can be made between composites with the same carbide content but with NbC particles of different grain size. As mentioned earlier in this report, NbC powder had a particle size of about 3.6μ whereas the metal powder was considerably coarser (9.8μ). A more unform dispersion of phases is apparent in "C-50Nb" and "C3-80Nb" (Figs. 13c and 14b) as compared to their compositional counterparts, "50Nb-31" and "80Nb-C" (Figs. 13b and 14c). The superior homogeneity obtained using the carbide raw material as opposed to the metal, generally produced a slightly higher strength composite.

Microstructural studies also showed if melting had occurred during processing. In high carbide content materials, this was quite apparent in that a eutectic structure was formed. In low carbide content composites, melting and recrystallization resulted in carbide particles which were greatly diminished in size and showed little preferred orientation. An example of this can be seen in Fig. 13a.

Presented in Figs. 15 and 16 are the microstructures of TaC-C composites of varying TaC content. Directionality in grain direction is quite evident for all of these materials. There was no evidence of melting in all but one of the various TaC-C pressings. This would appear reasonable in that the eutectic temperature of 3450°C is considerably higher than the normal 3200° to 3250°C processing temperatures for TaC-C composites.

Composites which had carbide contents of 50 vol% or less usually appeared somewhat porous as typified by the 26 vol% TaC-C and 53 vol% TaC-C bodies (Figs. 15a and 15b). However, these bodies exhibited strengths which were comparable to NbC-C composites of similar carbide concentration. At the higher carbide contents, the graphite phase generally appeared quite dense.
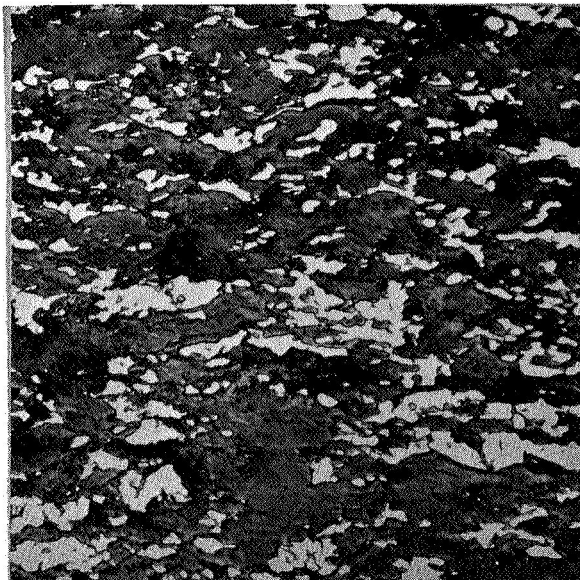
(a) "65Ta-B"
    26 vol% TaC
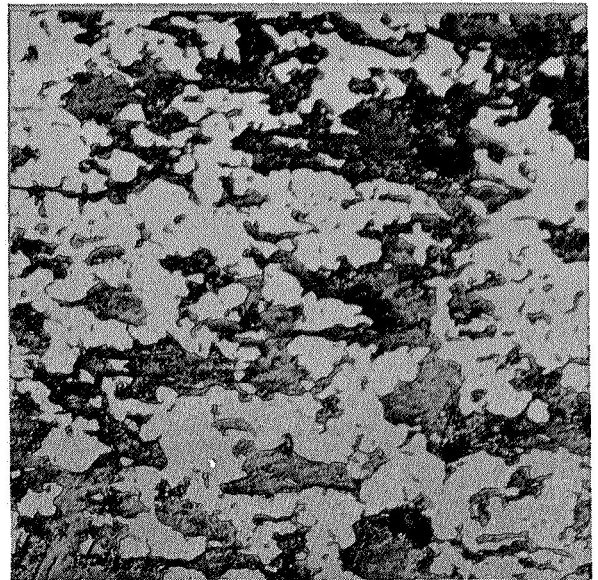
(b) "82.5Ta-A"
    53 vol% TaC
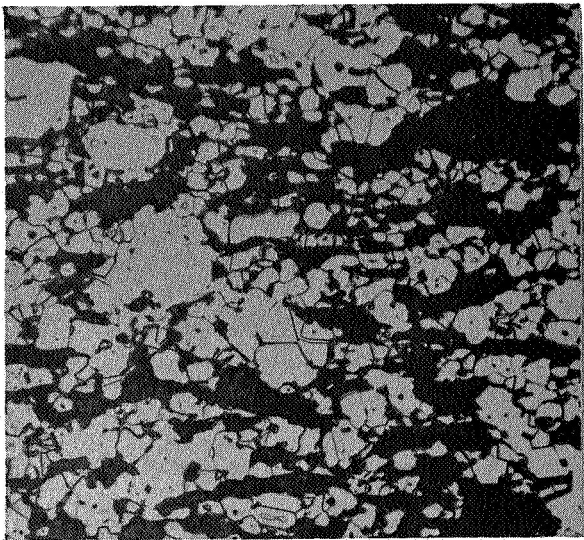
(c) "85Ta"
    61 vol% TaC
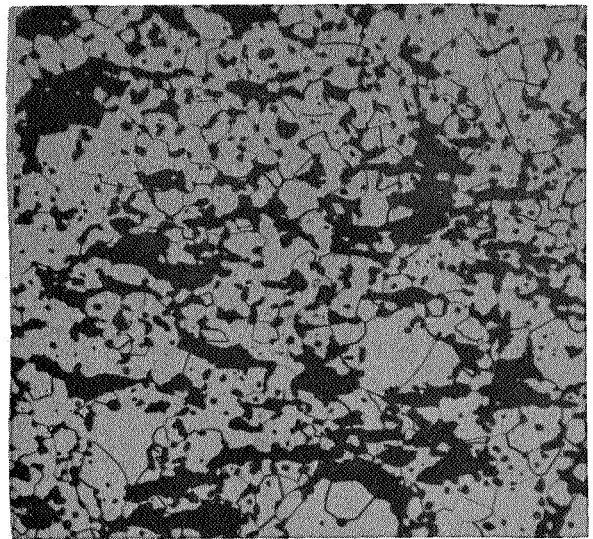
(d) "88Ta"
    71 vol% TaC

FIG. 15 - MICROSTRUCTURES OF TaC-C COMPOSITES
IN THE W/G DIRECTION (320x)

$\vdash \overline{50\mu} \dashv$
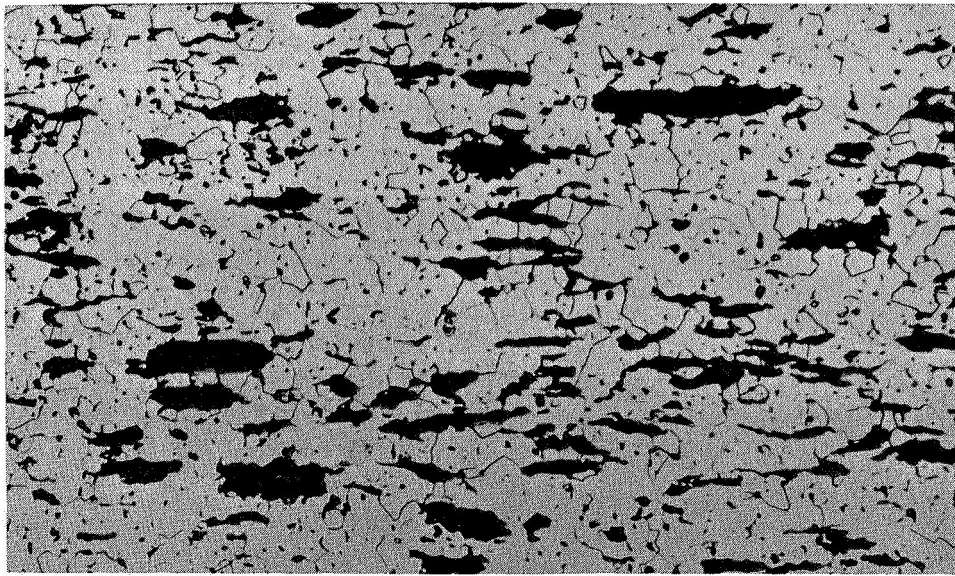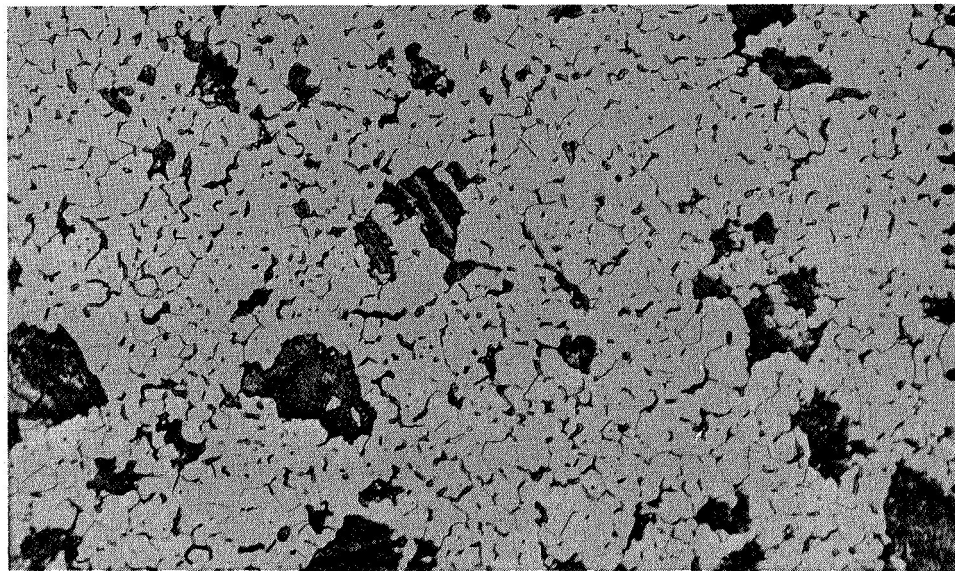
(a) W/G Direction

(b) A/G Direction

FIG. 16 - MICROSTRUCTURE OF 80 VOL% TaC-C COMPOSITE
SHOWING GRAIN ORIENTATION (320x)

As described later, mechanical strength tests showed that these materials were quite strong, indicating good sintering of the carbide matrix.

B. Mechanical Properties

1. Flexural Evaluations

The property of composites which has received the greatest attention is flexural strength. This has been predicated on the ease of fabricating a sample specimen shape and on the speed and simplicity of the test. A rapid screening of both room and high temperature behavior is thus accomplished.

a. NbC-C System

Room Temperature Evaluations - A plot of flexural strength as a function of carbide content for NbC-C composites is presented in Fig. 17. Strengths in the W/G direction exhibit a linear relationship. The assumption of linearity was examined using the statistical method of regression analysis. A correlation coefficient of 0.87 suggests that this assumption is valid.

In the A/G direction a nonlinear relationship exists. As the carbide becomes the dominant phase, the influence of the anisotropic behavior of graphite diminishes. The trend toward isotropic behavior with increasing carbide content is graphically illustrated in Fig. 18.

Flexural modulus of elasticity appears to increase in a nonlinear fashion as a function of carbide content as shown in Fig. 19. These curves show the dominance of low modulus graphite $(2.72 \times 10^6$ psi for ZTA or hot worked graphite)[6] at carbide contents below 50 vol%. As the carbide becomes the matrix, the relatively high modulus of NbC $(49 \times 10^6$ psi)[7] is reflected in the increasing slope of the curve.

IIT RESEARCH INSTITUTE

-33-
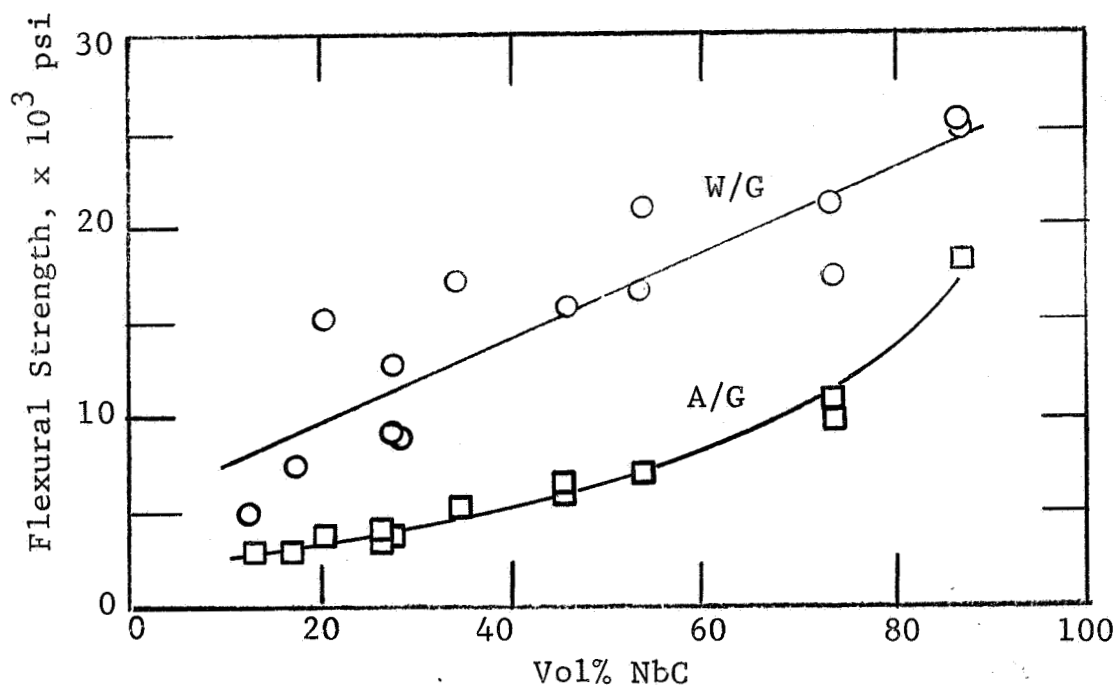
FIG. 17 - FLEXURAL STRENGTH AS A FUNCTION OF CARBIDE CONTENT FOR NbC-C COMPOSITES
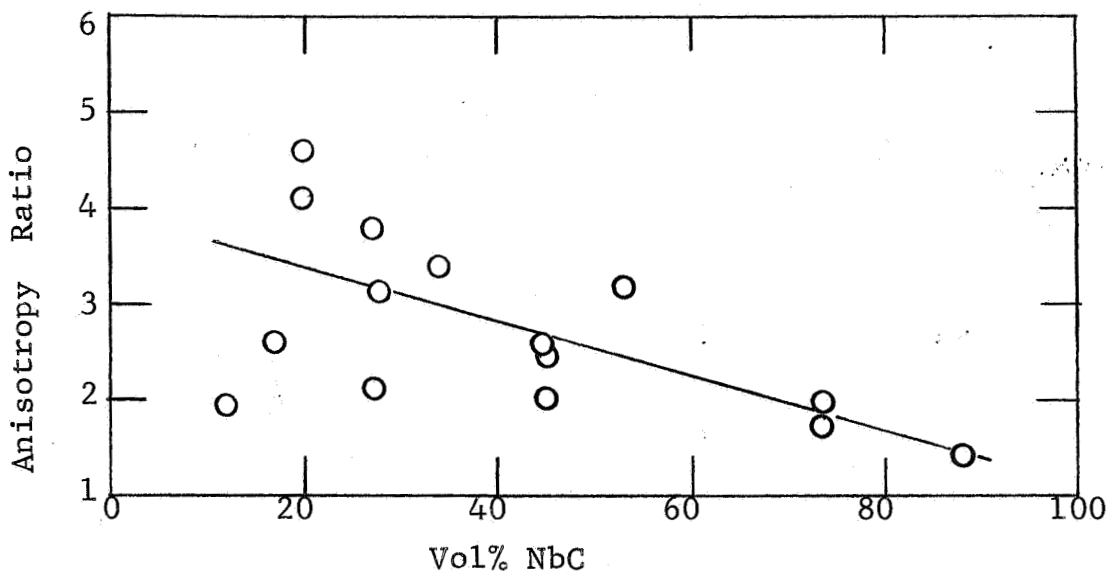
FIG. 18 - ANISOTROPY RATIO OF W/G TO A/G
FLEXURAL STRENGTH AS A FUNCTION
OF CARBIDE CONTENT FOR NbC-C
COMPOSITES

FIG. 19 - ELASTIC MODULUS IN FLEXURE AS A
FUNCTION OF CARBIDE CONTENT FOR
NbC-C COMPOSITES

The nonlinear relationship of flexural modulus with carbide content in the W/G direction contrasts with the linearity observed for flexural strength. Similar nonlinear trends for both E and σ as a function of porosity have been reported for Al_2O_3.[8]

High-Temperature Evaluations - All of the NbC-C composites exhibited higher strengths at 2000°C (Fig. 20). This increase in strength with temperature is similar to the behavior of graphite, and contrasts with the decrease in strength with temperature reported for pure NbC.[7] This behavior at 2000°C may be due to relief of residual stresses which are present in composites at room temperature.

At 2500°C, all samples tested in flexure displayed permanent deformation to varying extents. With one exception, the strengths at 2500°C were all lower than that of 2000°C. The exception was a composite containing only 12 vol% NbC which exhibited a peak strength at 2500°C. Apparently the carbide content in this material is low enough so that this composite behaves like pure graphite which has a peak strength at about this temperature.[9]

The 12 vol% NbC-C composite was the only material which could be loaded to failure at 2800°C. Composites incorporating higher amounts of NbC deformed plastically, and tests were terminated when the lower surfaces of the test samples made contact with the graphite boat (a distance of 3/16 in.) which supported the support pins and sample.

Of particular interest was flexural strength tests of pure NbC at 2000°C. Two samples which were tested are shown in Fig. 21. Specimen 6AT was loaded to a stress of over 29,000 psi which is the maximum for the equipment. The other sample, 1BT, was stressed initially to over 27,000 psi. This load was released
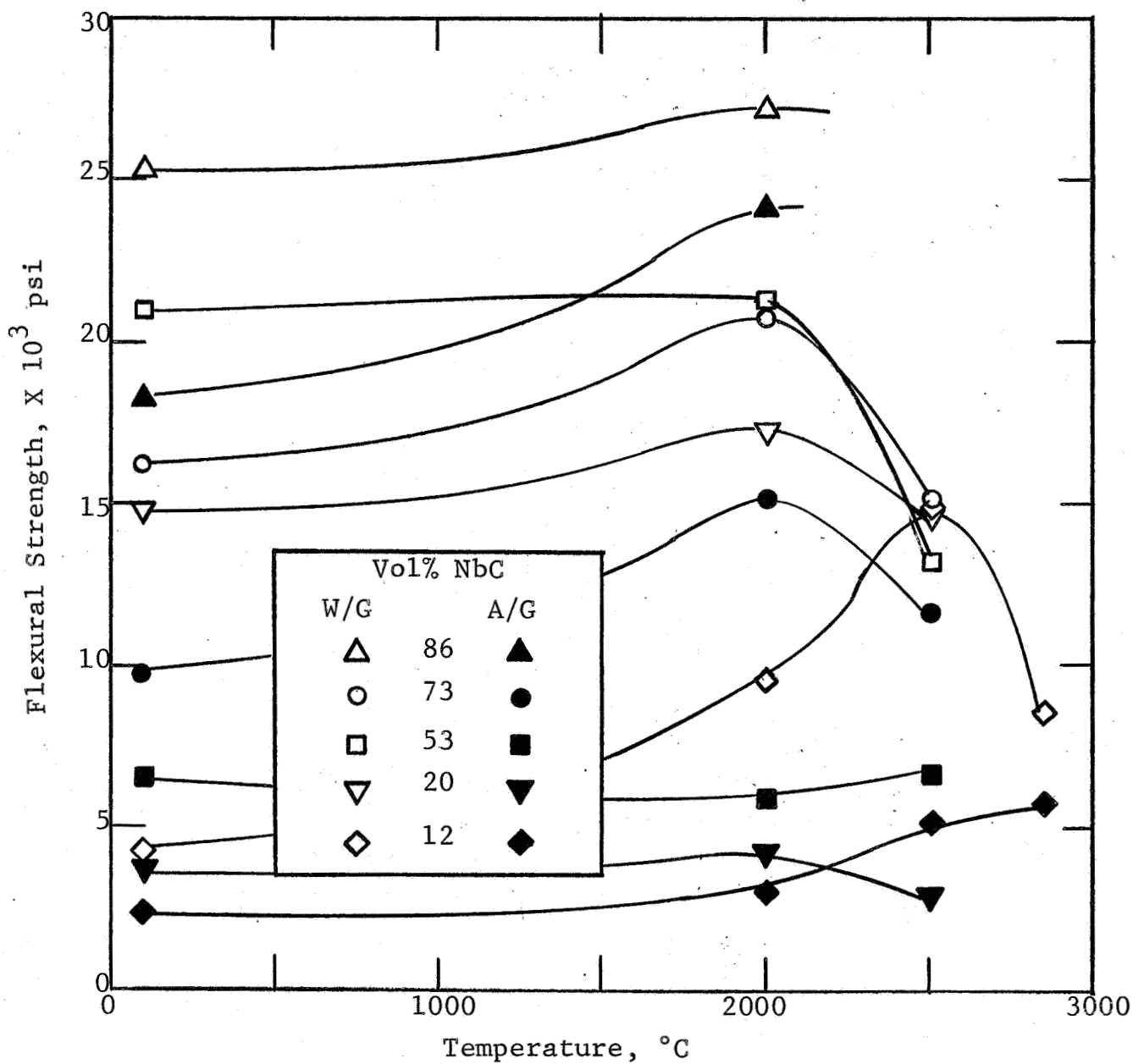
FIG. 20 - FLEXURAL STRENGTH AS A FUNCTION OF
TEMPERATURE FOR NbC-C COMPOSITES
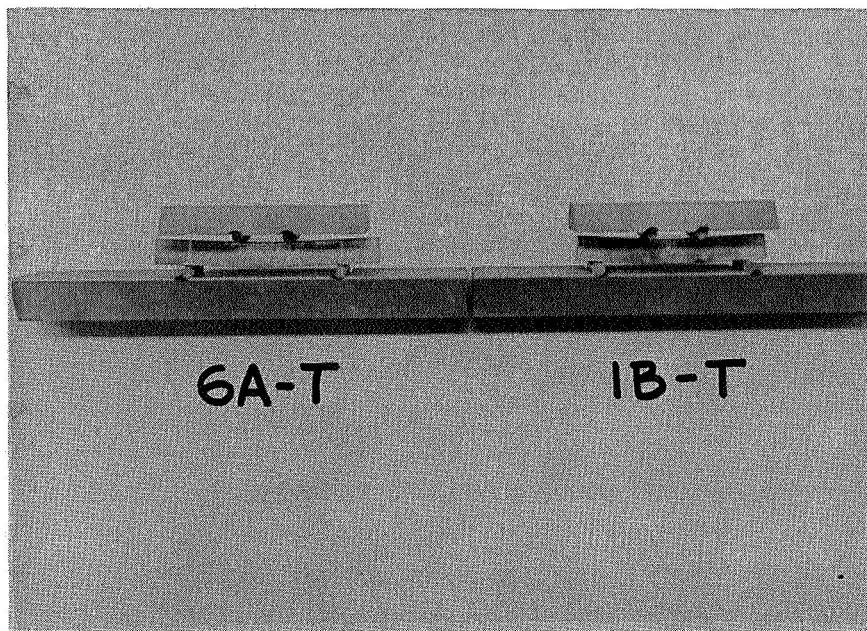
FIG. 21 - FLEXURAL TEST SPECIMENS OF PURE
NbC EVALUATED AT 2000°C

and then reapplied, and at a stress of 26,710 psi, failure occurred for both the sample and the support boat.

Both samples show some plastic deformation as seen in Fig. 21. However, neither has deformed enough to make contact with the support boat. The present information contrasts sharply with a 2000°C bending strength of 2,800 psi reported in the literature.[7]

Measurements were made to determine elastic modulus in flexure at elevated temperatures. A series of NbC-C composites were loaded to 12,000 psi in 2000 psi increments at 2000°C. Deflection was monitored visually using cathetometric techniques. The times involved at each stress level were about 30 sec. Plots of stress-strain are presented in Fig. 21, and modulus values are tabulated in Table II.

Permanent deformation occurred in all samples during testing. Separation of the plastic component from the elastic component could not be made. However, certain trends were observed in these experiments. The curves in Fig. 22 show that deflection under load was highest for the graphite matrix composite, and a decrease in deflection exists with increasing carbide content. Permanent deformation after removal of load exhibits a similar trend with carbide content.

Modulus values were calculated using deflections observed at 2000 psi for tangent E and at full load for secant E. Table II shows this data. The nonlinear behavior of the material at high temperature is clearly reflected in the lower values for secant moduli compared to the tangent moduli.

In Fig. 23, stress-strain plots are plotted for experiments conducted at 2500°C. The data here show that lower elastic moduli exist for the 52 vol% NbC-C and for pure NbC. Thus the inverse relationship between deflection and carbide content

Table II

MODULUS OF ELASTICITY IN FLEXURE AS A
FUNCTION OF TEMPERATURE FOR NbC-C COMPOSITES

Compositional Designation	Vol% NbC	Modulus of Elasticity, $E \times 10^6$ psi				
		Room Temp	2000°C		2500°C	
			Tangent	Secant	Tangent	Secant
C-40Nb	17	5.0	4.6	2.8	2.1	1.5
C2-70Nb	52	13.6	5.8	4.9	2.4	0.8
80Nb-C	73	24.8	12.9	5.1		
85Nb-A	86	28.8	11.4	9.4	7.3	2.3
88-6Nb	100	53.2	21.7	11.7	7.1	0.8
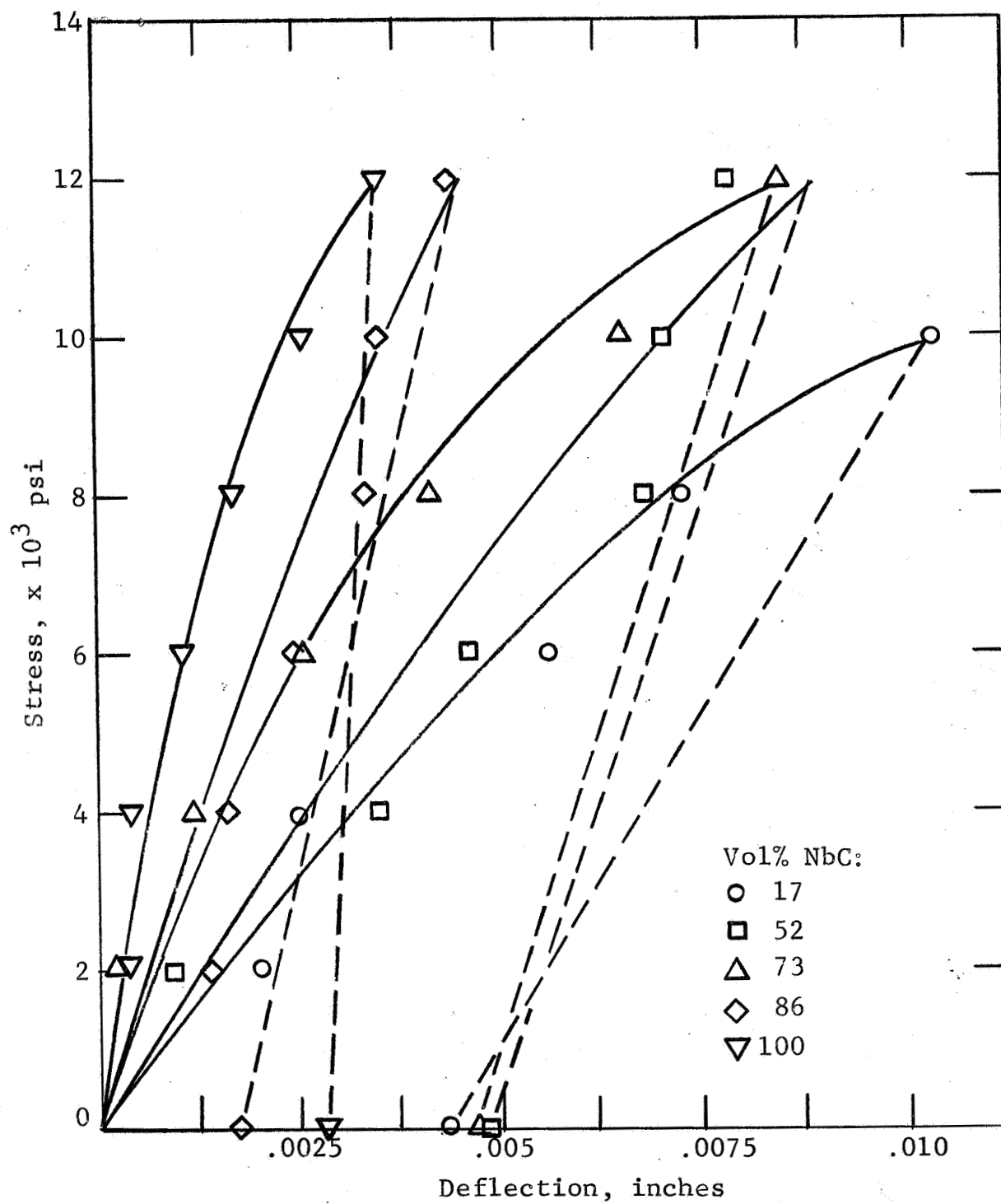
FIG. 22 - STRESS - DEFLECTION CURVES FOR NbC-C
COMPOSITES TESTED IN FLEXURE AT 2000°C
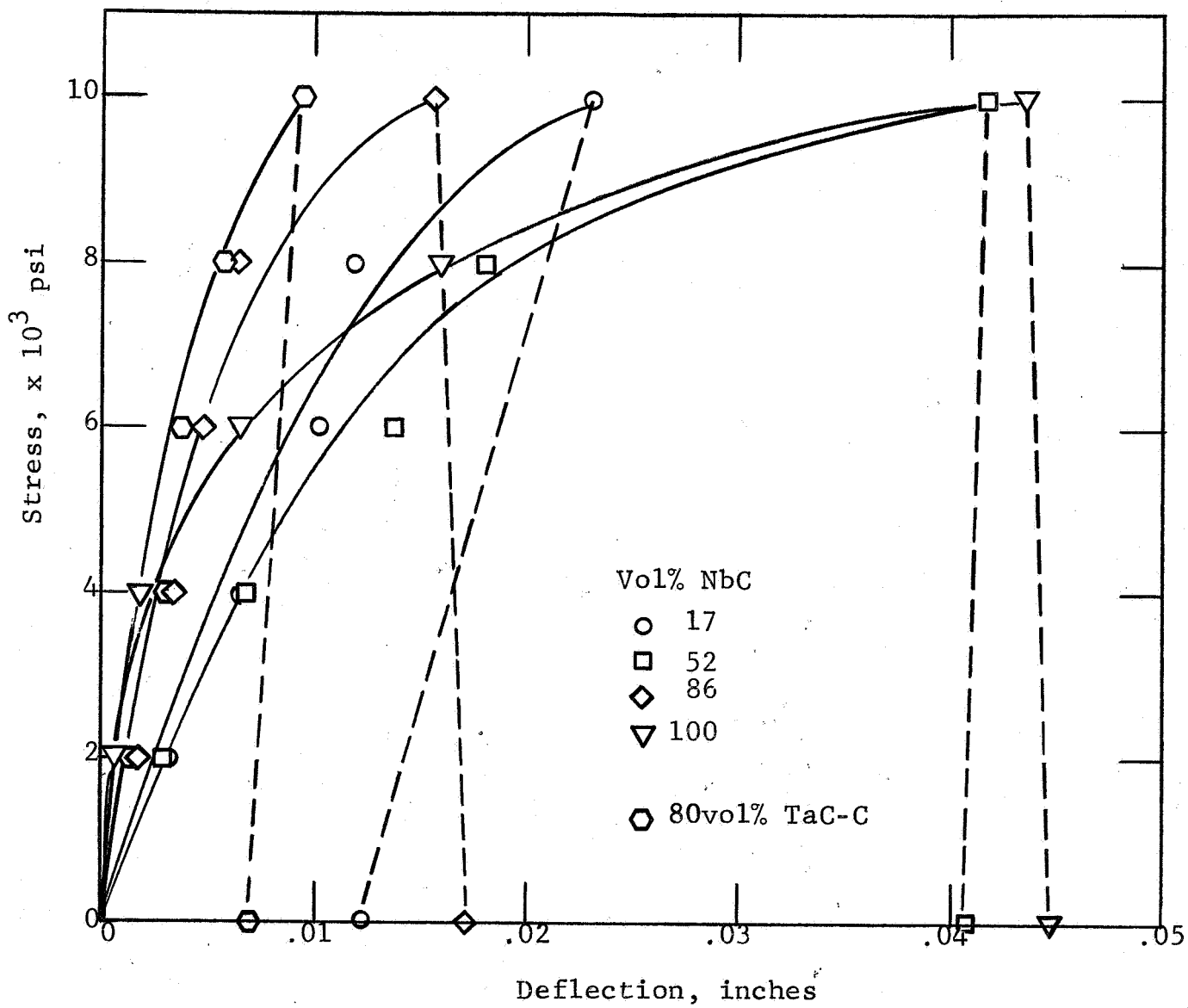
FIG. 23 STRESS - DEFLECTION CURVES FOR NbC-C
COMPOSITES TESTED IN FLEXURE AT 2500°C

observed at 2000°C no longer appears to hold. The moduli values in Table II also show the significant plasticity encountered at 2500°C.

Pure NbC displayed the smallest deflection at 2000°C and the highest at 2500°C. Apparently the plastic behavior becomes severe somewhere in the range 2000° to 2500°C under these flexural stresses. The significant deflection observed for composites containing about 50 vol% NbC may be due to the structure in which continuity of either phase is minimal. The carbide-carbon bond is probably not as strong as the carbide-carbide or carbon-carbon bond. It is possible that differential thermal expansion may cause weakening of the carbide-carbon bond at 2500°C leading to a condition which would be susceptible to high deformation.

When the strong plasticity of pure NbC is considered, the relatively small deflection observed for composites containing carbide contents of 70 to 85 vol% appears somewhat unusual. It is possible that the graphite in these composites act as inhibitors to dislocation movement.

These experiments, of course, are quite preliminary and much more experimentation is needed to establish compositional trends and mechanisms of behavior. Creep has several contributing factors and the existence of two phases in our composites makes analysis even more complex. Future experiments will be conducted for longer periods of time at temperature in attempts to determine secondary and tertiary creep stages as well as the primary.

b.   TaC-C System

Room-Temperature Evaluations - Room-temperature flexural strengths for TaC-C composites are similar to those for NbC-C composites, both in magnitude and in strength - carbide content relationships as shown in Fig. 24. The W/G strengths indicate a linear relationship, and the A/G strengths, a nonlinear relationship.

IIT RESEARCH INSTITUTE

-43-
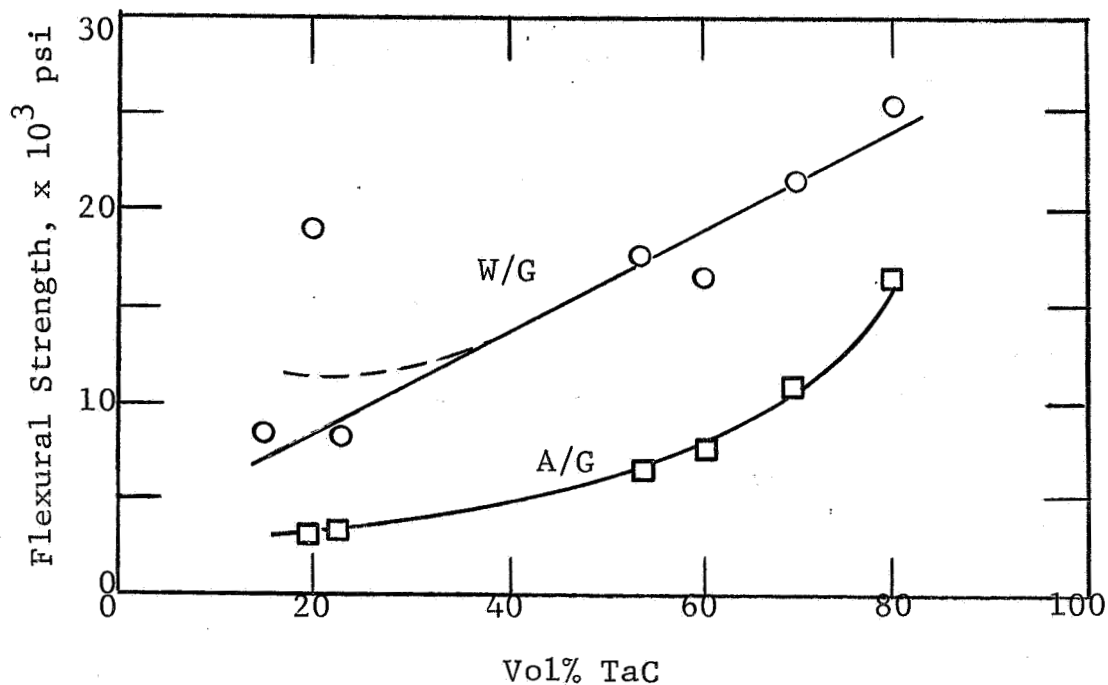
FIG. 24 - FLEXURAL STRENGTH AS A FUNCTION
OF CARBIDE CONTENT FOR TaC-C COMPOSITES
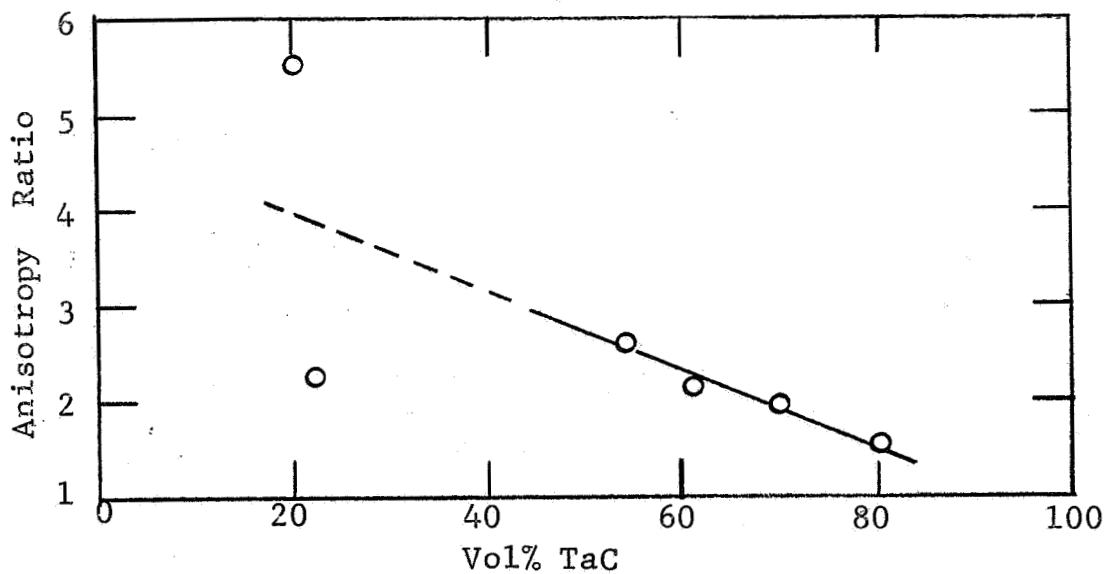
FIG. 25 - ANISOTROPY RATIO OF W/G TO A/G
FLEXURAL STRENGTH AS A FUNCTION
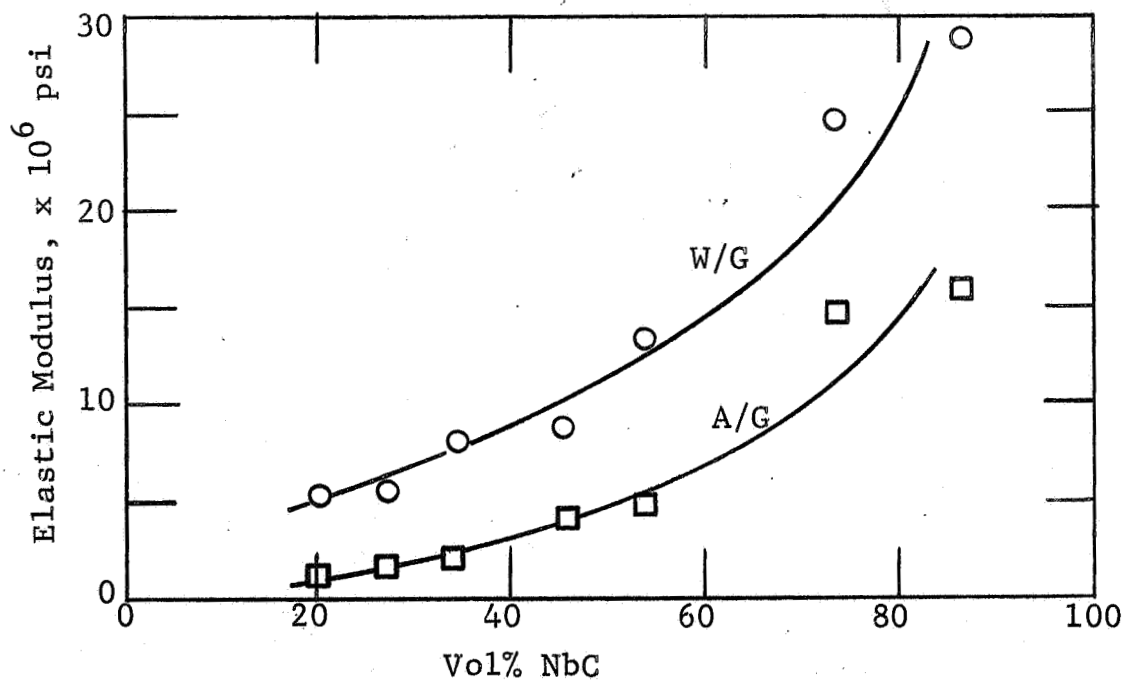OF CARBIDE CONTENT FOR TaC-C
COMPOSITES

The data point of 19,000 psi at 20 vol% TaC is a real one, and represents the only TaC-C composite which appeared to have reached the 3450°C solidus. This billet showed reaction with the mold and loss of material, indicating melting has occurred. The high strength can be attributed to high degree of graphite orientation and to liquid phase diffusion and sintering which undoubtedly occurred.

The lower strengths observed for graphite matrix bodies are representative of the results of a 3250°C processing temperature. It is evident that higher processing temperatures approaching 3450°C result in greatly improved bonding. However, such high temperatures are extremely difficult to predict and control, and the bulk of the TaC-C composites were fabricated at 3250°C.

The approach toward isotropic behavior with increasing carbide content is presented in Fig. 25. The trend at the higher carbide contents is quite clear, whereas the data for graphite matrix composites is strongly influenced by the processing temperature used. It would appear that as the carbide becomes the matrix, sintering of the carbide phase occurs and strength is no longer solely dependent on the carbide-carbon diffusion or extent of graphitization. At the 20 vol% TaC level, the anisotropy ratio of 5.5 is for a well-bonded composite having W/G and A/G strengths of 19,000 and 3430 psi, and the 2.3 ratio is for a material prepared at lower temperatures having strengths of 7080 psi (W/G) and 3340 psi (A/G). The increase in W/G strength at higher processing temperatures without an accompanying increase in A/G strength may be attributed to increased ordering and graphitization of the graphite matrix, which can result in lower A/G strength. An example can be seen with highly ordered pyrolytic graphite which has high W/G strength (25,000 psi) but low A/G strength (1500 psi).

Room-temperature moduli values are similar to those for NbC-C as shown in Fig. 26. At the higher carbide contents a sharp increase in modulus is indicated. This can be expected since the carbides display moduli which are at least an order of magnitude higher than that for graphite.

High-Temperature Evaluations - The high-temperature strengths of TaC-C composites followed a trend like that for NbC-C bodies. As shown in Fig. 27, a peak in strength occurs at 2000°C and lower strengths are observed at higher temperatures. In both systems, it is interesting to note that even the high carbide materials, in which the carbide is the dominant phase, showed increased strength at 2000°C. The 2000°C strength of pure TaC is listed as 17,000 psi by Shaffer[7] and also by Johansen.[10] This value is almost doubled by the 80 vol% TaC composite, and may be due to the graphite acting as crack stoppers.

It was evident in the tests at 2500° and 2800°C that TaC-C composites were less susceptible to plastic deformation than were the NbC-C. Most of the TaC-C composites could be stressed to failure at 2800°C without "bottoming" of specimens on the support boat whereas in the NbC-C system, enough plastic deformation occurred to permit contact between the bottom of the sample and the support boat.

c.   ZrC-C System

During this year's program, a limited amount of study was devoted to composites containing ZrC. Over the range of compositions evaluated, a linear relationship is indicated for both W/G and A/G strengths as a function of ZrC content (Fig. 28). It is possible that composites of higher carbide content may show a greater increase in A/G strengths, based on the nonlinear relationship observed for the TaC-C and NbC-C systems.
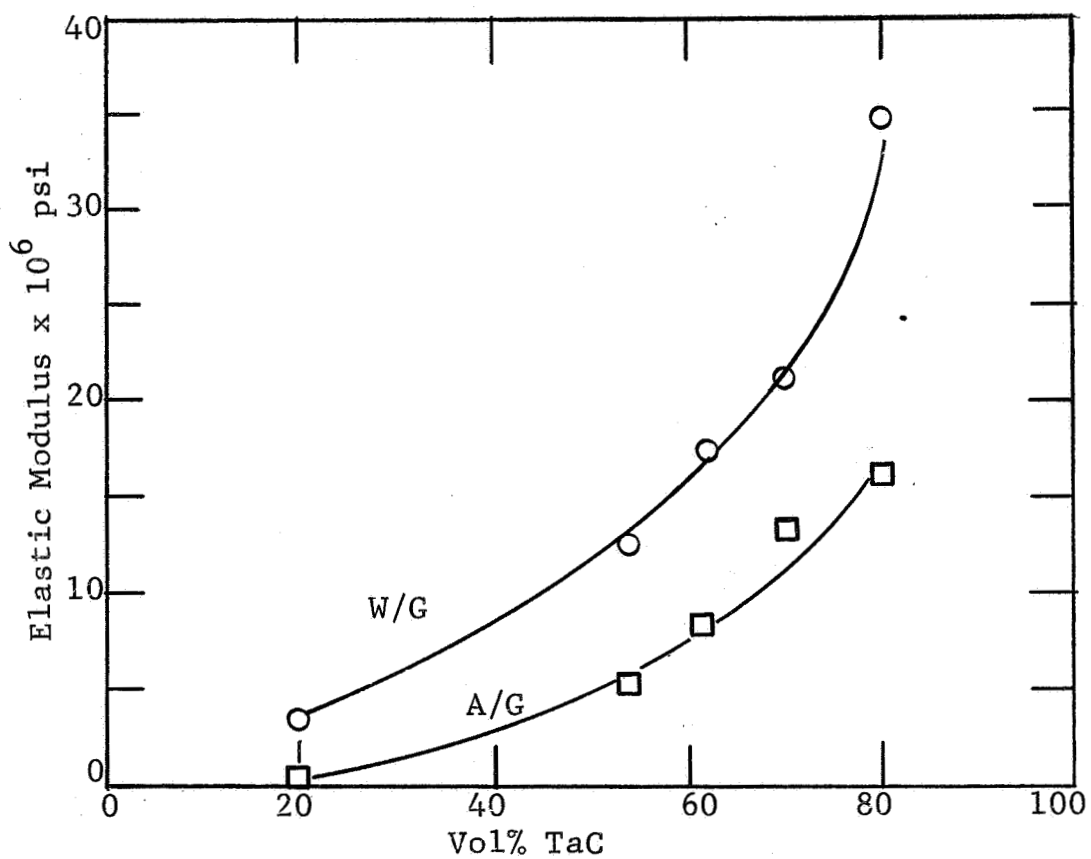
FIG. 26 -- ELASTIC MODULUS IN FLEXURE AS A FUNCTION
OF CARBIDE CONTENT FOR TaC-C COMPOSITES
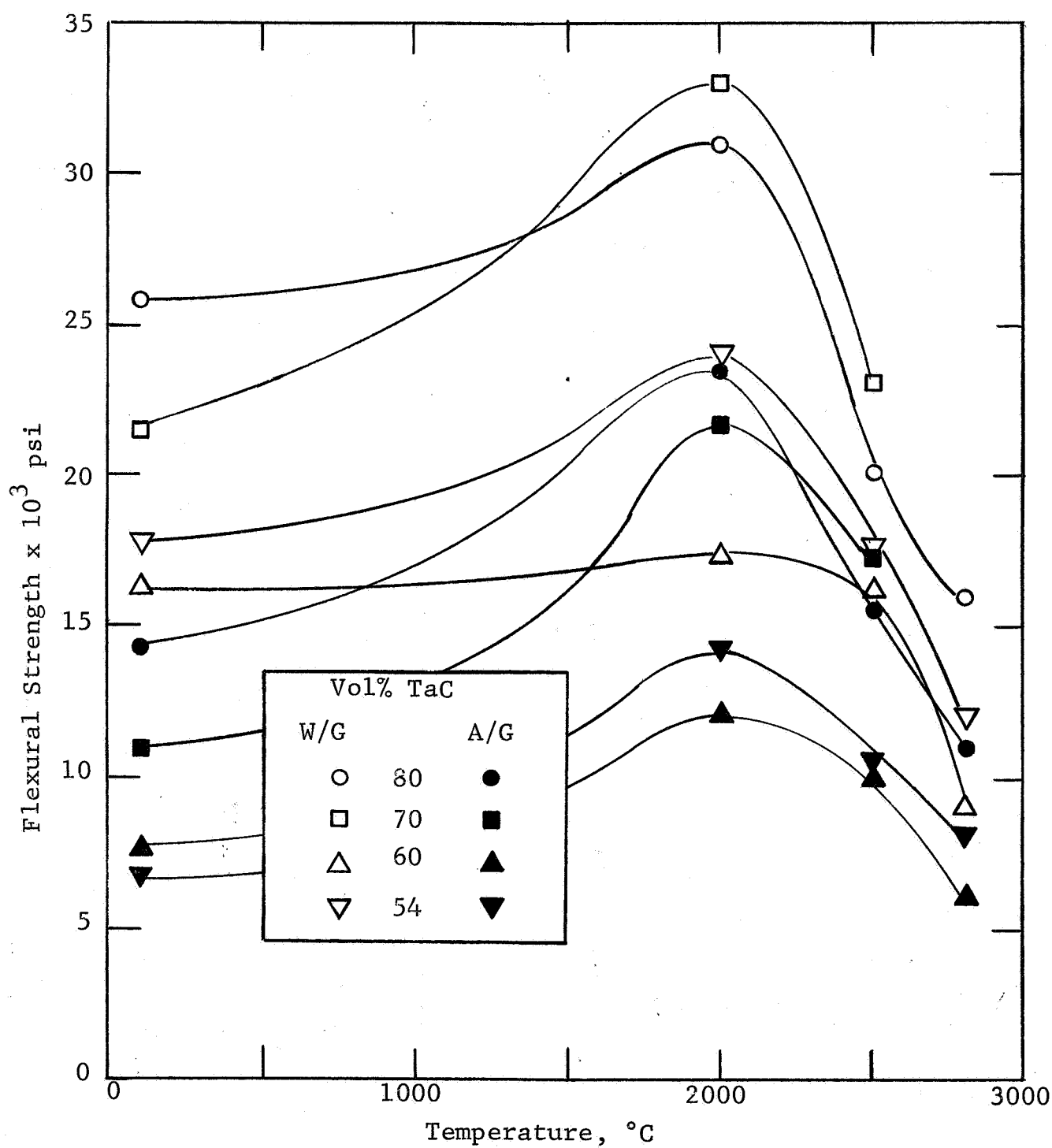
FIG. 27 - FLEXURAL STRENGTH AS A FUNCTION OF
TEMPERATURE FOR TaC-C COMPOSITES
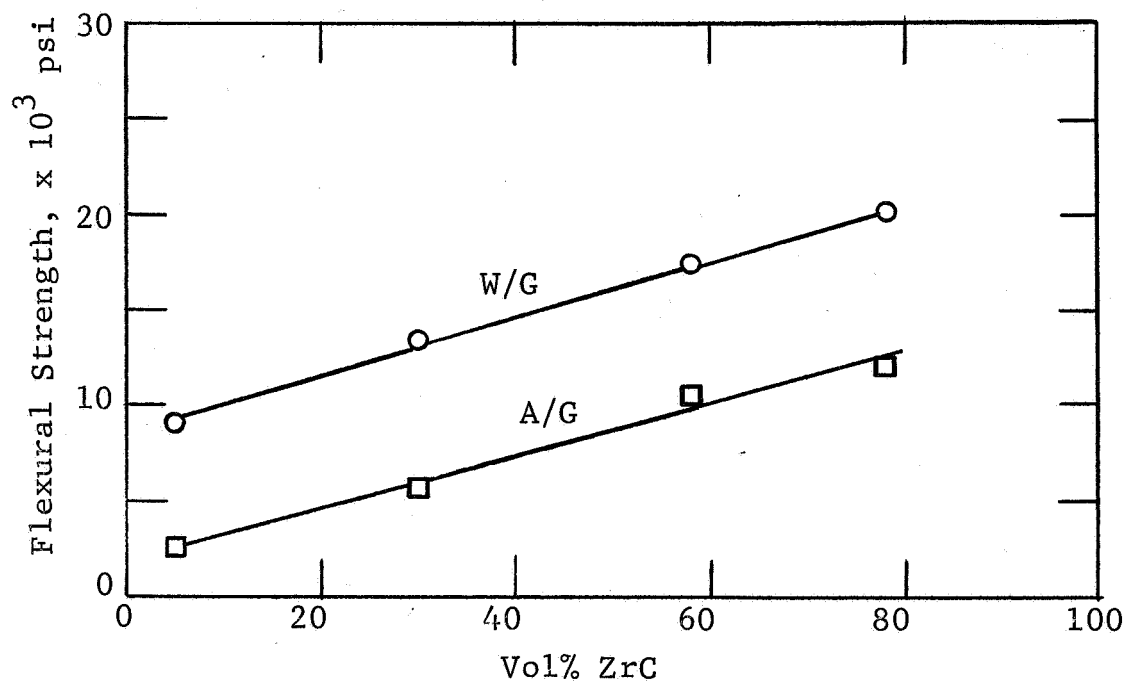
FIG. 28 - FLEXURAL STRENGTH AS A FUNCTION OF CARBIDE
CONTENT FOR ZrC-C COMPOSITES

In high temperature tests, all samples exhibited slightly higher strengths at 2000°C. However, plastic deformation became a greater factor at 2500°C, and the samples which could be stressed to failure showed low strengths. The superiority of TaC-C and NbC-C composites to ZrC-C compositions for refractory applications was quite clear from these evaluations.

2.   Tensile Strength

The results of a series of room temperature and 2000°C tests in the W/G direction are presented in Table III. Also included in this table are flexural data, either for the same billet or for billets of comparable composition and fabrication history. A plot of tensile strength vs carbide content for the two systems appear in Fig. 29. The relationship appears to be nonlinear and is virtually the same for the two systems.

NbC-C - There is a direct correlation between tensile strength and carbide content. The ratio of flexural to tensile strength was 1.9 for the composite containing 52 vol% NbC (Table III). This is comparable to the ratio of about 2 reported for carbides such as TiC and ZrC,[8] and somewhat lower than the value of 2.7 for ZTA hot worked graphite.[6] The ratio of 1.2 for the 85 vol% NbC composite was based on flexural data for a comparable billet ("84Nb"). It is likely that the flexural strength of the "84.1 Nb-L" composite was higher than the 23,200 psi value obtained for "84Nb."

At 2000°C, the 73 vol% NbC composite exhibited virtually no change in tensile strength whereas the others containing 52 and 85 vol% displayed a significant drop (Fig. 30). Such behavior appears unlikely in view of increases in flexural strength at 2000°C. More tests are necessary in order to determine if tensile strengths do not parallel the high-temperature trends observed for flexural strengths.
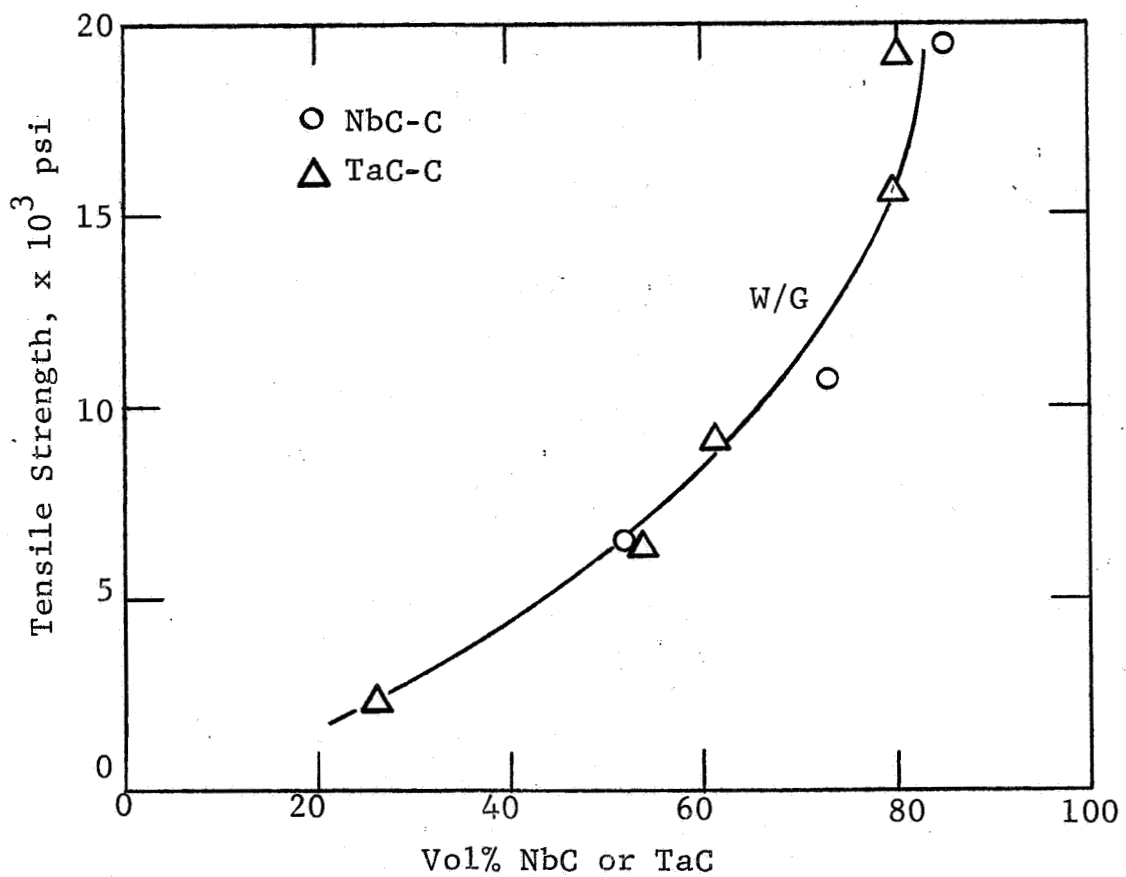
FIG. 29 - TENSILE STRENGTH AS A FUNCTION OF
CARBIDE CONTENT FOR NbC-C AND
TaC-C COMPOSITES

Table III

TENSILE STRENGTH OF METAL CARBIDE-
GRAPHITE COMPOSITES (W/G DIRECTION)

Compositional Designation	Vol% Carbide	Tensile Strength, psi		Flexural Strength, psi		Strength Ratio: Flexural/Tensile
		Room Temp	2000°c	Room Temp	2000°C	
C3-70Nb	52(NbC)	6,500	3,390	12,100*	12,510*	1.9
80Nb-E	73(NbC)	10,760	10,880	16,960**	20,770**	1.6
84.1Nb-L	85(NbC)	19,540	12,250	23,200**	24,700**	1.2
65Ta-C	26(TaC)	2,220		7,090**		3.2
82,5Ta-B	54(TaC)	6,330	8,770	17,850***	24,000***	2.8
85Ta	61(TaC)	9,010	9,980	16,260**	17,290**	1.8
M90Ta-A	80(TaC)	15,600	14,630	25,740**	31,000**	1.7
90Ta-B	80(TaC)	19,340	17,410	25,560***	32,000**	1.3

* Data obtained with samples from the same billet.
** Data obtained with samples from different billets of the same composition and processing history.
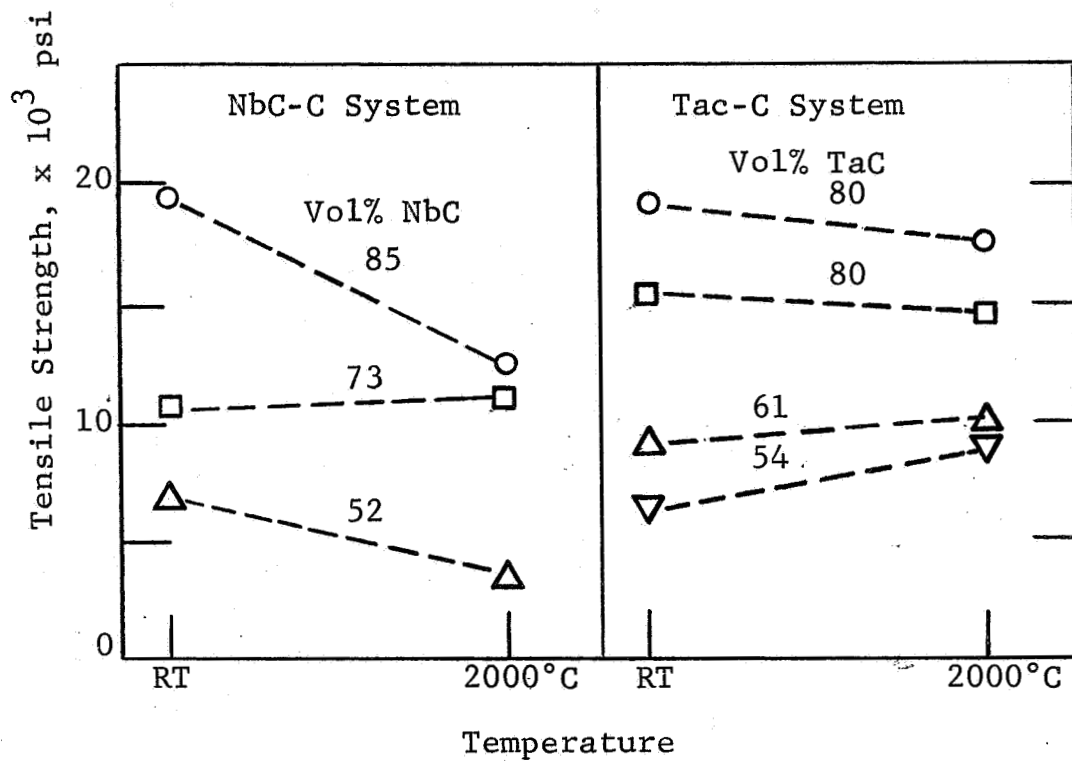
FIG. 30 - TENSILE STRENGTH AS A FUNCTION OF
TEMPERATURE FOR NbC-C AND TaC-C
COMPOSITES

TaC-C - Composites incorporating TaC also showed higher
tensile strengths with increasing amounts of carbide as would be
expected. High flexural-to-tensile ratios of 3.2 or 2.8 are
indicated for bodies containing 26 to 54 vol% TaC (Table III).
However, these ratios are based on flexural data for comparable
composites and appear somewhat high. For the sample (61 vol% TaC)
from which both flexural and tensile samples could be obtained,
the ratio was 1.8 which is similar to that for the 52 vol% NbC-C.
The ratio of 1.3 for "90 Ta-B" containing 80 vol% TaC is based
on a flexural strength value of 25,560 psi. A greater population
of data along with measurements of flexural and tensile strengths
from the same billet are needed to establish these ratios.

The high-temperature strengths (2000°C) were generally
the same or showed a slight increase as tabulated in Table III
and illustrated in Fig. 30. Based on the data obtained to date,
TaC-C composites show higher tensile strengths at 2000°C than do
the NbC-C composites. This trend is similar to that obtained for
flexural moduli and unlike that observed for flexural strength.
The fracture stress of a brittle material is not as high when
tested with a tensile specimen having a large surface area and
volume under the maximum stress as when tested in a flexural
test where the stress decrease from a maximum at the surface to
zero at the neutral axis.[11] Thus tensile values may be a better
representation of the strength of a material.

Additional work will be performed in tensile testing
in order to obtain a better picture of composition-dictated
trends, and also to investigate some high-temperature anomalies.
Larger billets will be fabricated in order to obtain A/G samples
and to assure adequate material for flexural testing as well.
It is possible that further modifications in sample configuration
and testing methods will be incorporated as more information is
gathered.

3. Compressive Strength

During this period, compressive strength tests were conducted at 2000°C in a Brew furnace in conjunction with a Riehle Testing Machine. Fixtures were fabricated of Poco Graphite. The results are tabulated in Table IV and graphically illustrated in Fig. 31 along with room temperature data. The only composites which failed in a brittle manner were the graphite matrix samples incorporating 25 or 20 vol% of NbC or TaC. Specimens containing higher amounts of carbide could not be stressed to failure because of plastic deformation. The stress values presented in the table are the maxima observed in the various tests. A fairly rapid decrease in load rate close to these maximum stresses shows the initiation of significant plastic deformation.

The compressive behavior of the higher carbide content composites at 2000°C is somewhat surprising in view of the brittle failure of flexural specimens at 2000°C at stresses which were about the same as the maxima observed in compression. Room temperature measurements had suggested that compressive strengths were about 2 to 4 times that in flexure. Furthermore, high carbide content samples exhibit increased flexural strength of 2000°C, similar to the behavior of pure graphite which displays increases in compressive strength with temperature as well.

The susceptibility of the higher carbide content composites to plastic deformation in compression at 2000°C will be studied further with additional tests. The crosshead speed will be increased from the present rate of .04 in./min in an attempt to minimize the time component of plastic deformation.

C. Thermal Properties

1. Thermal Expansion

In the continuing investigations of high-temperature properties, thermal expansion behavior of compositions incorporating

Table IV

COMPRESSIVE STRENGTH OF NbC-C and TaC-C Composites

Vol% NbC	Grain Direction	Compressive Strength, psi RT	2000°C	Vol% TaC	Grain Direction	Compressive Strength, psi RT	2000°C
25	W/G	12,000	11,160	20	W/G	110,300	13,740
	A/G		13,260		A/G	17,800	24,090
45	W/G		15,870*	54	W/G	46,100	16,520*
	A/G		17,930*		A/G	39,100	26,420*
52	W/G	29,300	16,460*	80	W/G	117,400	20,310*
	A/G				A/G	88,400	28,550*
85	W/G	187,000	18,170*				
	A/G		15,000*				

*No failure. Maximum load which could be applied due to onset of plastic deformation.
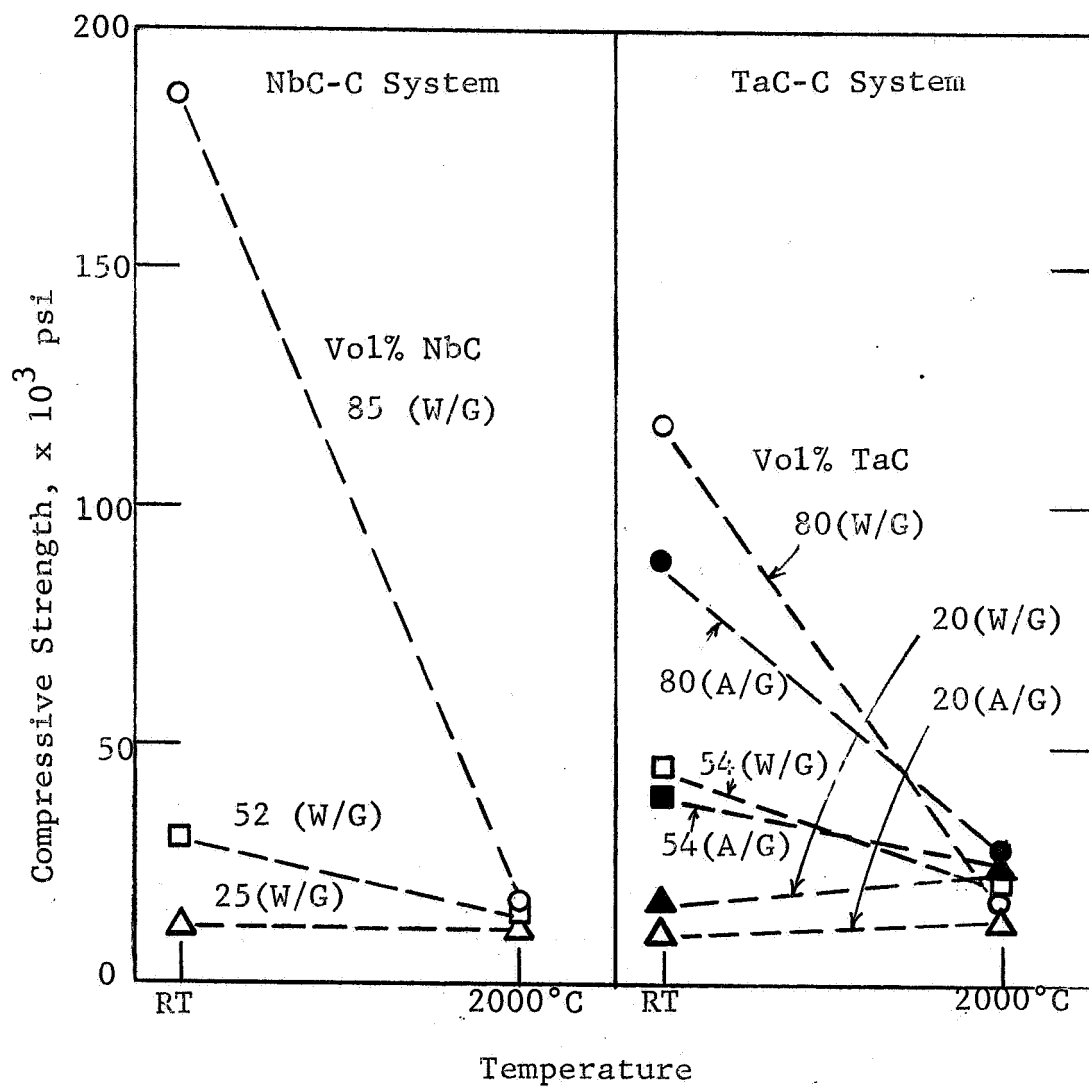
FIG. 31 - COMPRESSIVE STRENGTH AS A FUNCTION
OF TEMPERATURE FOR NbC-C AND TaC-C
COMPOSITES

TaC or NbC was measured. A cathetometer method was used in which the sample was heated in a graphite tube furnace and expansion monitored visually by sighting on the ends of the sample using Gaertner optical micrometers. Each sample was taken through the heating (to 2300°C) and cooling cycle twice. Sample dimensions were remeasured after removal from the furnace.

Table V contains coefficient of thermal expansion (CTE) values in both grain orientations for a range of graphite-matrix to carbide-matrix compositions in both the TaC-C and NbC-C systems. Compositions in which graphite is the matrix (C-50Nb and 65Ta-A) exhibit strong anisotropy, although not to the extent observed for ZTA (hot worked) graphite in which the A/G to W/G ratio is 15.[6] The CTE values are somewhat higher than those normally seen for ZTA, reflecting the influence of the higher thermal expansion carbide.

The trend toward isotropy with increasing carbide content is observed for both systems as shown in Figs. 32 and 33. Essentially nondirectional behavior is shown by composites containing about 80 vol% carbide. CTE values for pure NbC and TaC in the range room-temperature to 2500°C have been reported as 8.75 and 6.81 (in./in./°C x 10^6).[12] The values obtained for our composites appear reasonable in light of those values.

Measurement of samples after testing revealed some dimensional changes which were more pronounced for the graphite-rich materials. Similar permanent deformations in CTE samples have been reported by other investigators.[13] These changes were an increase in the A/G direction and a decrease in the W/G direction which may be due to a relaxation of stresses imparted to the composite during hot pressing. In the cooling process after fabrication, different expansion behavior in the anisotropic graphite crystals build up residual stresses. On subsequent

Table V

THERMAL EXPANSION OF NbC-C AND TaC-C COMPOSITES
FROM ROOM TEMPERATURE TO 2300°C

Compositional Designation	Composition Wt% Metal	Composition Vol% Carbide	Coefficient of Thermal Expansion, $\times 10^{-6}$ in/in/°C W/G	Coefficient of Thermal Expansion, $\times 10^{-6}$ in/in/°C A/G	Ratio A/G: W/G
C-50Nb	42	22	4.78	14.22	2.97
C-60Nb	57	35	5.13	10.63	2.07
70Nb	71	54	7.12	8.27	1.16
80Nb-B	80	73	7.49	6.97	0.93
85Nb	85	86	7.44	8.11	1.09
65Ta-A	65	26	3.29	12.17	3.70
82.5Ta-A	83	54	6.38	7.98	1.25
90Ta-A	90	80	7.05	7.35	1.05

FIG. 32 - COEFFICIENT OF THERMAL EXPANSION AS A
FUNCTION OF CARBIDE CONTENT FOR NbC-C
COMPOSITES (R.T. - 2300°C)
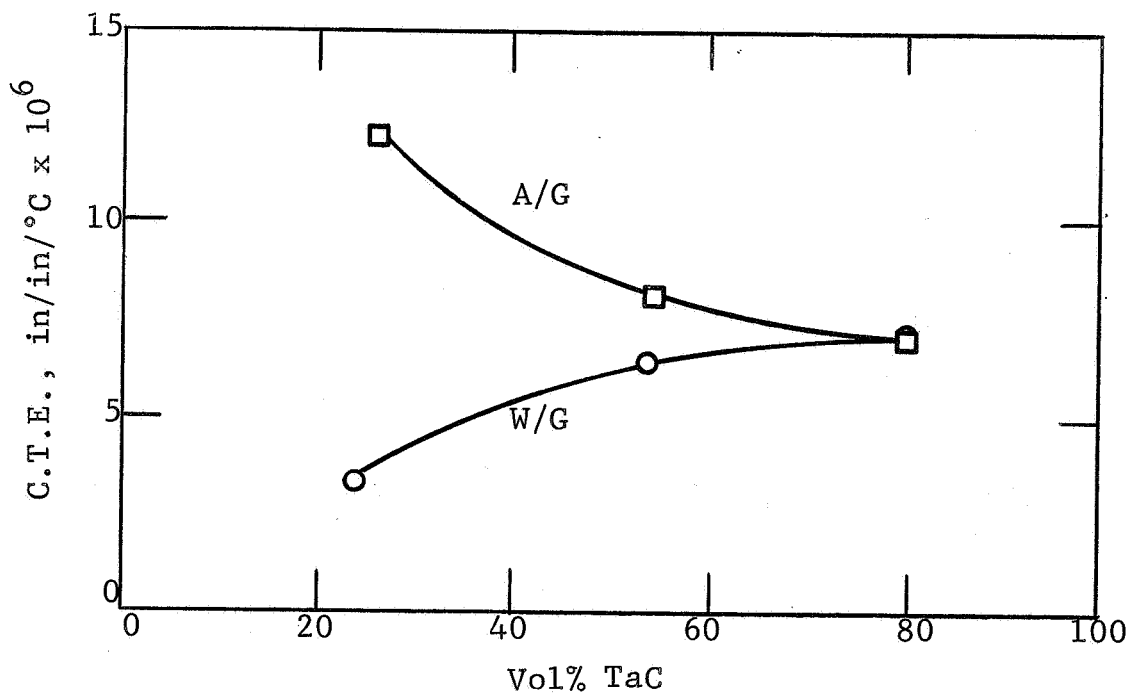
FIG. 33 - COEFFICIENT OF THERMAL EXPANSION AS A
FUNCTION OF CARBIDE CONTENT FOR TaC-C
COMPOSITES (R.T. - 2300°C)

heat treatment such as the CTE measurement, relief of these stresses would occur. This phenomenon will be discussed under another section, "Effect of Heat Treatment."

2. Compressive Creep

For a material to be useful for structural purposes at elevated temperatures, its resistance to creep or plastic deformation is of primary importance. Unless a system can maintain its dimensional stability under load, its utility would be severely limited. In order to determine high temperature structural integrity, a series of NbC-C and TaC-C composites were subjected to a compressive load of 2000 psi for 30 min at 2700°C. The results of these experiments are graphically illustrated in Fig. 34.

In general most of the materials tested exhibited little permanent deformation under these test conditions. In the NbC-C system, composites with carbide contents of about 50 to 75 vol% exhibited somewhat greater changes than did materials of lower or higher carbide levels. However, considerable scatter in the data along with the very small differences in the % changes makes it difficult to determine if this trend is real. For dense, well-bonded NbC-C composites in the compositional range examined, maximum permanent deformations of 2% can be expected under the conditions: 2700°C/2000 psi/30 min.

Similarly there is no clear trend of deformation as a function of carbide content in the TaC-C system. It is quite clear, however, that composites incorporating greater than 50 vol% TaC are more resistant to compressive deformation than are comparable NbC containing bodies (Fig. 34). This is probably related to the melting points of about 3500°C for NbC and 3900°C for TaC.[14] A direct relationship between critical resolved shear stress and melting point has been reported for single crystals of TiC, ZrC and NbC.[15] Therefore, at the same test temperature, it is probable
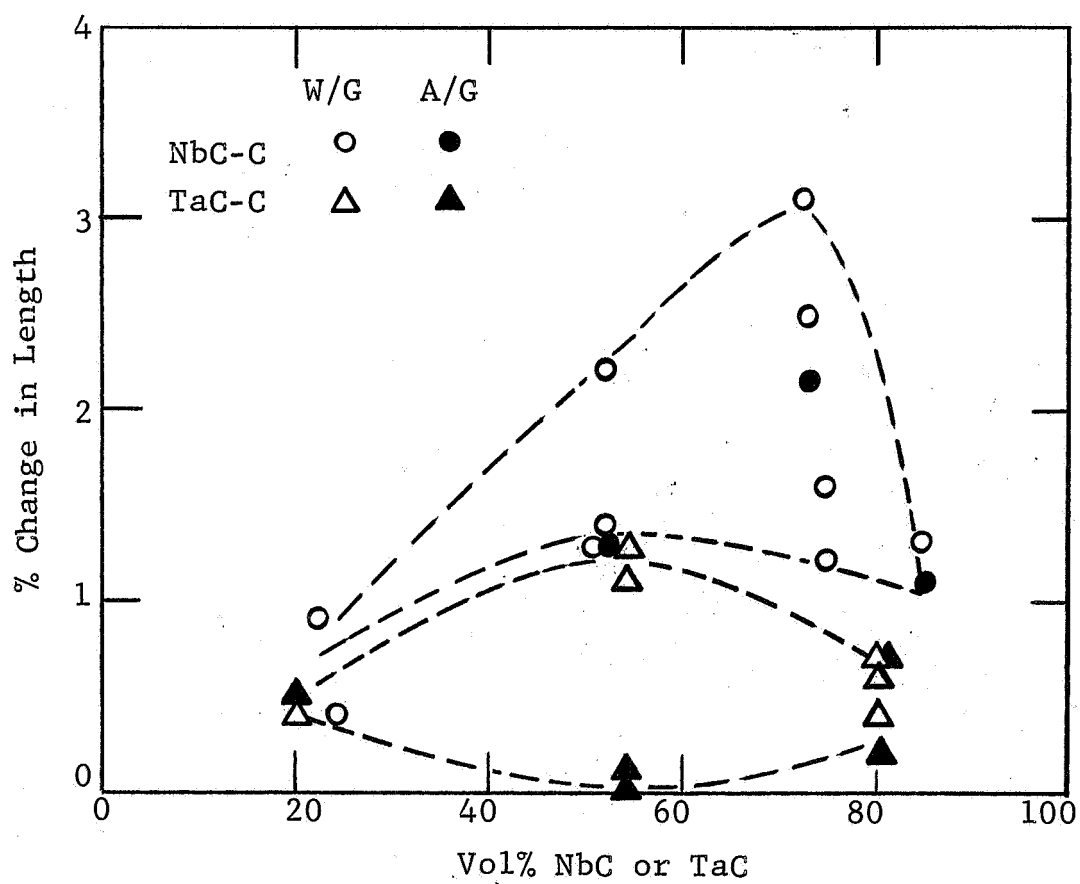
FIG. 34 - COMPRESSIVE DEFORMATION AS A
FUNCTION OF CARBIDE CONTENT
FOR NbC-C AND TaC-C COMPOSITES
(2700°C/2000 psi/30 minutes)

that the critical resolved shear stress is lower for NbC than for TaC. Thus dislocation movement may be expected to be greater in the lower melting NbC as compared to TaC, and the respective carbide matrix composites would probably show the same comparative behavior.

The curves in Fig. 34 suggest that there is little difference in behavior between the two systems for graphite matrix composites. This may be expected since the graphite would be the dominant species and the role of the respective carbides would be minimized. It has been shown than creep in a graphite will be smaller as the degree of graphitization increases.[16] Creep tests were conducted with both TaC-C and NbC-C composites prepared at relatively low temperatures and thus, which showed a lower degree of ordering. Deformations displayed by such materials were 3 to 4 times higher than comparable compositions which were well graphitized.

3. Thermal Conductivity

Thermal conductivity measurements have been made with two NbC-C composites, one of which contained 27 vol% NbC ("C3-50Nb") and the other, 73 vol% NbC ("80Nb-F"). The results of these determinations are tabulated in Table VI and illustrated in Fig. 35.

Very high thermal conductivity was shown for the W/G direction of the graphite matrix (27 vol% NbC) material at room temperature with a fairly rapid decline with temperature. The A/G values were relatively low, reflecting the anisotropy observed in mechanical properties. The curves for the high carbide material were at fairly low values, paralleling the behavior of pure NbC. The 73 vol% NbC-C also appears to be fairly isotropic.

Table VI
THERMAL CONDUCTIVITY OF NbC-C COMPOSITES

Compositional Designation	Vol% NbC	Thermal Conductivity, cal/sec cm °C			
		W/G	Temp, °C	A/G	Temp, °C
C3-50Nb	27	.661	86	.124	107
		.558	218	.0980	284
		.403	448	.0794	539
		.366	556	.0703	741
		.277	752		
80Nb-F	74	.186	86	.151	109
		.179	232	.150	297
		.169	410	.131	507
		.167	579	.126	708
		.148	813		
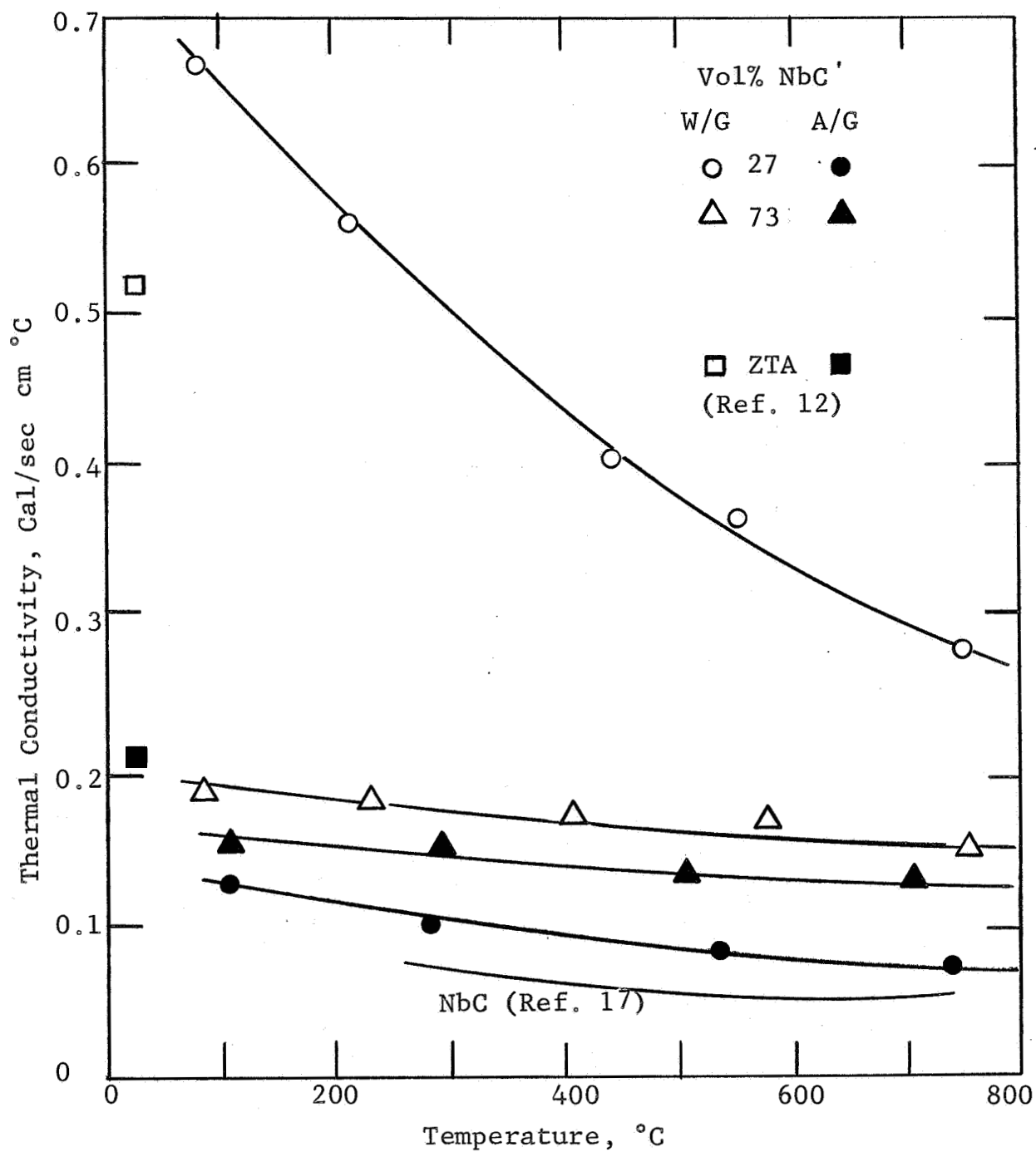
FIG. 35 - THERMAL CONDUCTIVITY OF NbC-C
COMPOSITES

The values for the W/G 27 vol% NbC composite appears to be rather high when compared to ZTA (hot worked graphite).[6] If these values are reproduced in a duplicate test now being conducted, this would mean that the graphite phase is extremely well graphitized and ordered. Determinations of specific heat and thermal conductivity up to 4000°F (2200°C) are also presently underway and will be reported in the near future.

D. Electrical Properties

Previous work on the measurement of electrical properties of metal carbide-graphite has revealed that a direct relationship exists between conductivity and flexural strength. With low carbide content composites in which graphite is the matrix, this relationship has been found to be linear.[2] Clear establishment of this conductivity-strength relationship over the complete compositional range is desirable in that it can constitute a nondestructive method for determining both degree of bonding and homogeneity. In addition, other properties such as thermal conductivity would be closely related to electrical conductivity since both are governed to a large extent by the fraction and morphology of the dispersed phase in two-phase systems.

1. Electrical Conductivity vs Carbide Content

Plots of electrical conductivity as a function of carbide content appear in Fig. 36. The relationship in the W/G direction is linear (correlation coefficient = 0.97) and in the A/G direction it is nonlinear. These relationships are the same as those observed for flexural strength, and reflect the trend toward isotropic behavior with carbide-rich composites. Extrapolation of the W/G curve indicates resistivity values of about 600μΩ-cm for graphite and 34μΩ-cm for NbC. These are in reasonable agreement with values of 700μΩ-cm for ZTA[6] and 35μΩ-cm for NbC.[14]
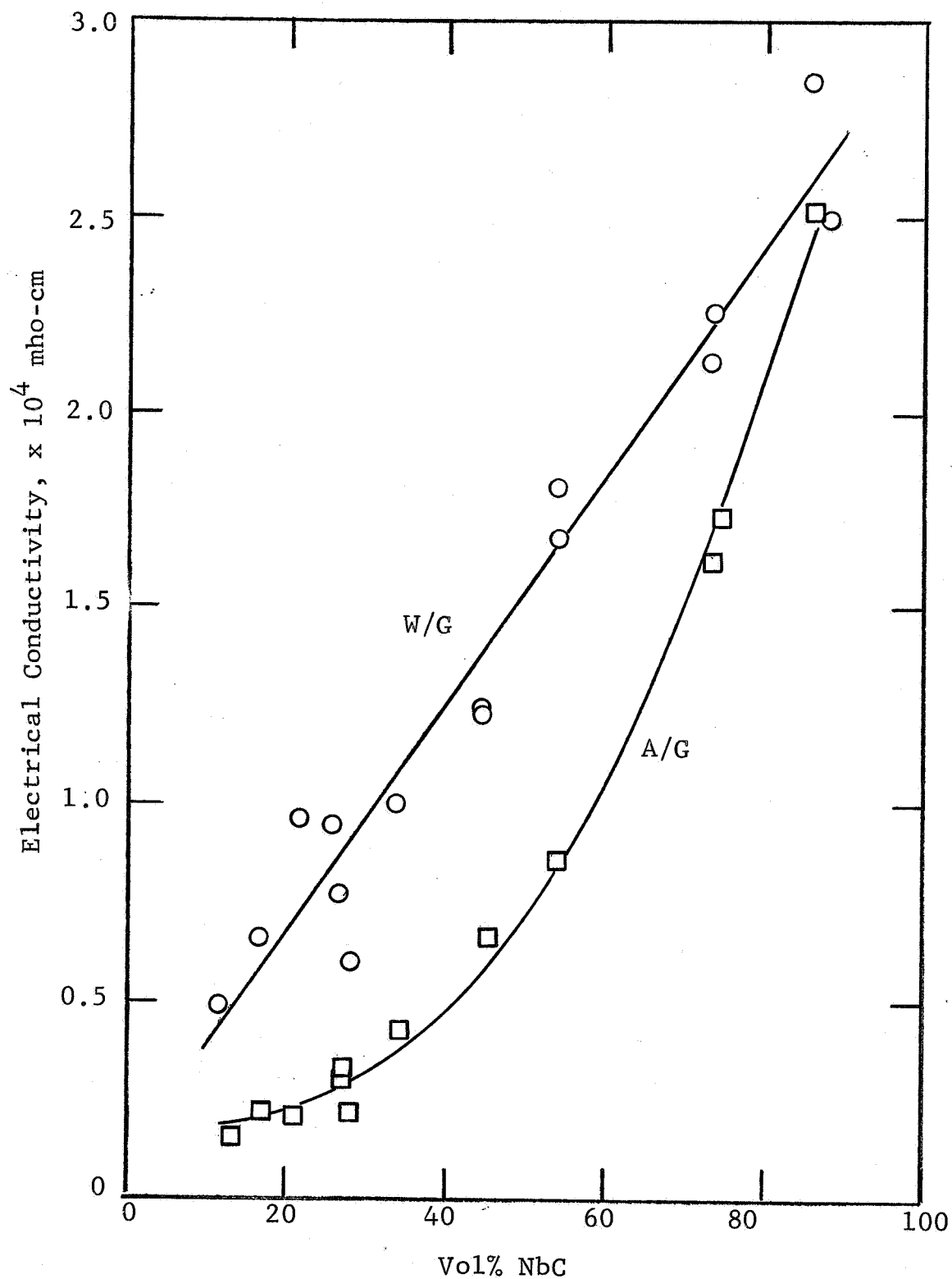
FIG. 36 - ELECTRICAL CONDUCTIVITY AS A FUNCTION
OF CARBIDE CONTENT FOR NbC-C COMPOSITES

The linearity shows the existence of an upper bound relationship (see section on Composite Characterization) or $\sigma_c = \sigma_1 V_1 + \sigma_2 V_2$ where: σ_c = composite conductivity; σ_1 and V_1 = conductivity and volume fraction of graphite phase; and σ_2 and V_2 = conductivity and volume fraction of the NbC phase. Apparently, good electrical contact exists between particles of the two phases at all carbide levels.

In the A/G direction, the shape of the curve suggests a lower bound relationship or: $1/\sigma_c = V_1/\sigma_1 + V_2/\sigma_2$. This may be explained by considering the microstructure of composites. A definite directionality of both phases results from the hot pressing procedure. If a greatly simplified model is used, the resistivity and conductivity can be depicted as follows:

$$1/\rho_c = 1/\rho_1 + 1/\rho_2 \qquad \rho_c = \rho_1 + \rho_2$$

$$\sigma_c = \sigma_1 + \sigma_2 \qquad 1/\sigma_c = 1/\sigma_1 + 1/\sigma_2$$
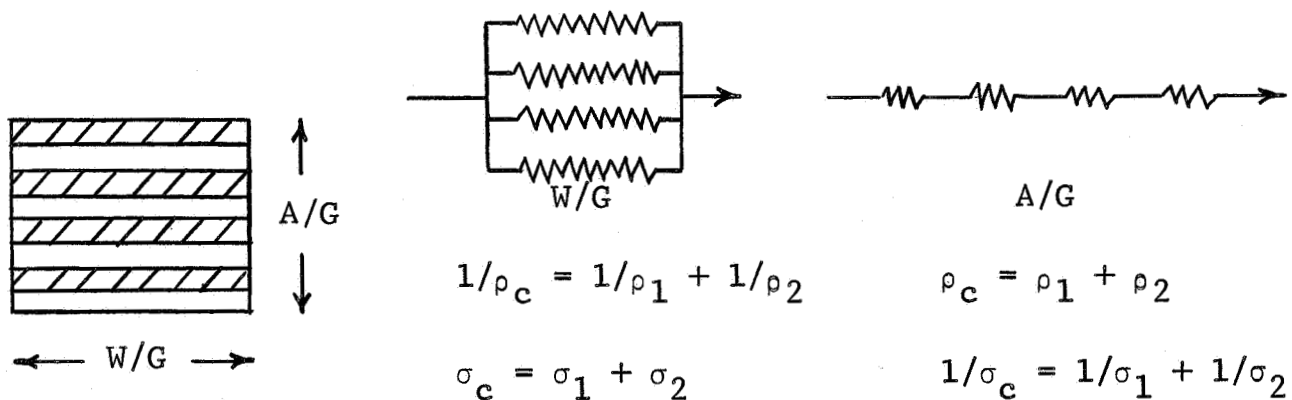
Thus the W/G direction would be a parallel model and the A/G direction approach a series model in terms of conductivity.

Similar relationships have been observed in the TaC-C system as illustrated in Fig. 37. However, comparison of W/G data with a theoretical curve (which assumes endpoints of $600\mu\Omega$-cm for graphite and $20\mu\Omega$-cm for TaC) indicates somewhat low conductivity for graphite-rich composites. As discussed earlier in flexural strength evaluations, good bonding was difficult to
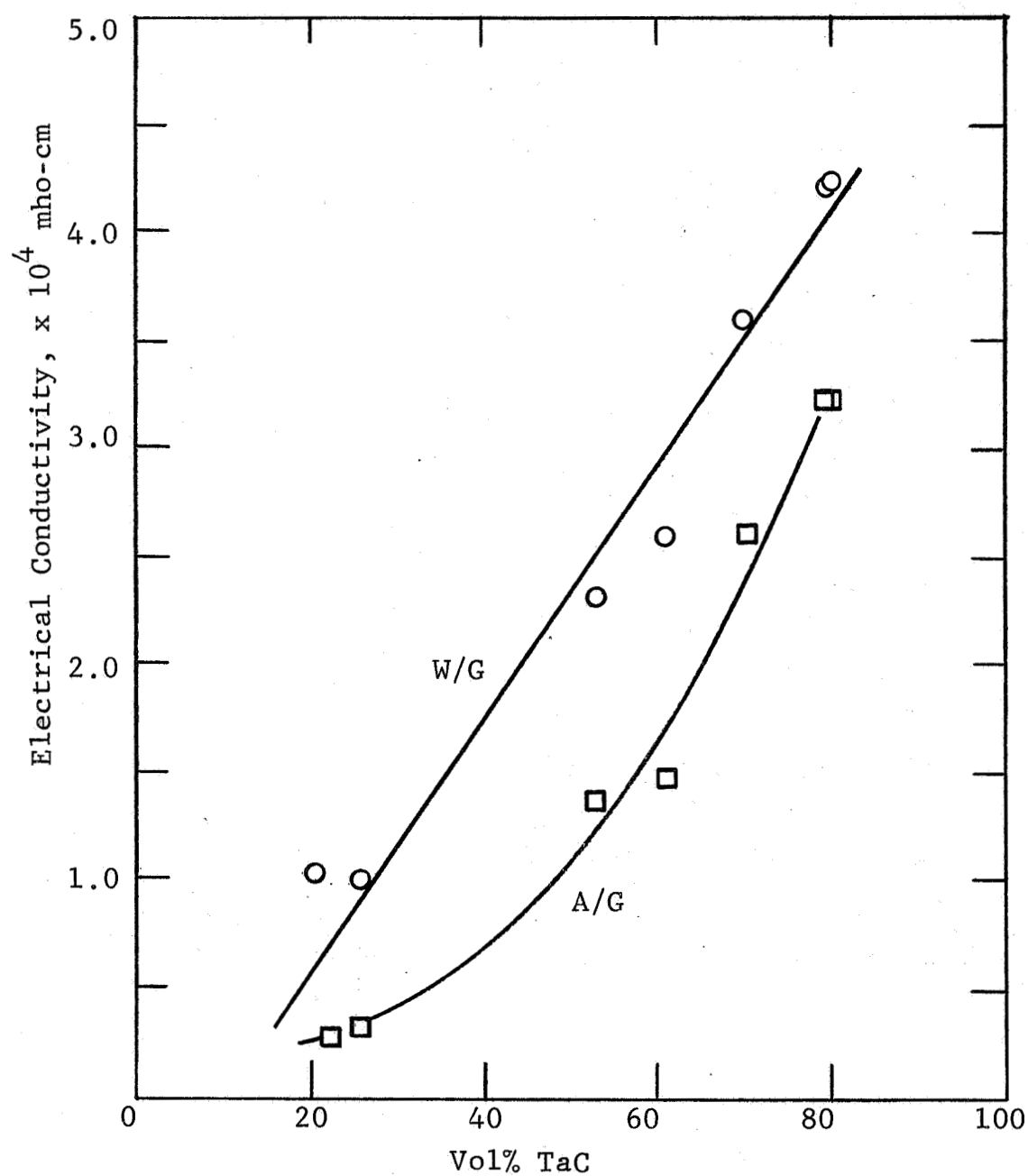
FIG. 37 - ELECTRICAL CONDUCTIVITY AS A FUNCTION
OF CARBIDE CONTENT FOR TaC-C COMPOSITES

achieve in low carbide content composites. Although the data
is limited, the poor bonding in graphite matrix TaC-C samples
does appear to be reflected in the electrical measurements.

2.   Electrical Conductivity vs Flexural Strength

The linear relationship between electrical conductivity
and flexural strength in the W/G direction appears to hold in the
NbC-C compositional range which has been evaluated (Fig. 38).
Analysis of W/G data by the statistical regression method shows
the correlation coefficient to be 0.90. This linear relationship
is to be expected since both electrical conductivity and flexural
strength are linear as a function of carbide content and should
thus be linear to each other.

In the A/G direction a nonlinear relationship is ob-
served. Most of the data points are at the low end of the scale,
both in strength and conductivity, leaving gaps at about 1.0 and
2.0×10^4 mho-cm. In looking at the conductivity-composition
curve in Fig. 34, these gaps correspond to composites containing
60 to 70 vol% and about 80 vol% NbC. Materials in these ranges
will be fabricated in the near future for evaluation.

The properties depicted in Fig. 36 can be of value in
predicting strength from electrical measurements. Although there
is considerable scatter in the data, minimum W/G strengths may be
listed as follows: 1.0×10^4 mho-cm, >10,000 psi; 2.0×10^4 mho-cm,
>15,000 psi; and 2.4×10^4 mho-cm, 20,000 psi. As more informa-
tion is gathered, a graph of this type can become increasingly
accurate and valuable as a method for nondestructively indicating
strength.

E.   Composite Characterization

Fracture and deformation characteristics of all mate-
rials are strongly affected by microstructure. For single phase
polycrystalline materials the amount and distribution of porosity
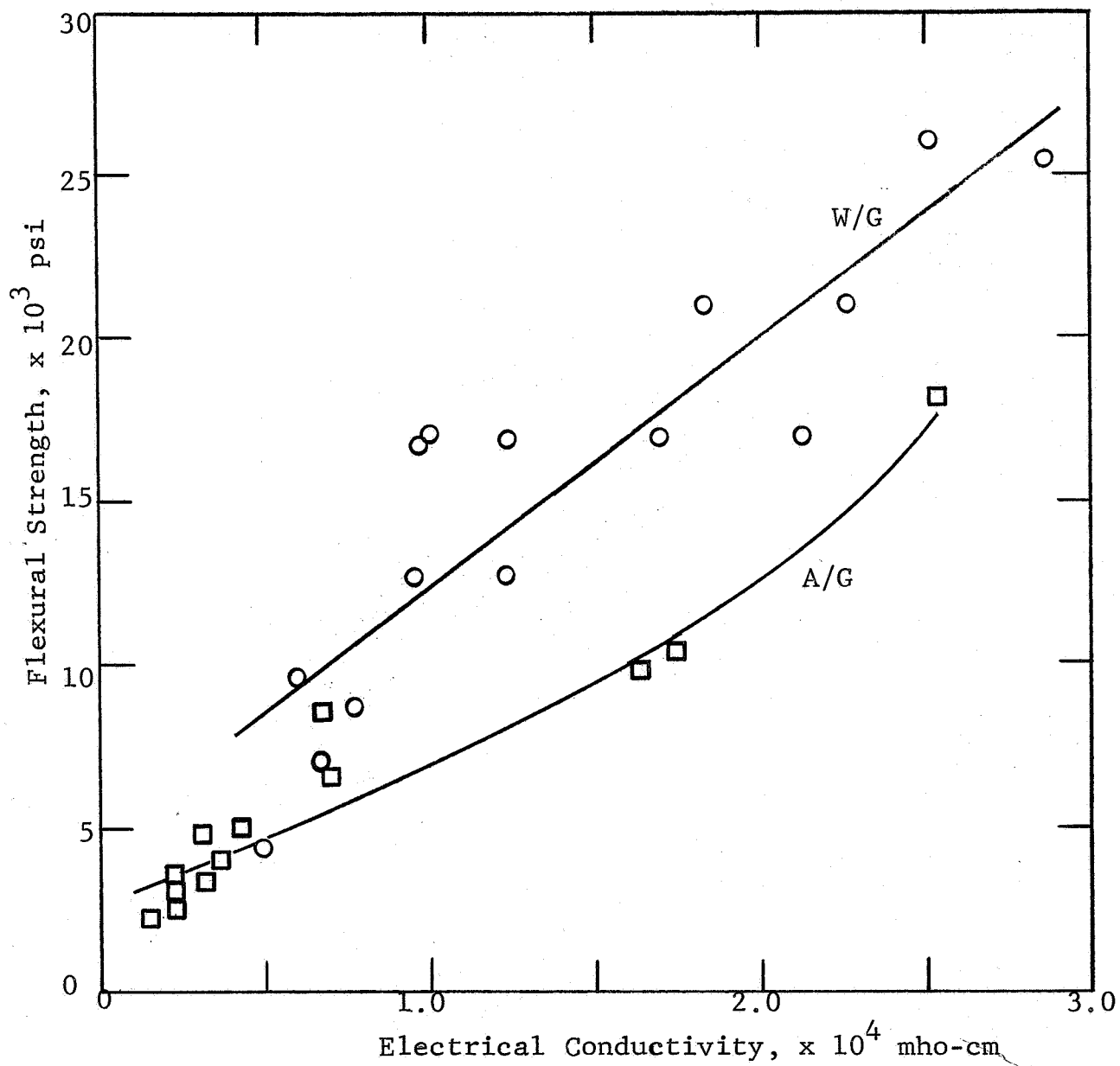
FIG. 38 - RELATIONSHIP BETWEEN FLEXURAL STRENGTH
AND ELECTRICAL CONDUCTIVITY FOR
NbC-C COMPOSITES

together with grain size distribution determine the observed mechanical properties. Materials containing two phases, where one phase can be a dispersed second phase or a pore phase, can be classified by their essential microstructural variables as follows:

1. Distinction between the continuous phase and the dispersed phase
2. Volume fraction of the two phases
3. Shape of dispersed phase particles
4. Size and distribution of dispersed phase particles
5. Mean separation between neighboring dispersed phase particles and their distribution
6. Grain structure of the matrix
7. Relation between grain structure of the matrix and dispersed phase
8. Nature of the interface between matrix and dispersed phase

In view of the complications involved in the study of multiphase materials many investigators[18] have resorted to applying mixing law theory to the behavior of these materials. This type of theory has been used to predict the mechanical and physical properties of particulate and fibrous composites.[19] This research has brought to light that many material properties are interrelated and are controlled by the same microstructural characteristics given in the above list of variables. Thus, if one property of a material is known, it should be possible to predict other properties of the same material. The factor which brought about the study of the use of mixing laws with regard to the carbide-graphite composites under investigation on this program was the observation that the flexural strength of the composite increased in a linear manner with increased carbide content for a "with" grain orientation and that in the "across" grain

orientation the strength increase was nonlinear (Fig. 17). The appearance of these curves was that of upper and lower bounds as derived by Paul[20] in his study of changes in elastic modulus of two phase systems, Fig. 39. A review of mixing law concepts is shown in Fig. 40. Paul assumed composite materials were oriented in such a manner that the grains were under equal strain for upper bound limits and the grains were under equal stress for lower bound limitations (Fig. 40). The upper bound is a series relationship for elastic modulus:

$$E_C = V_1 E_1 + V_2 E_2 \tag{4}$$

while the lower bound is a parallel relationship:

$$\frac{1}{E_C} = \frac{V_1}{E_1} + \frac{V_2}{E_2} \tag{5}$$

where E is elastic modulus and V is the volume fraction of constituent materials. Hirsch[21] has derived a relation which combines Paul's equations such that if the degree of orientation can be determined, the relationship can be predicted:

$$\frac{1}{E_C} = X \left[\frac{1}{V_1 E_1 + V_2 E_2} \right] + (1-X) \left[\frac{V_1}{E_1} + \frac{V_2}{E_2} \right] \tag{6}$$

Hashin[22] and Counto[23] assume a model in which the particle is surrounded by a matrix. All of these other theories fall within the boundaries established by Paul. In addition to effects due to the respective amounts or volume fractions of the two phases, the size and distribution of dispersed particles also affect properties.

For this program the assumption is made that the carbide composites under study fail as a brittle material and that strength and elastic modulus can be related through the strain in the material at failure:

$$\sigma = E\epsilon \tag{7}$$
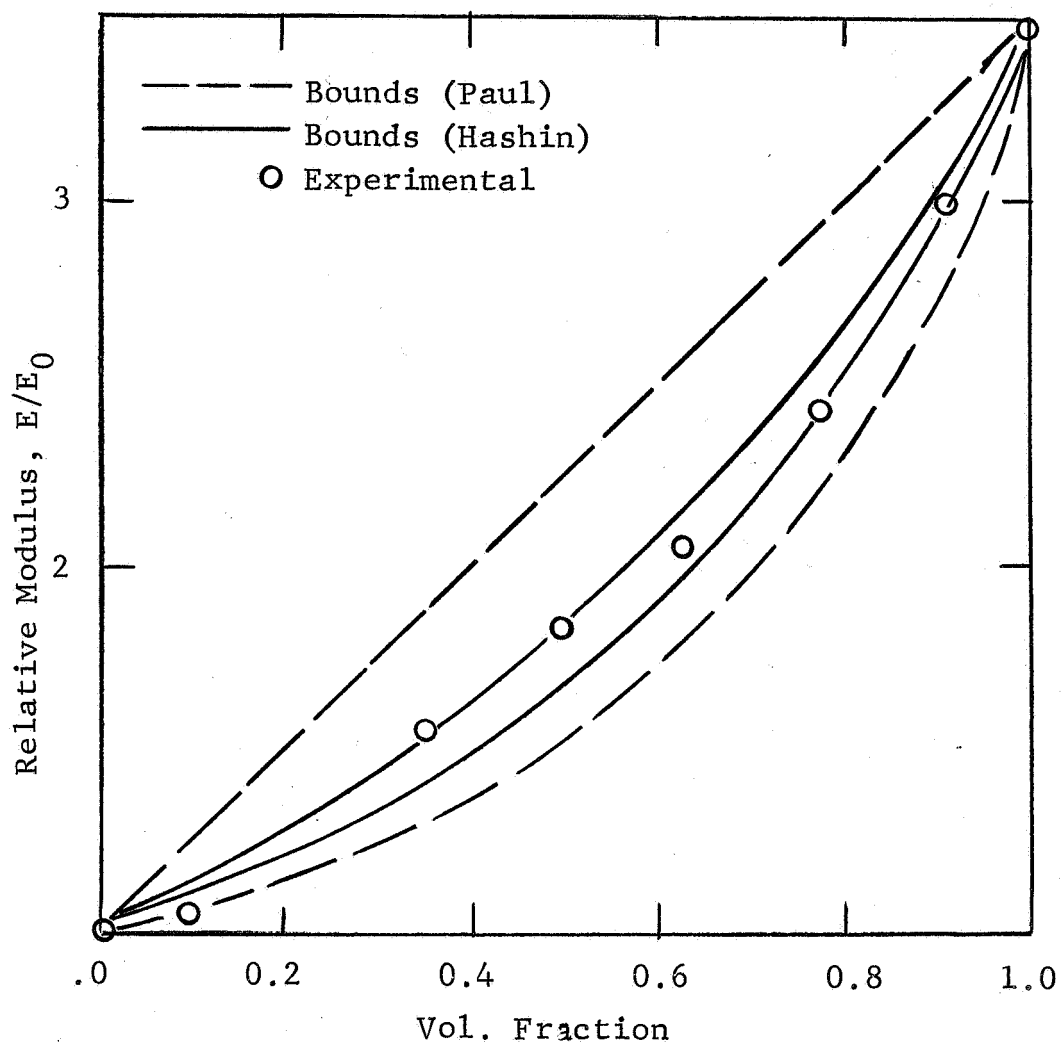
FIG. 39 – UPPER AND LOWER BOUNDS FOR YOUNG'S
MODULUS COMPARED WITH EXPERIMENTAL
RESULTS FOR WC-Co ALLOY
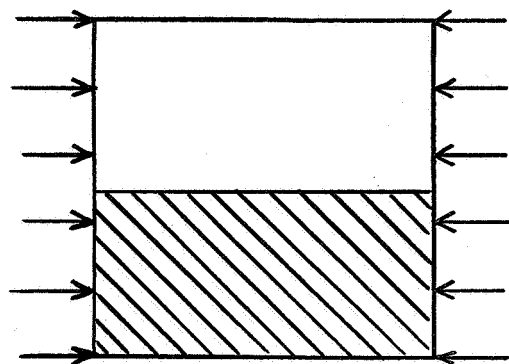
(a)

Upper Bound:
Uniform Strains
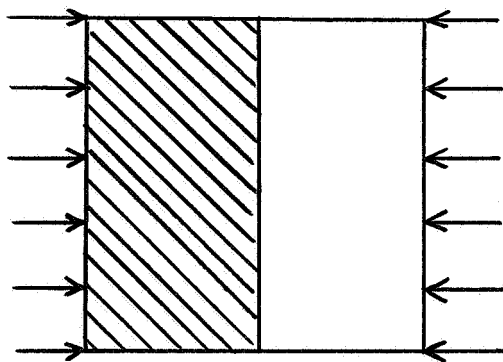
(b)

Lower Bound:
Uniform Stresses
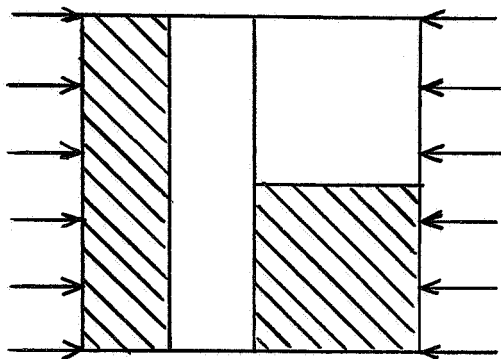
(c)

Hirsch's Model
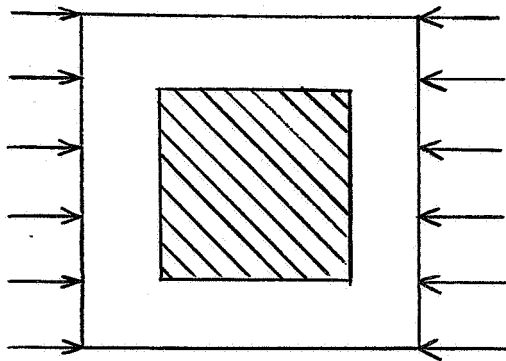
(d)

Counto's Model

FIG. 40 - SIMPLIFIED STRUCTURAL MODELS FOR COMPOSITES

where σ is the failure stress and ϵ is the failure strain. In addition, there is evidence[24] that for brittle materials failure is strain dependent and not stress dependent. Thus there is a direct relation between stress and elastic modulus for materials which are elastic to failure.

Orientation and grain structure can be seen in Fig. 13. The effect of grain orientation and grain size on strength is listed in Table VII. Here there is also a comparison between electrical conductivity and strength, as well as microstructural variables. The table shows that with increasing grain size strength and electrical conductivity decrease. This phenomena is probably due to decreased contact area between grains with increasing grain size.[25]

Having observed this phenomena, the next step was to try and relate the mechanical and electrical properties through the mixing laws and thus establish a method of characterizing mechanical strength through the expedient of electrical measurement. The latter measurement is easier and less time consuming to perform than the actual mechanical measurement.

A plot of flexural strength vs volume of carbide content is shown in Fig. 41. The data for flexural strength indicates that the "across" grain orientation is more sensitive to orientation than that of the "with" grain. While the "with" grain plots as an upper bound of full orientation, the lower, "across" grain, data substituted into the Hirsch model shows that the orientation should be about half parallel and half series orientation. A similar plot is shown in Fig. 42 for electrical conductivity and volume percent carbide. Here the "with" grain data plots as a Paul upper bound while results of the "across" grain test, using the Hirsch model, plots as if the orientation were 90% parallel orientation. It is obvious that while the "with" grain data

Table VII

RELATIONSHIP BETWEEN CARBIDE GRAIN SIZE,
STRENGTH, AND ELECTRICAL CONDUCTIVITY

Compositional Designation	Vol% NbC	Flexural Strength, psi	Electrical Conductivity $10^2/\rho(\mu\Omega\text{-cm})$	Carbide Grain Size, μ
C-50Nb	21	16,620	0.96	3
50Nb-C	28	9,500	0.59	10
C-65Nb	45	16,880	1.24	3
65Nb-A	45	12,690	1.23	10
C2-70Nb	54	20,960	1.82	3
70Nb	54	17,050	1.68	10
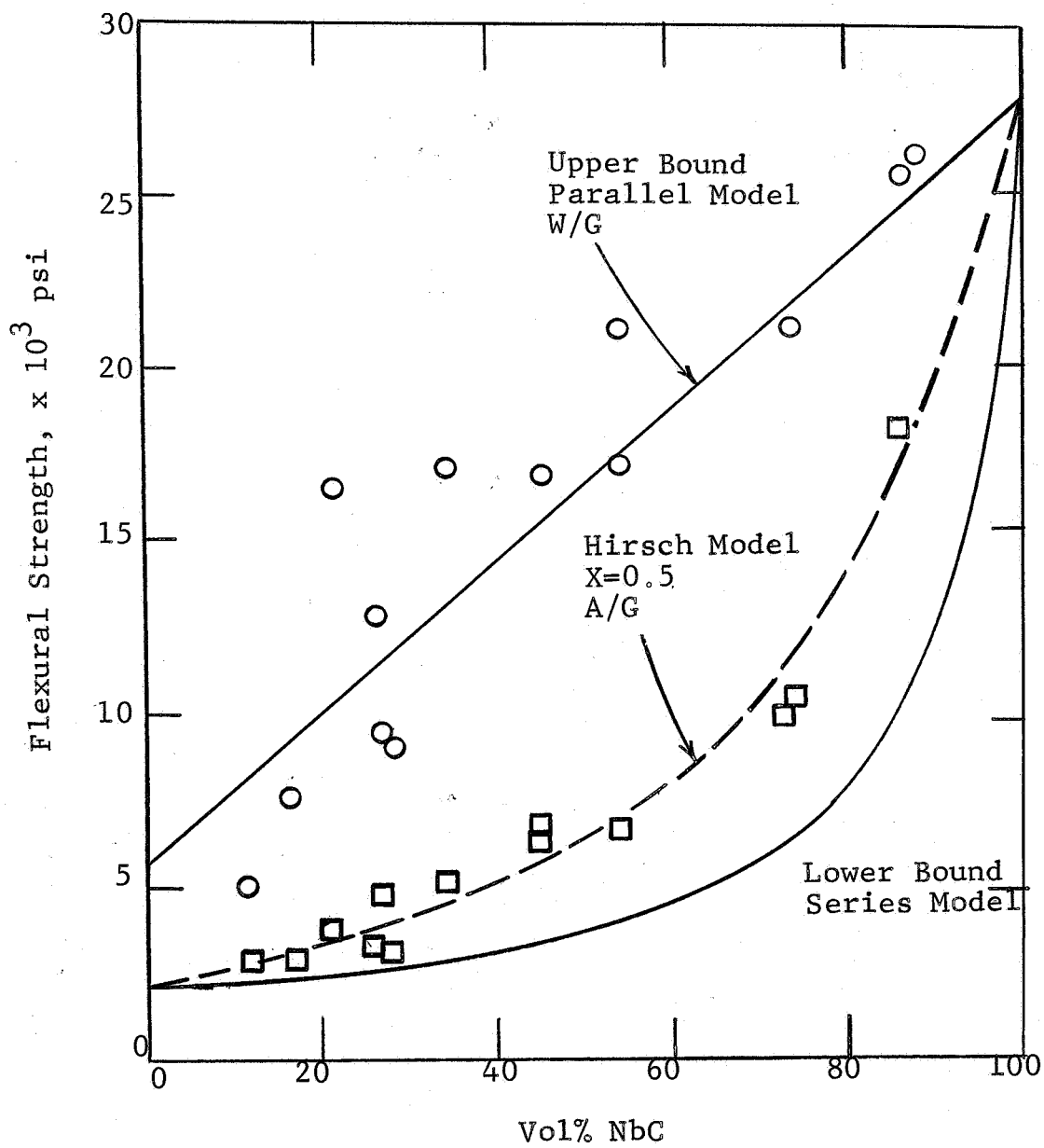
FIG. 41 - APPLICATION OF MIXING LAWS
RELATIONSHIPS TO FLEXURAL
STRENGTH
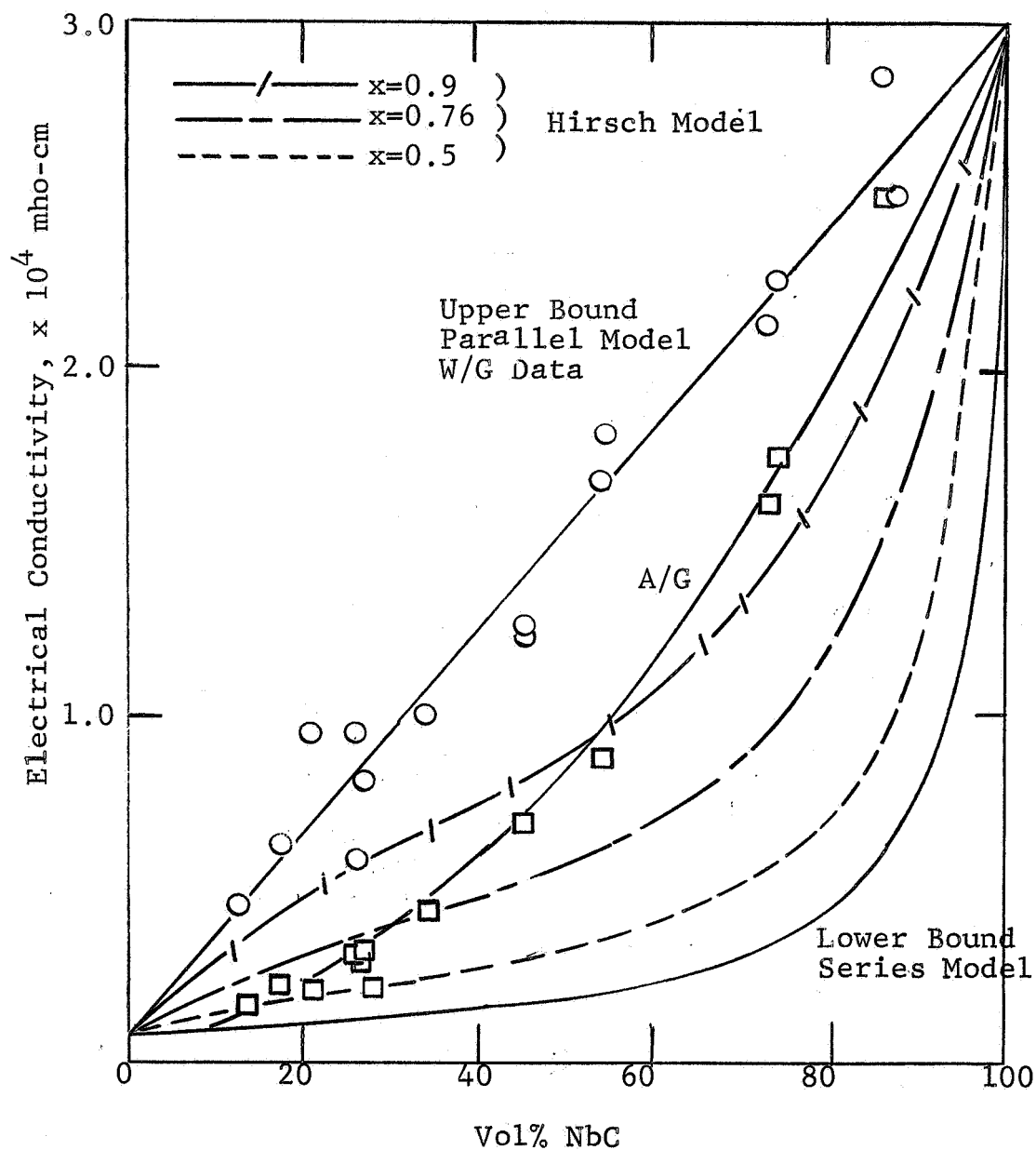
FIG. 42 - APPLICATION OF MIXING LAW
RELATIONSHIPS TO ELECTRICAL
CONDUCTIVITY

will plot as a Paul upper bound for both flexural strength and electrical conductivity, the "across" grain relationships are still not well enough understood for accurate characterization using the mixing laws. However, a plot of strength vs conductivity shows good correlation and could be used to help characterize NbC-C composites (Fig. 38).

Other properties such as elastic modulus and tensile strength have shown a nonlinear relationship with carbide content in the "with" grain direction, in contrast with the linear relationship observed for flexural strength. Other investigators[8] have shown an exponential relationship between transverse strength or elastic modulus with porosity for alumina. Thus, if graphite were regarded as porosity in the metal carbide-graphite composites, the nonlinear relationship would appear more valid than the linear. The nonlinear relationship would agree more with the work of Hashin and Hirsch than with that postulated for the carbide flexural data which has been analyzed to date.

Considerably more work must be done with the mixing laws and their relationship to strength and other properties. The experimental work performed during this program has shown the promise of this type of investigation with regard to characterizing strength from electrical measurements. However, a great deal remains to be done (even though mixing law theory is presently used to help characterize electrical properties of multiphase materials) to provide a better understanding with regard to bonding and grain orientation and their relationship to strength, strain and elastic properties.

F.   Effect of Processing Temperature

1.   Liquid Phase Processing

The use of increasingly higher processing temperatures to exploit diffusion bonding and high degrees of graphitization

has resulted in several pressings in which the metal carbide-carbon was wholly or in part liquid. With compositions of high NbC content (greater than 70 vol%), fabrication at temperatures above the solidus of 3220°C yielded poorly bonded composites having long needles of primary graphite in a eutectic structure.[2] Loss of material through reaction with the mold and extrusion around the plungers also lead to considerable heterogeneity.

In the present work, a series of low metal content (less than 50 vol% carbide) compositions were processed at about 3200°C in an attempt to exploit more rapid diffusion, and hence bonding, afforded by higher temperatures. It was felt that since liquid (eutectic) formation would be in relatively isolated islands, gross melting and loss of material would not occur. Evaluation of these materials revealed a heterogeneity in density. This lack of uniformity is caused by differences in carbide content from one portion of the billet to another. As illustrated in Fig. 43, this effect is in the form of a cone which is visible to the eye due to different light-reflecting characteristics.

The cone contains greater amounts of carbide, and the periphery has lesser amounts. Photomicrographs of these two areas for a 30 vol% NbC composite appear in Fig. 44. Also shown is a eutectic structure which existed in the material extruded around the punch during hot pressing, indicating that the eutectic temperature, 3220°C, had been attained.

It is felt that this phenomenon is due to a combination of extrusion around the top punch and reaction with the mold wall of a mobile eutectic phase. The reason the cone has its base at the bottom graphite punch may be due to differences in pressure at the top and bottom punches. Although the system is designed so that the sample is pressed from both ends, the pressure at the bottom may be distributed in part to the carbon black insulation
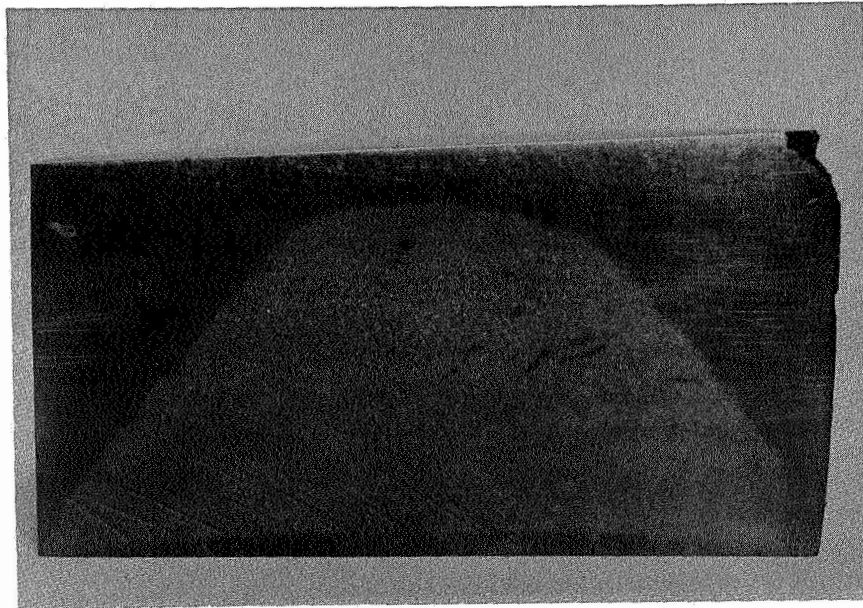
FIG. 43 - CONING EFFECT IN NbC-C COMPOSITE
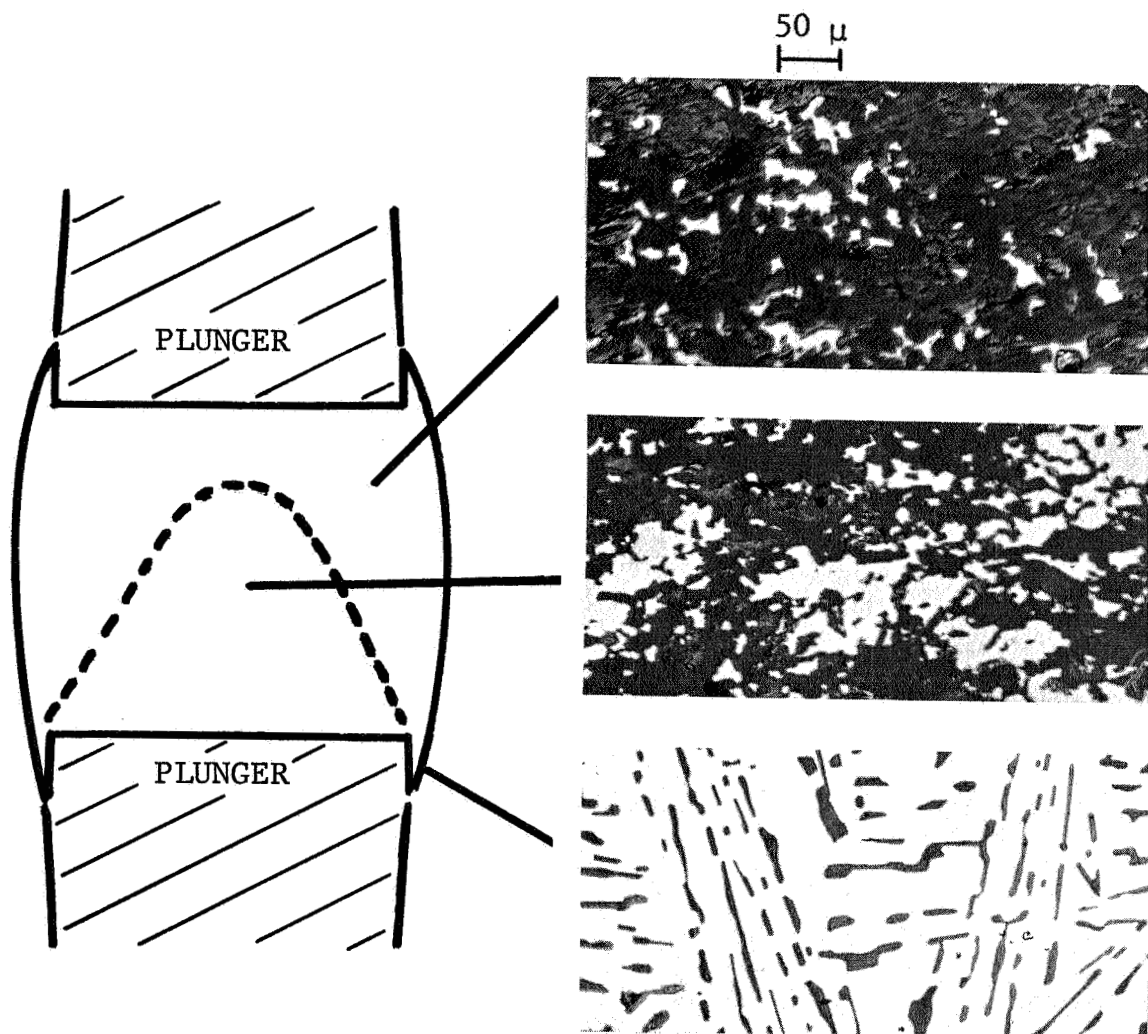
FIG. 44 - "CONING" EFFECT IN Nb-C COMPOSITE SHOWING
          HETEROGENEITY IN CARBIDE CONTENT
          AND FORMATION OF EUTECTIC STRUCTURE (320x)

under the bottom of the mold. Thus, the carbide-graphite particles toward the top of the charge may be in more intimate contact and more susceptible to eutectic formation.

Despite the heterogeneity shown by these materials, variations in flexural strength between "cone" and "noncone" samples were surprisingly small, being on the order of 10 to 15%. Furthermore, the strength values of 15,000 psi for 20 vol% NbC-C and 17,000 psi for 34 vol% NbC-C were about the highest observed in our experiments for composites containing these amounts of NbC. Thus, the beneficial effect of liquid phase hot pressing on strength was quite apparent. However, when the "coned" billet is considered as one piece instead of many smaller sections, differences in thermal expansion, conductivity and possibly high-temperature creep behavior may make this an undesirable material.

2. Temperature Calibration Experiments

A series of hot pressings were conducted to determine the temperature at which liquid formation occurred in the NbC-C system. The experiments were also designed to assess possible temperature gradients in the hot pressing mold. The NbC-C eutectic temperature has been variously reported as 3305±15°C,[26] 3220±40°C,[27] and 3220±50°C.[28] On the basis of our work, the latter temperatures would appear to be more realistic.

In these studies, eutectic mixtures of NbC-C were to be the "thermometer," i.e., formation of the eutectic structure would show if the solidus had been reached. Three pressings involving layers of various materials were conducted at 3200°C (two) and 3100°C, and were designated Sand-1, Sand-2 and Sand-3. The compositional makeup of these pressings are presented in Fig. 45.

Sand-1 - As shown for Sand-1 in Fig. 45, one eutectic layer was located toward the top of the mold and the other toward
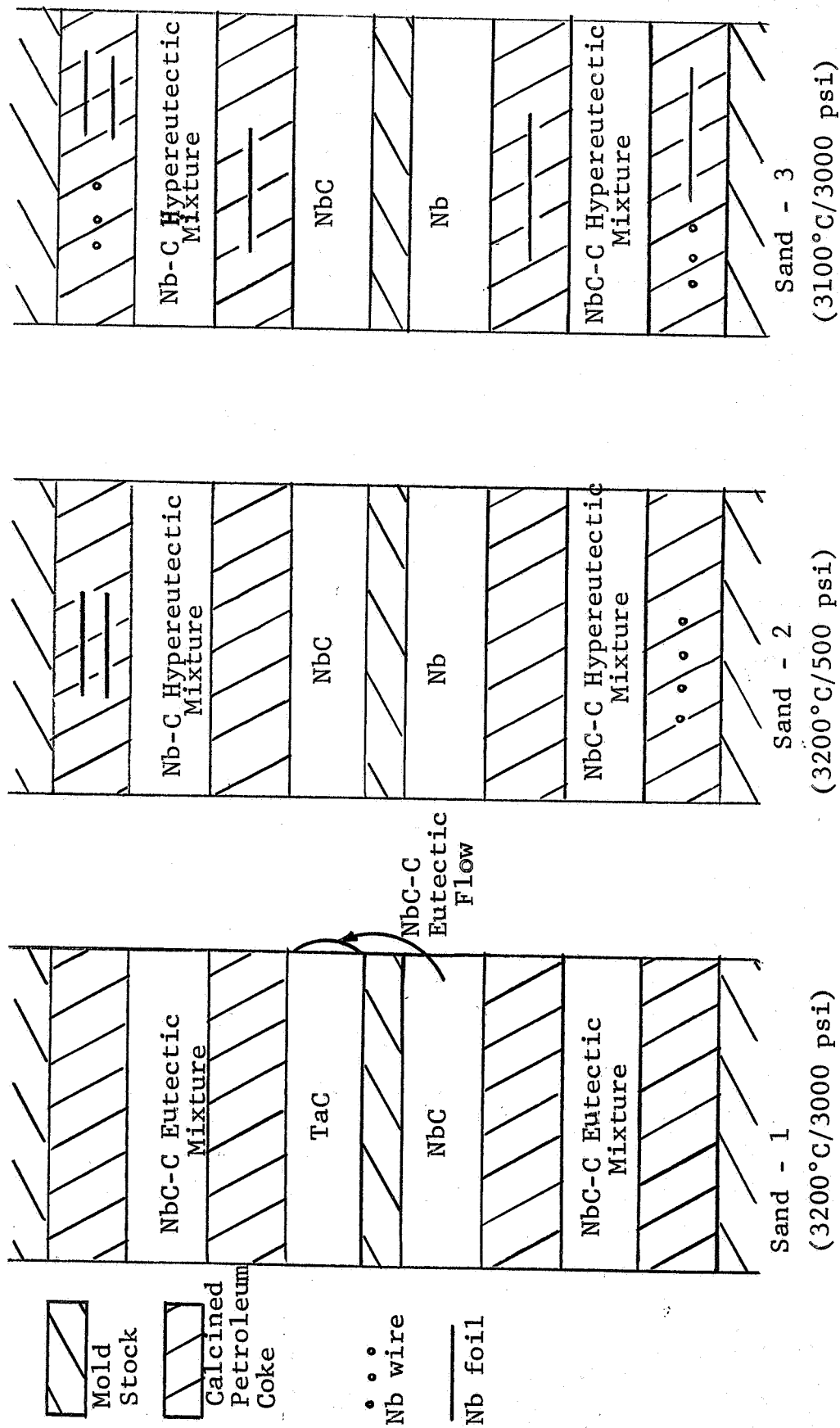
FIG. 45 - MATERIALS HOT PRESSED IN TEMPERATURE CALIBRATION STUDIES

Mold Stock

Calcined Petroleum Coke

Nb wire

Nb foil

Sand - 1
(3200°C/3000 psi)

NbC-C Eutectic Mixture

TaC

NbC-C Eutectic Flow

NbC

NbC-C Eutectic Mixture

Sand - 2
(3200°C/500 psi)

Nb-C Hypereutectic Mixture

NbC

Nb

NbC-C Hypereutectic Mixture

Sand - 3
(3100°C/3000 psi)

Nb-C Hypereutectic Mixture

NbC

Nb

NbC-C Hypereutectic Mixture

the bottom in an effort to determine possible temperature gradients. Also included were layers of TaC and NbC to determine possible diffusion of these materials into their carbonaceous surroundings. Layers of petroleum coke were used to separate the various layers so that the reactions in individual layers would be clearly defined.

The various materials were hot pressed at an indicated 3200°C and 3000 psi. Opening of the mold after the run revealed that most of the material had been lost through extrusion and reaction with the mold. The only layer which was clearly remaining was that of TaC. This suggested a very high mobility of NbC and/or NbC-C eutectic at these temperatures. Apparently the temperature attained was above the NbC-C eutectic but below that of TaC-C (3450°C).

Photomicrographs of two areas are shown in Fig. 46. The eutectic structure (NbC-C) in Fig. 46 was material which had extruded from the NbC layer and had solidified on the side adjacent to the TaC on cooling. The TaC phase appears rather porous; sectioning of samples from this layer and determination of densities revealed a range from 93.2 to 95.2% theoretical. Little if any solid solution between NbC and TaC occurred.

The layers depicted in Fig. 47 are for adjacent layers of NbC-C and calcined petroleum coke. Evidently much of the carbide had been extruded from the original eutectic (75 vol% NbC) mixture, leaving behind a structure corresponding to about 20 vol% carbide. The shape of the carbide particles suggests melting and recrystallization. This micrograph also shows very limited diffusion of carbide into the coke layer.

The beneficial effect of a liquid phase in producing dense graphite is also apparent in this micrograph (Fig. 47).
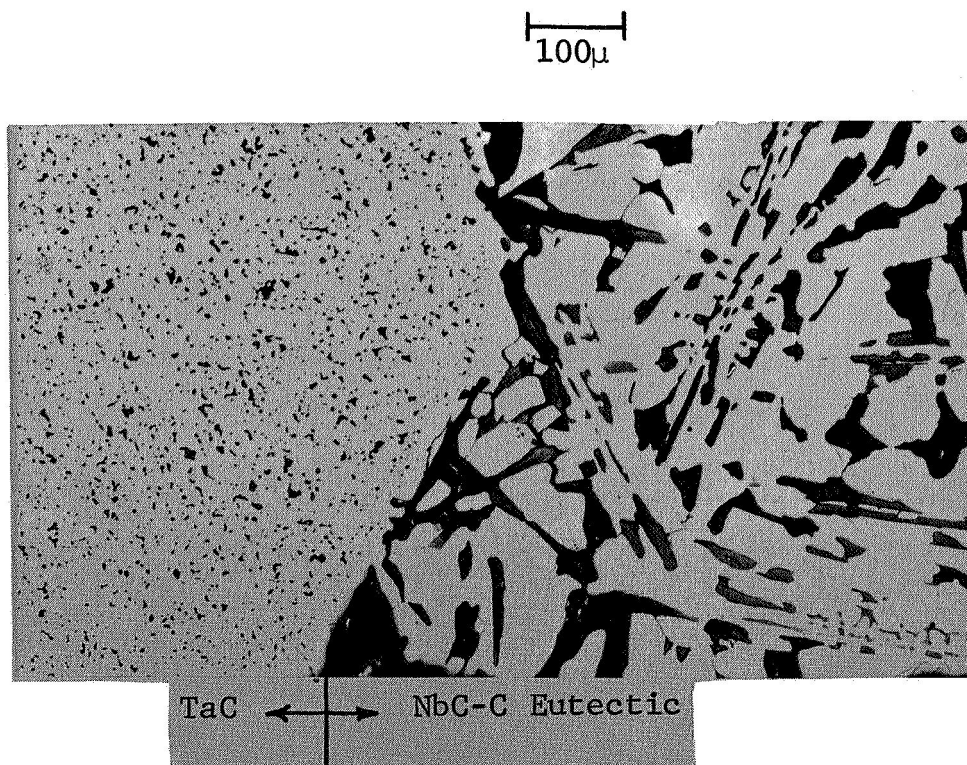
FIG. 46 - SAND-1: MICROSTRUCTURES OF TaC
AND PRECIPITATED NbC-C EUTECTIC (125x)
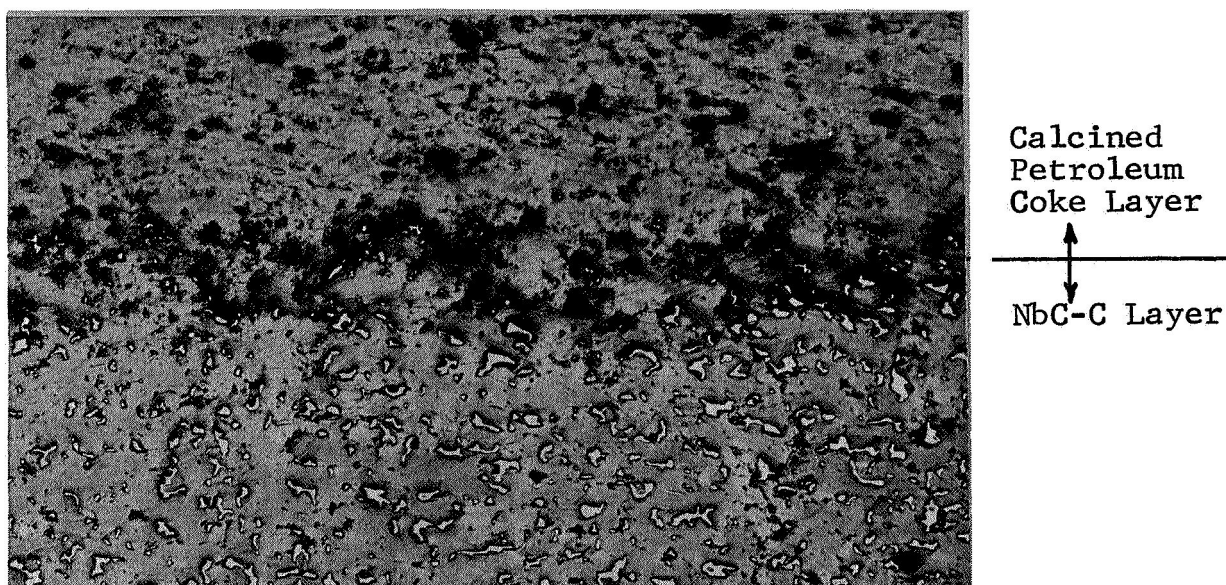
FIG. 47 - SAND-1: MICROSTRUCTURES OF ADJACENT COKE
AND COKE-CARBIDE LAYERS SHOWING DIFFERENCES
IN GRAPHITE STRUCTURE (125x)

The carbon source in both layers was calcined petroleum coke. The layer which did not incorporate NbC was quite porous whereas the layer containing the carbide exhibits a dense graphite phase. Apparently movement of a liquid eutectic phase through the carbon and precipitation of graphite upon cooling results in the formation of a dense structure. A similar behavior has been shown[2] for graphite in which molybdenum carbide was the mobile liquid phase.

Sand-2 - In view of the gross loss of material in the first experiment, a similar test was conducted at the same indicated temperature of 3200°C but at a reduced pressure of 500 psi. Some additions in materials were instituted in this pressing. As shown in Fig. 43, niobium metal foil and wire were imbedded into petroleum coke layers to act as diffusion couples. The purpose was twofold: one was to determine extent of carbide formation, and the second was to determine carbide diffusion into the graphite.

Examination of the mold interior after this pressing revealed that although material loss was again evident, much higher retention was realized with reduced pressure. The formation of a eutectic structure was evident in all of the layers as shown in the photomicrographs in Fig. 48. The Nb-C and NbC-C mixtures were designed as hypereutectics and both show excess graphite which had come out of solution. The carbide-carbon eutectic structure is also seen in the two layers which were originally pure metal and metal carbide containing no free carbon. During the pressing the metal formed the carbide and at the very high temperature, both carbide layers dissolved carbon from their environs in eutectic melting. Apparently diffusion of carbon into the carbide becomes quite rapid under these conditions. Graphite precipitates in these layers were observed at the boundaries with adjacent carbon layers.
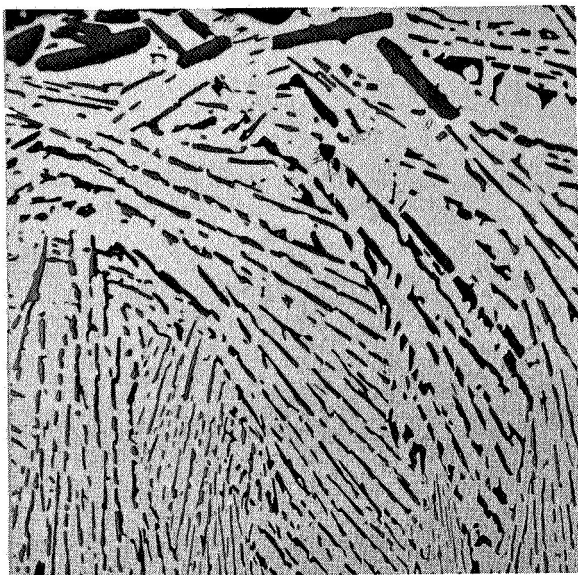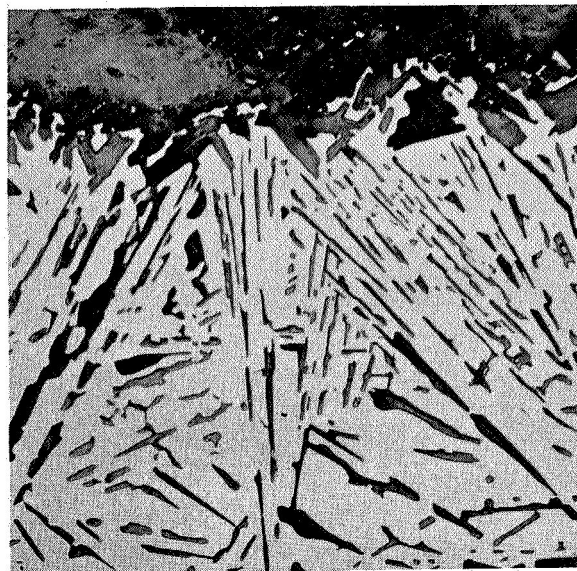
a) NbC Layer

b) Nb Layer
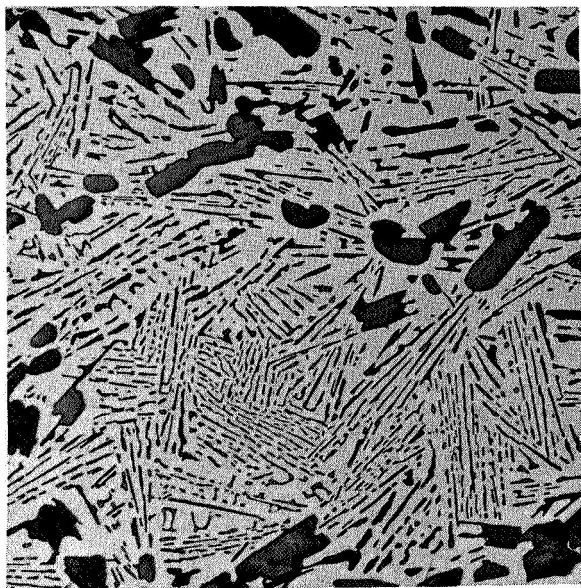
c) Nb-C Hypereutectic Layer
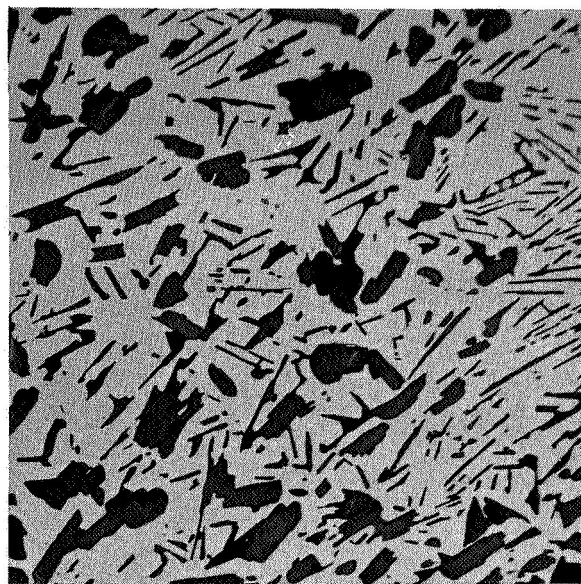
d) NbC-C Hypereutectic Layer

FIG. 48 - SAND-2: MICROSTRUCTURES OF NbC-C EUTECTICS
FORMED IN HOT PRESSING (125x)

A somewhat finer structure can be seen for the Nb-C and NbC layers which were in upper portions of the mold (Figs. 48a and 48c). This may be due to a slightly faster quench of the upper portions since heat loss on cooling would occur more rapidly toward the top, or open part of the hot pressing system.

Macroscopic examination of the coke layer containing the metal foil showed little evidence of metal carbide phase. Microstructural study revealed areas containing small amounts of NbC particles, similar to that seen in Fig. 47. Apparently much of the material had been lost through plastic flow.

On the other hand, the wire was retained in the coke matrix. As shown in Fig. 49, deformation of the wires due to the pressing direction is evident. Also in evidence is considerable material flow for one of the wires. Eutectic structure can be observed in both pieces showing that the metal had formed the carbide which in turn reacted with carbon to form the eutectic. The original diameter of the wire was 0.020 in. A volume gain of about 70% can be expected in the carbide formation plus eutectic reaction. The structure on the left side of Fig. 49 conforms to such dimensional growth, whereas the larger growth for the structure on the right may be due to concentration of material flow in a particular area.

Sand-3 - A third experiment was conducted in which the processing temperature was lowered to 3100°C. Some eutectic melting occurred in this pressing but the bulk of the NbC-C materials remained solid. There appeared to be a temperature gradient from top to bottom in that the wires in the top coke layer (see Fig. 45) formed eutectic structures whereas those in lower layers showed no evidence of such melting.

The various metal and metal carbide containing layers all exhibited melting and eutectic formation only at the interface

500μ
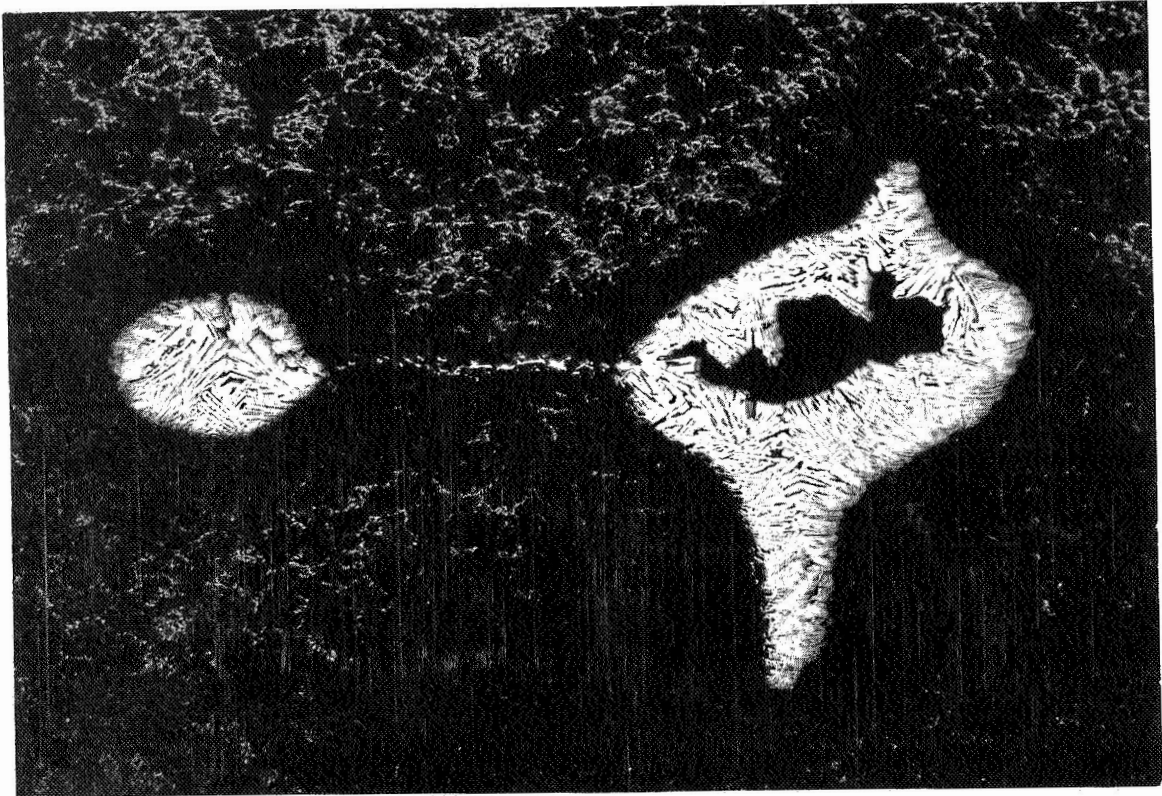
FIG. 49 - SAND-2: MICROSTRUCTURE SHOWING NbC-C EUTECTIC
FORMATION OF Nb METAL WIRE IN GRAPHITE MATRIX (30x)

between layer and mold. Microstructural examination of the "Nb-C hypereutectic" layer revealed eutectic and hypereutectic adjacent to the mold wall (Fig. 50a) and no eutectic formation within the layer (Fig. 50b). In both the NbC and Nb layers, a hypoeutectic structure (Fig. 51), i.e., primary NbC in a eutectic matrix, was observed at the layer-mold interface, and there was no evidence of any graphite toward the interior of these layers. It appears that melting and solution of a limited amount of graphite had occurred at the mold wall. Figure 52 shows the edge of the "NbC-C hypereutectic" layer. Examination of this area shows a zone of a NbC-C mixture which had not undergone melting, a hypereutectic zone, a hypoeutectic zone, and solid carbide. This gradation suggests that the layer was rich in carbide at the edge adjacent to the mold wall. The indicated segregation resulting in the carbide enriched zone is not understood at this time.

Summary - These experiments have enabled us to modify our temperature monitoring so that we might process NbC-C composites at as high a temperature as possible without gross loss of material through liquification.

Also shown by the studies was the ability of niobium to readily form the carbide and subsequently dissolve carbon to form the eutectic. Apparently at higher temperatures carbon is continually dissolved until the mixture is of either eutectic or hypereutectic composition.

It is also apparent that the presence of a liquid NbC-C eutectic phase enhanced densification of graphite. Part of this may be attributed to increased plastic flow. Another contributing factor is the high density and orientation of the graphite phase which precipitates from the eutectic. Full exploitation of such improvement in graphitization realized with the presence of a

$\vdash\!\overline{100\mu}\!\dashv$
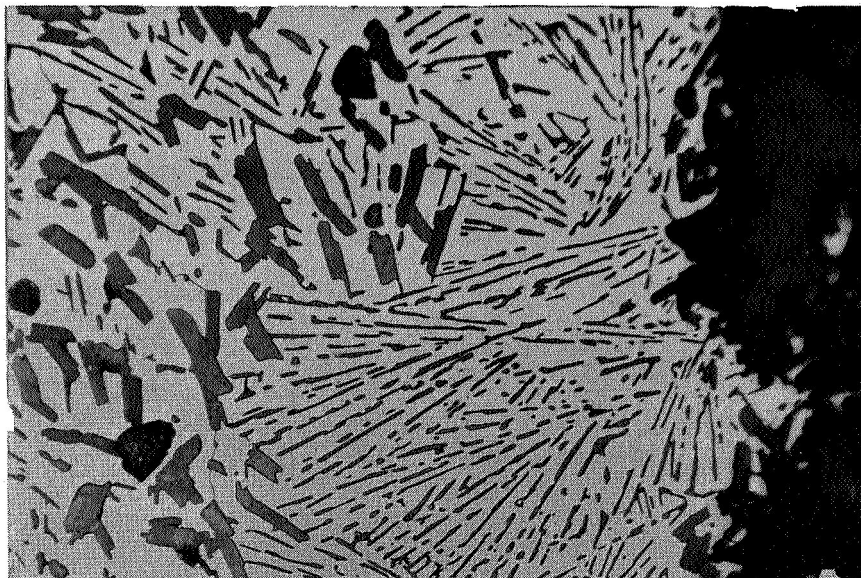
(a) Edge of Layer Adjacent to Mold Wall
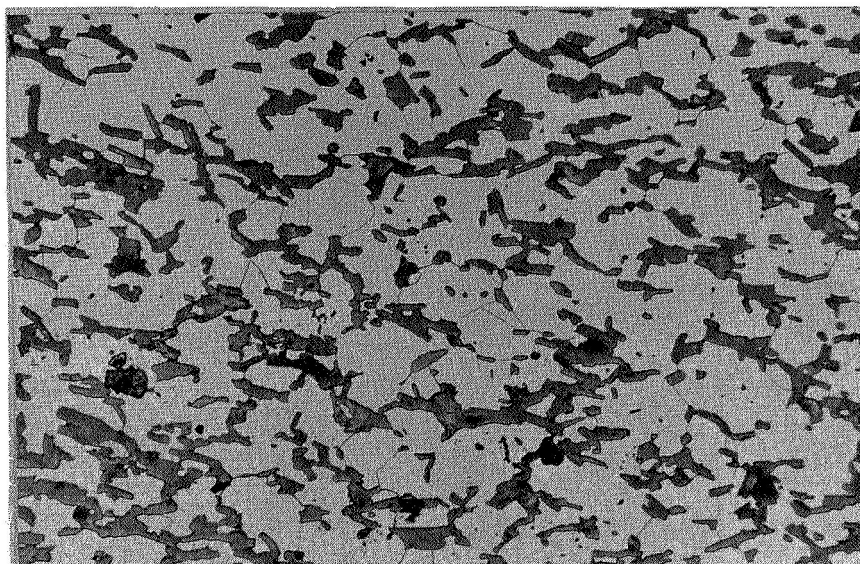
(b) Interior of Layer

FIG. 50 - SAND-3:   MICROSTRUCTURE OF Nb-C HYPEREUTECTIC
LAYER SHOWING FORMATION OF EUTECTIC STRUCTURE
IN THE AREA ADJACENT TO THE MOLD WALL(125x)
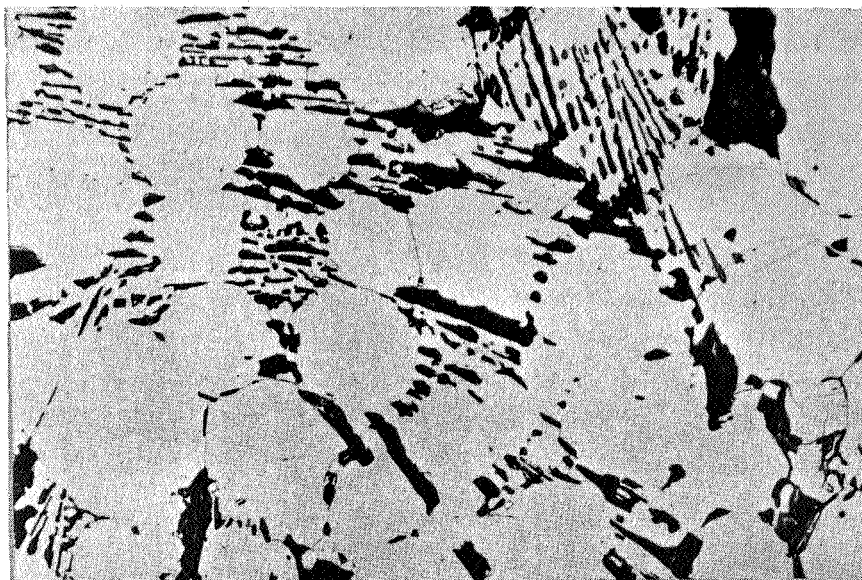
FIG. 51 - SAND-3:   HYPOEUTECTIC STRUCTURE
              AT EDGE OF Nb LAYER SHOWING
              PRIMARY NbC IN NbC-C EUTECTIC (125x)
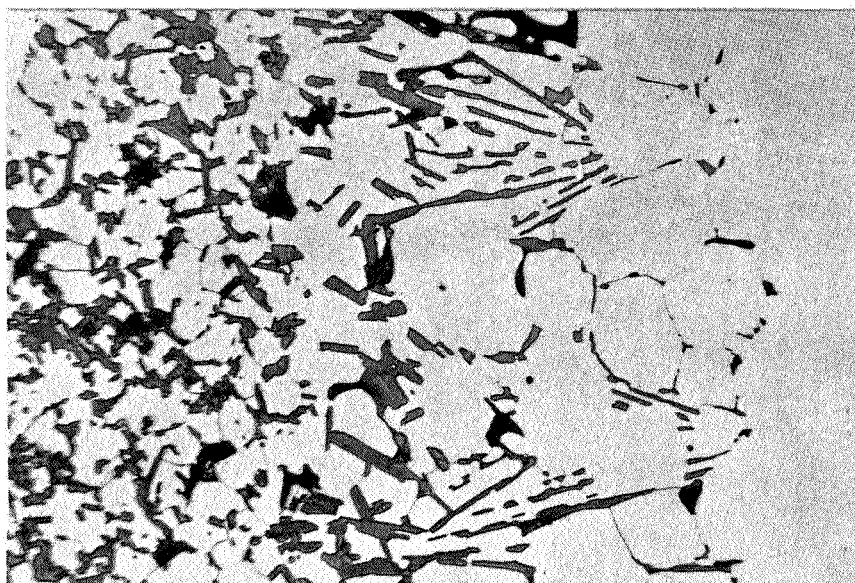
FIG. 52 - SAND-3:   EDGE OF NbC-C LAYER
              SHOWING HYPEREUTECTIC AND
              HYPOEUTECTIC STRUCTURE (125x)

liquid carbide phase can lead to very high strength graphite matrix composites.

G. Heat Treatment Studies

In the determinations of thermal expansion of composites, it was observed that permanent dimensional changes had occurred in the samples due to the heat treatment. These changes were an increase in the A/G or c-axis direction and a decrease in the W/G or ab-plane direction, and were more pronounced with graphite-rich materials. A relaxation of stresses imparted to the composite during hot pressing, may be responsible for such changes. In the cooling process after fabrication, different expansion behavior in the anisotropic graphite crystallites builds up residual stresses which would be relieved on subsequent heat treatment.

1. Heat Treatment Effects on Dimensions

Experiments were conducted on the effect of heat treatment on flexural strength and electrical resistivity as well as dimensional changes. Composites in both the NbC-C and TaC-C systems were subjected to a heat treatment of 2500°C for 1 hr in an argon atmosphere. In addition, some NbC-C samples were held at 2800°C for 1 hr. The resulting dimensional changes as a function of carbide content are presented in Figs. 53 and 54.

As shown in Fig. 53 for the NbC-C system, expansion in the A/G direction and contraction in the W/G direction diminish with increasing carbide content. This is logical in that as the carbide becomes the dominant phase, stress relief of the minor graphite phase is further restricted by the isotropic cubic carbide. It is felt that the changes are not due to an ordering effect for the graphite crystallites. Such ordering would produce the opposite effect, i.e., increase in the W/G and decrease in the A/G direction, as shown by other investigators.[29]
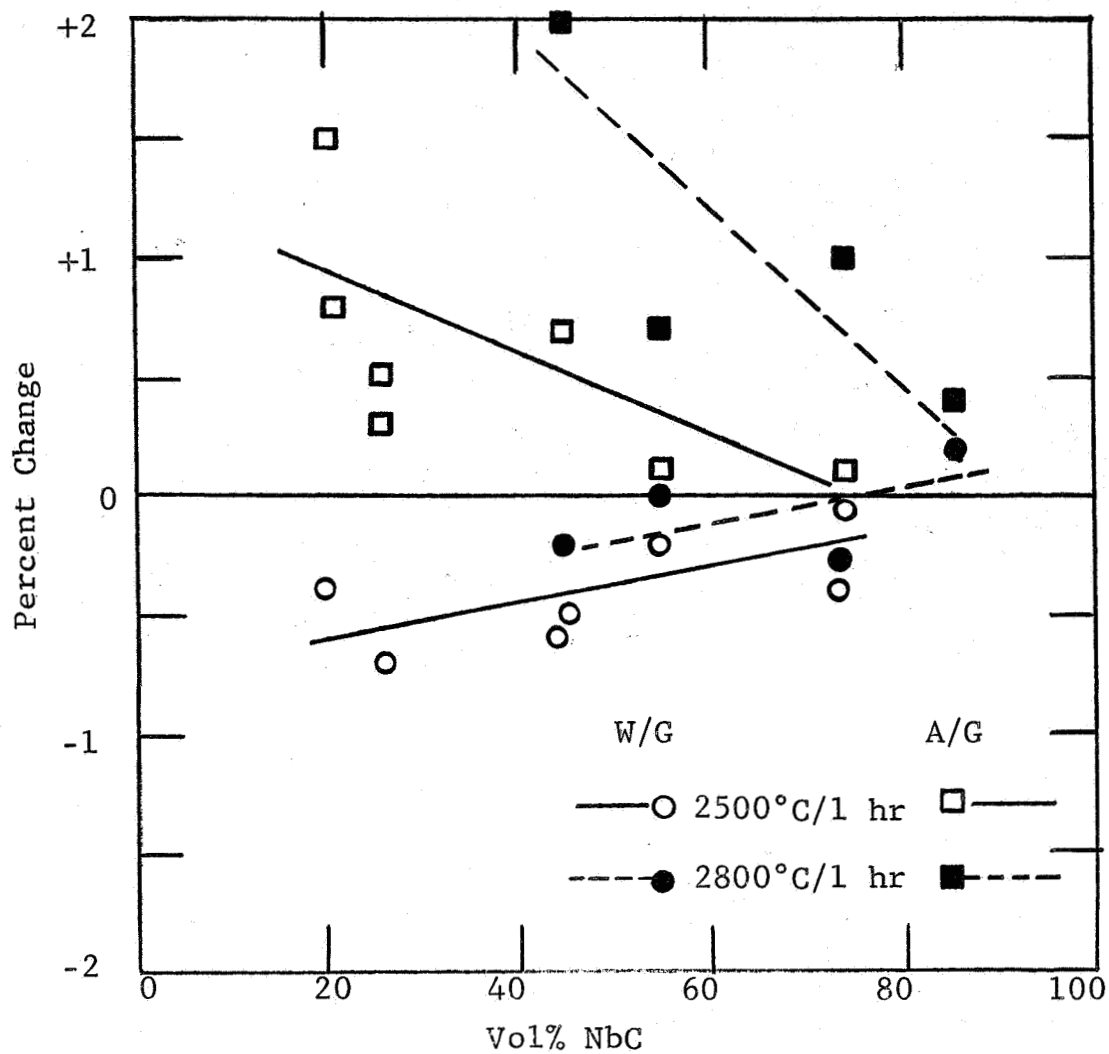
FIG. 53 - HEAT TREATMENT EFFECTS ON DIMENSIONS
OF NbC-C COMPOSITES
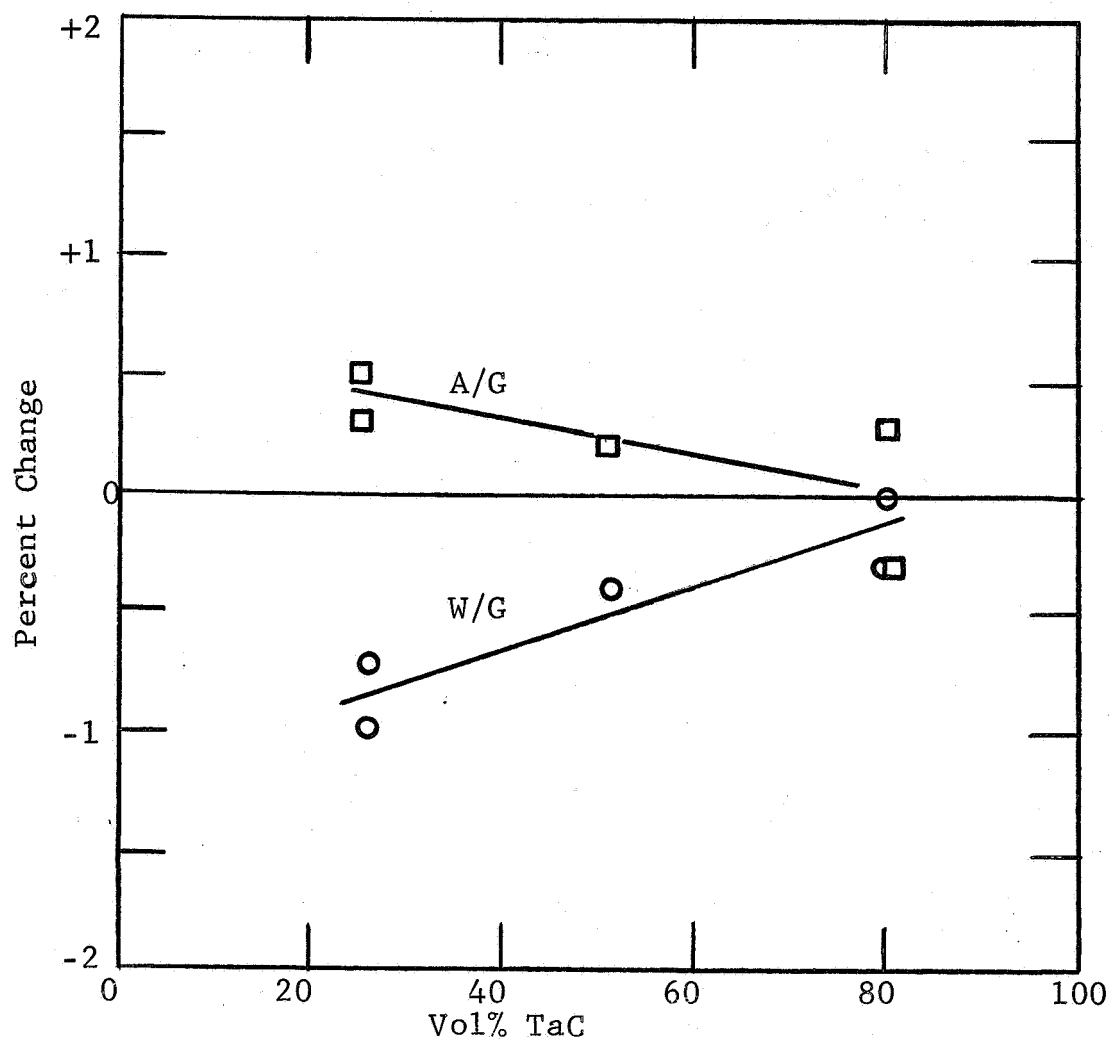
FIG. 54 - HEAT TREATMENT EFFECTS ON
DIMENSIONS OF TaC-C COMPOSITES
(2500°C/1 hour)

The data for NbC-C composites heat treated at 2800°C indicates an additional increment of change in the A/G direction at the higher temperature. Shrinkage in the W/G direction appears to be somewhat smaller, and changes again are inversely related with carbide content. These data suggest that even greater dimensional changes may occur at higher temperatures; tests will be conducted at 3000°C and possibly higher in order to establish this trend.

Changes for TaC-C composites followed relationships similar to those for NbC-C as shown in Fig. 54. These materials will also be subjected to higher temperatures at possibly longer times so that an end point might be attained.

2. Heat Treatment Effects on Electrical
and Mechanical Properties

Most of the samples exhibited little change in electrical resistivity or flexural strength due to heat treatment. Exceptions were two materials of high carbide content in the NbC-C system (C3-80Nb and 80Nb-B) which had displayed low strengths (6,600 and 13,000 psi, respectively) in earlier tests. Normally composites containing 73 vol% NbC exhibit strengths of about 17,000 to 20,000 psi.

Changes in electrical resistivity and flexural strength are presented in Table VIII. Permanent decreases in resistivity occurred for all samples; they were particularly pronounced for some of the C3-80Nb specimens. The flexural strengths of the heat-treated samples confirm the improved bonding suggested by the changes in electrical conductivity. In two of the samples (C3-80Nb, samples 1C and 4A) macroscopic cracks were evident both before and after heat treatment. The significant drop in resistivity and increase in flexural strength indicate that some sintering had occurred in these flaws.

Table VIII

EFFECT OF HEAT TREATMENT ON MECHANICAL AND ELECTRICAL PROPERTIES
OF SELECTED NbC-C COMPOSITES

Compositional Designation	Sample No.	Grain Direction	As Pressed		2500°C/1 Hour	
			Flexural Strength, psi	Electrical Resistivity, μΩ-cm	Flexural Strength, psi	Electrical Resistivity, μΩ-cm
80Nb-B	5C	W/G	13,260*	50.1	18,240	44.0
	5A	W/G		49.8	23,750	44.6
	5B	A/G	5,280*	64.3	10,460	57.2
	7B	A/G		61.1	10,380	57.1
C3-80Nb	5A	W/G	6,660*	52.1	16,530	45.6
	5C	W/G		56.3	16,630	48.2
	1C	W/G		232	12,130	45.5
	1A	A/G	4,010*	82.6	12,830	61.1
	4A	A/G		284	7,950	63.0
	2B	A/G		160	10,260	53.1

*Averages for 4 or more samples

3. Heat Treatment Effects on Microstructure

Typical microstructures of C3-80Nb before and after heat treatment appear in Fig. 55. The "before" structure is rather porous in comparison to the "after" structure, indicating that densification had occurred. This was reflected to a small degree in bulk density measurements in which a change of about 0.5% was observed. The photomicrographs also show that there was no carbide grain growth. Although increased bonding indicates some sintering the heat treatment conditions apparently were insufficient to cause grain growth.

Heat treatment of composites at 2500°C appears to be extremely beneficial in upgrading mechanical properties of high carbide content composites which are poorly bonded. These particular annealing conditions failed to change the properties of graphite matrix composites and TaC-C samples. Thus, it would appear that improvement in strength occurs due to improved bonding by sintering rather than by relief of stresses. Furthermore, materials which have been processed to relatively high strengths are also unaffected. It is possible that a higher temperature treatment may be beneficial for TaC-C in which sintering of TaC could occur.

These experiments show that an annealing step subsequent to hot pressing of composites can be quite important in obtaining sound materials. Equally important is the dimensional stability which would be achieved prior to actual use at elevated temperatures.

IV. FUTURE WORK

Composites in the NbC-C and TaC-C systems have shown the most promise for high-temperature, structural applications. Thus, future studies will be primarily concerned with these systems and emphasis will be placed on developing more isotropic

50 μ

(a) Before Heat Treatment
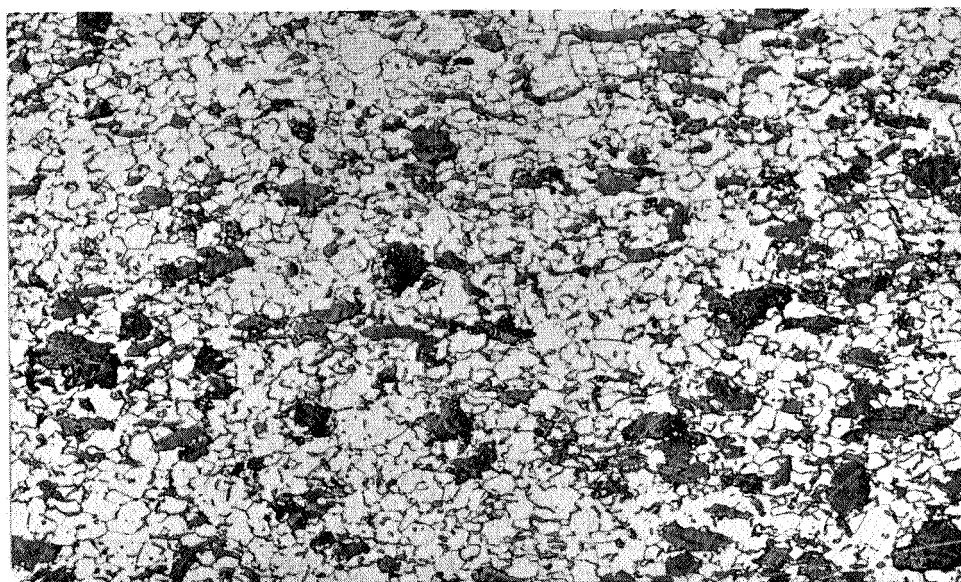
(b) After Heat Treatment

FIG. 55 - TYPICAL MICROSTRUCTURES OF 80 VOL% NbC-C
COMPOSITE (C3-80Nb) BEFORE AND AFTER
2500°C/1 HR HEAT TREATMENT (200x)

materials with good resistance to high temperature deformation. To accomplish this purpose the work scope will consist of the following:

1. Carbon Source - Variations in carbon source which contrast with the needle coke used in earlier studies will be evaluated. Materials to be studied include graphite powders and resin cokes.

2. Particle Size and Shape - These parameters will be varied so as to obtain different morphological relationships between the graphite and carbide phases.

3. Use of Sintering Aids - Small amounts of additives will be incorporated in the TaC-C system to obtain liquification at temperatures lower than the 3450°C eutectic temperature. This will permit exploitation of the densification and improved bonding obtainable in liquid phase sintering at processing temperatures of 3200°C or lower.

4. Property Evaluation - The effects of the above mentioned variables upon physical and mechanical properties of composites in both grain directions will be determined. Particular attention will be paid to creep behavior of these materials at temperatures ≥ 2500°C and to the degree of anisotropy.

It is anticipated that these investigations will yield information which can be used to optimize high-temperature properties of carbide-graphite composites containing NbC or TaC. The information should also be applicable to compositions incorporating other metal carbides.

V. CONTRIBUTING PERSONNEL AND LOGBOOK RECORDS
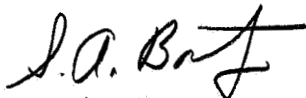
The following personnel have participated in this research program: S. A. Bortz, Y. Harada, J. L. Sievert, G. Besbekis, and R. Baker. All data pertaining to this program are recorded in IITRI Logbook Nos. C 16816, C 16973, C 16974, C 16986, C 16989, C 17303, C 17308, C 17314, C 17320, C 17323, C 17830, C 17838, and C 17905.

Respectfully submitted,
IIT RESEARCH INSTITUTE

Y. Harada
Associate Ceramist
Ceramics Research

APPROVED:

S. A. Bortz
Senior Engineer
Ceramics Research

Appendix A

<u>THERMAL MECHANICAL PROPERTIES</u>
<u>WHICH AFFECT THERMAL SHOCK</u>
<u>AND THERMAL STRESS</u>

IIT RESEARCH INSTITUTE

Appendix A

THERMAL MECHANICAL PROPERTIES
WHICH AFFECT THERMAL SHOCK
AND THERMAL STRESS

The behavior of materials in response to temperature gradients and rate of temperature change is perhaps the most important consideration in designing for severe temperature environmental conditions. The scope of this discussion will be directed toward understanding the properties which affect thermally induced stresses and proper control of these properties to reduce thermal stresses.

A.   Thermal Shock and Thermal Stress

In the literature of materials technology there still appears to be some confusion as to the definition of thermal stress and thermal shock. The following paragraphs will attempt to define these phenomena.

Thermal shock and thermal stress loading have always been problems in using brittle materials because these materials cannot withstand rapid changes in temperature. Many investigators have looked at the problem of thermal stresses in ceramics. They have developed steady-state procedures for examining the resistance of ceramic bodies to changes in temperature. Others have looked at the thermal shock resistance of ceramics and have developed quench tests for this type of study. Analysts have also developed elastic equations for calculating thermal stresses within various geometric solids when the temperature gradients are known. Recently, there has been additional work to develop equations for the plastic state.

Thermal stresses are defined as those resulting from a temperature gradient. A body that is evenly heated and free to expand or contract in all directions will have no thermal stresses. If the body is restrained from expanding, stresses are developed within the body proportional to the restraining force. A free body unevenly heated so that a temperature gradient is established also develops thermal stresses. Under these conditions, the cooler portions of the body provide the restraining force for the hotter sections.

Thermal shock as differentiated from steady-state thermal stress usually refers to cases in which a body experiences sudden changes in temperature due either to a change in external environment or to internal heat generation. It is the transient feature of temperature distribution that distinguishes thermal shock stresses from steady-state thermal stresses. Although thermal shock stresses are determined by temperature distribution, (and are little different from what they would be if the same temperature distribution could be obtained in the steady-state condition) such stresses are often greater than those due to slow heating and cooling because of steeper temperature gradients that can be generated in this way.

Another distinction between ordinary thermal stress and thermal shock is that the rate of application of the stresses in thermal shock is very rapid. Such properties as specific heat and conductivity, which do not enter directly into consideration for thermal stresses under known conditions of temperature, become important in thermal shock applications. These properties determine the rate of climb or fall of temperature, temperature gradients, and the rate of change of the gradients, which in turn govern strains and strain rates. Since some materials

are more sensitive than others to stress gradients or to strain rate (due to microstructural and elastic property effects), thermal shock tests may rate materials differently than tests involving slowly applied thermal gradients.

B.   Property Changes Which Affect Thermal Shock and Thermal Stress

Thermal shock, as well as thermal stress, is induced by temperature gradients. The principal material properties that determine thermal stress resistance of ceramic materials are tensile strength (σ); Young's elastic modulus (E); Poisson's ratio (μ); coefficient of thermal expansion (α); thermal conductivity (K); thermal diffusivity (a); and emissivity (e); each of these is a function of temperature.

Most problems encountered are three-dimensional. Equations for three-dimensional problems are difficult to solve, and it is desirable to reduce the problem to a one or two dimensional problem. If the body is very thin as in a plate, the temperature can be considered as a function of x and y, and any variation in Z can be neglected. The problem is said to be one of plane stress, since only the stresses in the xy plane through the center are considered.

At the other extreme when the Z dimension of the body becomes very large compared with other dimensions, but where the temperature does not vary with Z, all planes perpendicular to the Z axis can be considered similar. Such a case is encountered if a long cylinder is quenched. If the ends are constrained from axial motion by end plates, it is apparent from the symmetry of the problem that all planes will be constrained from axial motion. A plane of unit thickness "A" can then be analyzed on the basis that $\epsilon_Z = 0$. The case of a long hollow cylinder

without end restraint is that of the generalized plane strain problem. For a linear temperature distribution:

$$T = t_i \left(\frac{r_o - r}{r_o - r_i}\right)$$

The equation for stress can be shown as:

$$\sigma_t = \frac{E\alpha t_i}{3(1-\mu)(r_o - r_i)} \; fn \; (r, \; r_o, \; r_i) \qquad (1)$$

For a logarithmic temperature distribution:

$$T = \frac{t_i}{\ln\left(\frac{r_o}{r_i}\right)} \; \ln\left(\frac{r_o}{r}\right)$$

The equation then becomes:

$$\sigma_t = \frac{E\alpha t_i}{2(1-\mu) \; \ln(r_o/r_i)} \; fn \; (r, \; r_o, \; r_i) \qquad (2)$$

where σ_t is the tangential stress; t_i the inside temperature; r_o the outside radius; r_i the inside radius; r any intermediate radius; and T the temperature at a radius r. The above equations are used for analyzing steady-state thermal stress conditions.

Now consider the analysis of thermal shock. First, it is necessary to know what the temperature distribution is at a time (t) after the surrounding temperature has been changed. Thermal stresses are then calculated using equations in the theory of elasticity. For a thick wall which is at a temperature (t_i) throughout, the surface temperature changes suddenly to t_o. The equation for temperature of a point in the wall is:

$$t = t_o + (t_i - t_o) \; f \left(\frac{X}{2\sqrt{\alpha T}}\right) \qquad (3)$$

where t is the temperature in the wall of a distance (X) from the surface of a time (T) after the sudden temperature changes of

the surface; α is the thermal diffusivity, and $f\left(\frac{X}{2\sqrt{\alpha T}}\right)$ is a function which is called Gauss' error integral. Figure A-1 is a plot of this relationship which can be used to determine temperature distribution through a thick wall. The thermal diffusivity of a material is related to other thermal properties such as density (ρ), thermal conductivity (K) and specific heat (C_p) by the equation:

$$\alpha = \frac{k}{\rho C_p} \tag{4}$$

Elastic stress equations to be considered when calculating stresses have to do with the analysis of a composite cylinder where the outer ring (A) is affected by the change in temperature and the inner ring (B) is not (Fig. A-2). For the dynamic case, using Eq 3, a plot can be made of the temperature gradient through the cylinder wall which is shown schematically in Fig. A-3. From these analytical considerations it is possible to determine the effect of material properties on thermal stress or thermal shock. The temperature differential at which thermal stress fracture will occur is a function of these relationships:

$$\Delta T = (\sigma, 1/E, 1/\alpha, K, 1/e) \tag{5}$$

In addition, particle size, porosity, surface condition, residual stresses, and grain bonding of ceramic bodies introduce major variables which strongly affect mechanical properties, and to a lesser extent, thermal properties. Still another variable introduced when correlating thermal stress data with physical properties is the effect of the volume under stress on the strength value obtained. This depends on the homogeneity of the material (distribution of flaws). The effective surface energy required for crack propagation is a variable affecting the damage to be incurred after fracture has been nucleated. This

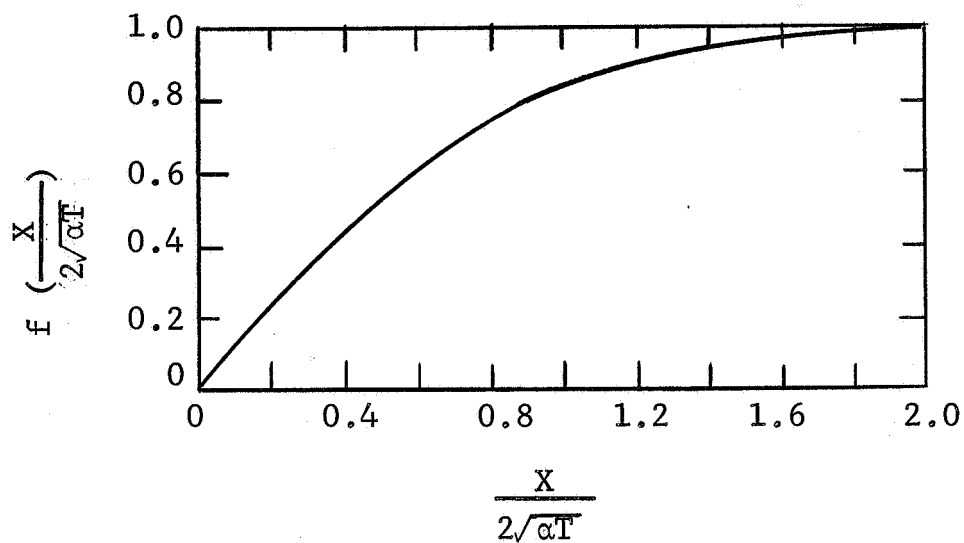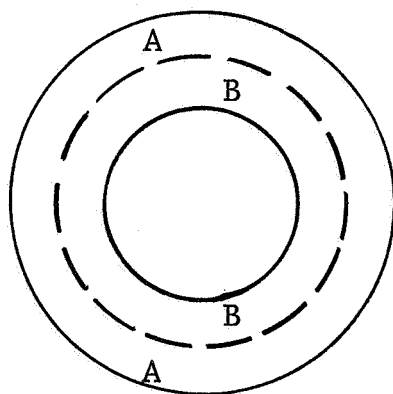FIG. A-1 - GAUSS' ERROR INTEGRAL

(A) $\epsilon_{\text{circumferential}} = \alpha\Delta T$
   outer ring

(B) $\epsilon_{\text{inner}} = 0$ since $\Delta T = 0$

Therefore, $\Delta\epsilon = \alpha\Delta T$

FIG. A-2 - DETAIL OF CYLINDER SHOWING HOW MATERIAL
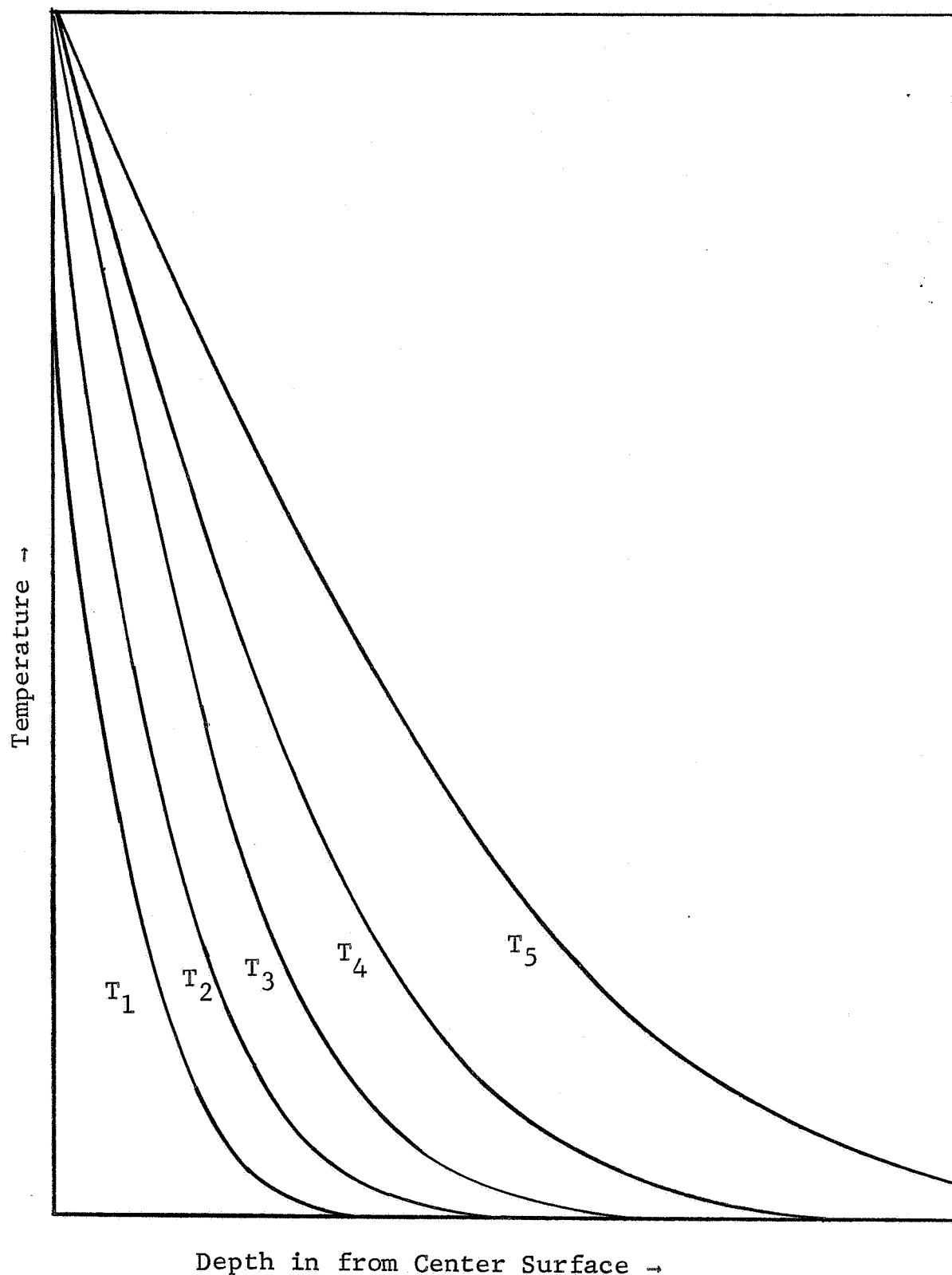IS DIVIDED BETWEEN HEATED AND UNHEATED
SECTIONS

Fig. A-3 - TEMPERATURE DISTRIBUTION AS A
FUNCTION OF TIME

damage is also a function of the elastic energy stored at fracture and available for crack propagation. Consequently, it is not possible to designate a single factor called "resistance to thermal stress" as a material property as can be done with fundamental physical properties, such as density or coefficient of expansion. Instead, the environmental conditions and component shape greatly influence the observed failure.

In the analysis of resistance to thermal stresses, the assumption is made that the material is elastic and obeys Hooke's law up to the fracture stress. For brittle nonmetals, these assumptions are quite good at low temperatures, and E is almost independent of T at low temperatures. As the temperature increases, there is a decrease in E owing to grain boundary relaxation, and at still higher temperatures plastic or viscous flow may take place. Measurement of E is possible in either tension or bending. At higher temperatures, where some plastic flow can occur, stress distribution is different from that assumed, and a low value of E results. However, in thermal stress calculations the assumption is made that Hooke's law applies, and the best approximation for elevated temperatures is to employ E measured in bend tests, even though this may not be a true elastic constant.

Poisson's ratio, μ, which enters into the equation for thermal stress resistance, is relatively constant with temperature and between materials (varying from 0.18 to 0.35). At higher temperatures, the measured value of μ increases to a limit of 0.50 where plastic flow begins.

The temperature-dependent mechanical properties of a ceramic material normally decrease slowly and linearly at first with increasing temperature and then drop off more rapidly at some critical temperature.

1. Thermal Conditions

When specimen size is sufficiently large, conditions approach the case where surface temperature is altered without changing the mean body temperature. The thermal stress resistance can be considered independent of the coefficient of heat transfer between the material and its surroundings, the surface, and the thermal conductivity. For moderate rate of temperature change, the thermal stress is approximately proportional to the normal distance from the center axis (r_m) and the coefficient of heat transfer (h) and is inversely proportional to the thermal conductivity (K). Thermal stress resistance for this case is inversely proportional to specimen dimensions. For steady-state conditions, the temperature drop for a given heat flow is directly proportional to wall thickness, and increased thermal stresses occur. However, if the temperature change (not heat flow) is maintained constant, no stress change occurs.

The rate of heating or cooling is an important factor in the development of thermal stresses and is affected both by the conditions imposed and by the physical properties of the material concerned. Measurements of the heat transfer coefficient (h) are largely for the steady-state condition and few data are available for transient conditions. The assumption that h remains constant (the condition taken for most thermal stress calculations) is only an approximation for most practical cases, and can be expected to hold closely only for small temperature differences. It is a reasonable approximation for ceramic bodies having poor thermal stress resistance; it is a poor assumption for the better refractory materials. Another complicating factor is the neglect of changes in thermal conductivity with temperature. A sharp change in heat capacity changes the temperature distribution and, consequently, the stress, especially in the transient state.

While these changes are not usual in ceramic materials, a sharp decrease in the thermal conductivity of dense crystalline ceramics does normally occur.

2. Microstructure

In this section the relation between porosity or grain size and the mechanical and physical properties of ceramics will be discussed. The work of various investigators to develop empirical equations which relate microstructure to physical and mechanical properties will be referenced.

For pure crystalline materials the porosity, purity, and grain size become quite important. Porosity has its greatest effect on strength,[30] and this relation can be found using the following equation:

$$S = S_o e^{-cP} \tag{6}$$

where
- S = strength of a porous material
- S_o = strength of material with zero porosity
- P = fractional porosity
- c = material constant
- e = 2.718

Decreasing porosity from 10 to 2% provides an increase in strength by a factor of two. Larger scatter on individual measurement also occurs at low porosities, indicating that strength is becoming less dependent on total porosity and more dependent on surface defects.

The effect of porosity on elastic modulus has also been examined by Murray[31] who found that the variation of E with porosity is less than the variation of transverse strength.

Loeb[32] predicts linear relationships between thermal conductivity and porosity. Loeb's equation takes the form:

$$K = K_o (1-P) \tag{7}$$

where K = thermal conductivity of material of fractional porosity, P

          K_o = thermal conductivity for zero porosity

          P = porosity

Generally, thermal conductivity increases by about 10% for a decrease in porosity from 10 to 2%.

The effect of increased grain size on strength of ceramic materials is deleterious. On the basis of the Griffith crack theory, strength should be inversely proportional to the square root of the grain diameter. Reduction of grain size from several tens of microns to several microns approximately doubles the strength.

Crandall,[33] and Spriggs and Vasilos[34] have developed an equation which shows the effect of grain size on strength:

$$\sigma = \sigma_o G^{-a} \tag{8}$$

where σ_o = strength of polycrystalline material with a specific grain size

          G = average grain size (μ)

          a = material constant

Increased grain boundary area and consequent increased scattering of energy by the grain boundary "material" will decrease thermal conductivity. Thus with fine grain size material, an increase in strength will be somewhat offset by the decrease in thermal conductivity, but the overall thermal stress resistance factor will be increased by a factor of two. If, in addition to the previous criterion of low porosity, fine grain size is also added, there may be an improvement in thermal stress

resistance by a factor of four with respect to the material of 10% porosity and 20μ grain size, due mainly to the effects on strength.

In summary, the important factors to be controlled in order to improve thermal stress and thermal shock resistance of a material are; increased strength, thermal conductivity, and Poisson's ratio, decreased elastic modulus, coefficient of expansion, and emissivity. Effect of porosity must be a trade-off between strength, elastic modulus, and thermal conductivity. The effect of grain size is a trade-off between strength and thermal conductivity. The above analysis provides a guide to the direction for further research with respect to control of material properties.

REFERENCES

1. Harada, Y., "Graphite-Metal Composites," IIT Research Institute, Report No. IITRI G6003-F4, (July 28, 1965).

2. Harada, Y., "Graphite-Metal Composites," IIT Research Institute, IITRI Project G6003 Final Report, (August 1, 1966).

3. Davidson, K.V., Riley, R.E. and Taub, J.M., "Carbide-Graphite Composites: Second Progress Report," Los Alamos Scientific Laboratory, LA-3652-MS, (June 15, 1967).

4. Riley, R.E., LASL (private communication).

5. Davidson, K.V., Riley, R.E. and Taub, J.M., "Carbide-Graphite Composites," Los Alamos Scientific Laboratory, LA-3569-MS, (October 19, 1966).

6. Turner, J.H. and Carter, M.B., "Research and Development on Advanced Graphite Materials: Volume XXXIII. Investigation of Hot Worked Recrystallized Graphites," WADD TR 61-72, (June, 1964).

7. Shaffer, P.T.B., "High Temperature Materials: No. 1," Materials Index, Plenum Press, New York (1964).

8. Coble, R.L. and Kingery, W.D., "Effect of Porosity on Physical Properties of Sintered Alumina," J. Am. Ceram. Soc. 39 (11) 377-85 (1956).

9. The Industrial Graphite Engineering Handbook, Union Carbide Corporation, (1965).

10. Johansen, H.A. and Cleary, J.G., "The Ductile-Brittle Transition in Tantalum Carbide," J. Electrochem. Soc. 113 (4) 378-381 (1966).

11. Kingery, W.D., Introduction to Ceramics, Wiley and Sons: New York (1960) p. 607.

12. Miccioli, B.R. and Shaffer, P.T.B., "High Temperature Thermal Expansion Behavior of Refractory Materials: I, Selected Monocarbides and Binary Carbides", J. Am. Ceram. Soc. 47 (7) 351-56 (1964).

13. Miccioli, B.R., "Carbide-Graphite Polyphase Systems," Preprint, presented at Am. Ceram. Soc. Electronics Div. and 18th Pacific Coast Regional Meeting, San Diego, California (27-29 October 1965).

14. Storms, E.K., "A Critical Review of Refractories," Los Alamos Scientific Laboratory, LA-2942, p. 52, (August 13, 1964).

15. Williams, W.S., "Influence of Temperature, Strain Rate, Surface Condition, and Composition on the Plasticity of Transition-Metal Carbide Crystals," J. Appl. Phys. 35 (4) 1329-1338 (1964).

16. Seldin, E.J., "Research and Development on Advanced Graphite Materials: Volume VI. Creep of Carbons and Graphites in Flexure at High Temperatures," WADD TR 61-72, (June, 1962).

17. Hague, J.R. et al, "Materials Selection Handbook," ASD-TDR-63-4102 (October, 1963).

18. Holliday, L., "Composite Materials," Elsevier Publishing Company New York - Chapter II p. 28-62.

19. Ibid p. 9-18.

20. Paul, B., "Prediction of Elastic Constants of Multiphase Materials," Transaction of Metallurgical Society of AIME Volume 218(February, 1960) p. 36-41.

21. Hirsh, T.J., "Modulus of Elasticity of Concrete Affected by Elastic Moduli of Cement Paste Matrix and Aggregate," Proceeding Am Concrete Inst Volume 59 (March, 1962) p. 427.

22. Hashin, Z. and Shtrikman, S., "A Variational Approach to the Theory of Elastic Behavior of Multiphase Materials," J. Mech Physical Solids Volume 11 (1963) p. 127-140.

23. Holliday, L., "Composite Materials," Elsevier Publishing Company New York p 406.

24. Bortz, S.A. and Lund, H.H., "The Brittle Ring Test," Proc. Conference on Mechanical Properties of Engineering Ceramics, p 383-406 (North Carolina State College, R leigh, N.C.) Interscience: New York (1961).

25. Knudson, F.P., "Dependence of Mechanical Strength of Brittle Polycrystalline Specimens on Porosity and Grain Size," J. Amer. Ceram Soc., 42, (8) (1959).

26. Rudy, E., et al., "Ternary Phase Equilibria in Transition Metal-Boron-Carbon-Silicon Systems," Aerojet-General Corporation, AFML-TR-65-2, Part I, Volume V (Jan. 1966).

27. Nadler, M.R. and Kempter, C.P., "Some Sodidus Termperatures in Several Metal-Carbon Systems," J. Phys Chem. 64(10) 1468-71 (Oct. 1960).

28. Adelsberg, L.M., Cadoff, L.H. and Tobin, J.M., "Group IV B and VB Metal Carbide-Carbon Eutectic Termperatures," J. Am. Ceram. Soc. 49(10) 573-74 (Oct. 1966).

29. Meers, J.T., "Some Effects of Annealing Pyrolytic Graphite," Fifth Carbon Conference, Pergamon Press, New York (1962) p. 461-465.

30. P. Murray, et al, "Factors Affecting the Thermal Shock Resistance of High-Temperature Materials," <u>Mechanical Properties of Nonmetallic Brittle Materials</u>, edited by W.H. Walton, Interscience Publishers, Inc., New York (1958) pp. 269-276.

31. P. Murray, et al, in "Ceramic Fabrication Processing," MIT, J. Wiley and Sons, New York (1958) p. 147.

32. A.L. Loeb, "A Theory of Thermal Conductivity of Porous Materials," <u>J. Am. Ceram. Soc.</u>; Volume 37, (1954) p. 96-99.

33. W.B. Crandall, et al, in "Mechanical Properties of Engineering Ceramics," Interscience Publishers, New York (1961) p. 349.

34. R.M. Spriggs and T. Vasilos, "Effect of Grain Size of Transverse Bend Strength of Alumina and Magnesia," <u>J. Am. Ceram. Soc.</u>, Volume 46, No. 5 (May 1963) p. 224-228.

DISTRIBUTION (Cont'd)

	Copies
General Atomic Division General Dynamics Division P. O. Box 608 San Diego, California 92112 Attention: Dr. J. L. White	1
Missile and Space Systems Division Douglas Aircraft Co., Inc. 1177 Jadwin Avenue Richland, Washington Attention: Mr. J. O. Gibson	1
Battelle Northwest 3000 Stevens Drive Richland, Washington 99352 Attention: Dr. Ralph Cooper	1
National Aeronautics & Space Administration Lewis Research Center Cleveland, Ohio Attention: Mr. Merv Ault	1

DISTRIBUTION

IIT RESEARCH INSTITUTE

Copies

University of California   2
Los Alamos Scientific Laboratory
P. O. Box 1663
Los Alamos, New Mexico   87544
Attention: Mr. K. V. Davidson, CMB-6

University of California   2
Los Alamos Scientific Laboratory
P. O. Box 1663
Los Alamos, New Mexico   87544
Attention: Mr. Haskell Sheinberg, CMB-6

University of California   2
Los Alamos Scientific Laboratory
P. O. Box 1663
Los Alamos, New Mexico   87544
Attention: Dr. Charles P. Kempter

Westinghouse Astronuclear Laboratory   1
Pittsburgh, Pennsylvania
Attention: Dr. Leonard France

Westinghouse Astronuclear Laboratory   1
Pittsburgh, Pennsylvania
Attention: Dr. J. M. Tobin

Westinghouse Astronuclear Laboratory   1
Pittsburgh, Pennsylvania
Attention: Mr. Jack Blay

Union Carbide Corporation   2
Nuclear Division (Y-12)
Oak Ridge, Tennessee
Attention: Dr. John M. Napier

Space Nuclear Propulsion Office   2
National Aeronautics & Space Administration
Lewis Research Center
Cleveland, Ohio
Attention: Dr. N. R. Thielke